Dynamic Performance Evaluation of Fabric Reinforced Brick Masonry wall

Submitted By

Student Name: Abrar Hussain

Registration No: 31-FET/MS CE/F22

Supervisor: Prof. Dr. Syed Abid Ali Shah

Co-Supervisor: Dr. Zeeshan Alam

DEPARTMENT OF CIVIL ENGINEERING

FACULTY OF ENGINEERING AND TECHNOLOGY

INTERNATIONAL ISLAMIC UNIVERSITY, ISLAMABAD

July, 2025

All rights reserved. No part of this thesis may be reproduced, distributed, or transmitted in any form or by any means, including photocopying, recording, or other electronic or mechanical methods, by any information storage and retrieval system without the prior written permission of the author.

Dedication:

To my parents

And

"It is with my deepest gratitude and warmest affection that I dedicate this thesis to my supervisor "**Dr. Abid Ali Shah**" & Co supervisor "**Dr. Zeshan Alam**" who have been constant source of knowledge and inspiration for me in this whole period.

CERTIFICATE OF APPROVAL

Title of Thesis: Dynamic Performance Evaluation of Fabric Reinforced Brick Masonry Wall

Name of Student: Abrar Hussain

Registration No: 31-FET/MS CE/F22

Accepted by the Department of Civil Engineering, Faculty of Engineering and Technology, International Islamic University (IIU), Islamabad, in partial fulfillment of the requirements for the Master of Science degree in Civil Engineering.

Viva voce committee:

Prof. Dr. Sayed Abid Ali Shah (Supervisor)
Professor, DCE, FET, IIU, Islamabad

Dr. Muhammad Noman (Internal)
Assistant Professor, DCE, FET, IIU, Islamabad

Dr. Rana Faisal Tufail (External)
Assistant Professor, DCE, Comsats University, Wah

Prof. Dr. Sayed Abid Ali Shah (Chairman, DCE)
Assistant Professer DCE, FET, IIU Islamabad

Prof. Dr. Muhammad Amir (Dean, FET)
Professor DCE, FET, IIU Islamabad

Author's Declaration

I, **Abrar Hussain** hereby state that my MS thesis titled "**Dynamic Performance Evaluation of Fabric Reinforced Brick Masonry Wall**" is my own work and has not been submitted previously by me for taking any degree from International Islamic University, Islamabad or anywhere else in the country/abroad.

At any time if my statement is found to be incorrect even after my graduation, the University has the right to withdraw my MS Degree.

Abrar Hussain

Reg No: 31-FET/ MS CE/F22

Plagiarism Undertaking

I solemnly declare that research work presented in this thesis titled "**Dynamic Performance Evaluation of Fabric Reinforced Brick Masonry Wall**" is solely my research work with no significant contribution from any other person. Small contribution/help wherever taken has been duly acknowledged and that complete thesis has been written by me.

I understand the zero-tolerance policy of the HEC and International Islamic University, Islamabad towards plagiarism. Therefore, I as an author of the above titled thesis declare that no portion of my thesis has been plagiarized and any material used as reference is properly referred/cited.

I undertake that if I am found guilty of any formal plagiarism in the above titled thesis even after award of MS Degree, the University reserves the right to with- draw/revoke my MS degree and that HEC and the University have the right topublish my name on the HEC/University website on which names of students areplaced who submitted plagiarized work.

Abrar Hussain

Reg No: 31-FET/MS CE/F22

Acknowledgements

Firstly, I would like to thank **ALLAH ALMIGHTY** for giving me strength and skills to carry out this research work successfully. I am always deeply obliged to my beloved father and mother for her support and encouragement, and always prayed for my success in this life and the life hereafter. My deep gratitude goes to **Prof. Dr. Abid Ali Shah & Prof. Dr. Zeshan Alam** who expertly guided and motivated me throughout this research work with his generous remarks and technical support. His unwavering enthusiasm kept me constantly engaged with my research work and helped me make my tasks enjoyable. It's a great honor for me to work under his supervision. May **ALLAH ALMIGHTY** grant him countless blessings, Ameen.

It is a great pleasure to express my deepest thanks and gratitude to my mentor **Prof. Dr. Abid Ali Shah & Prof. Dr. Zeshan Alam** from Islamic International University Islamabad for his moral support, motivation, continuous review, and positive feedback on my research work. Without their keen input, this work could not have been completed successfully.

Lastly, Thanks to my well-wishers for their endless love and support.

Abrar Hussain

Reg No: 31/FET/MS CE/F22

Abstract

The dynamic performance of masonry structures is critically impacted by natural disasters like earthquakes, which induce cracks and compromise structural integrity. Structural enhancement emerges as a viable solution to enhance the durability and strength of masonry walls, particularly through the use of innovative reinforcement materials. This research investigates the effectiveness of fabric-reinforced masonry walls by incorporating Chicken Mesh Fiber, Steel Mesh Fiber, and Glass Fiber into their construction. The study emphasizes the comparative analysis of these materials in improving load-bearing capacity, crack resistance, and overall resilience against seismic forces.

The experimental framework involved constructing masonry walls specimens, each measuring 600 x 600 mm with a thickness of 114.5 mm. These walls were divided into control and test groups, where control specimens utilized conventional materials, while the test specimens integrated different fiber meshes within the plaster. Comprehensive testing procedures, including static compression tests, dynamic Pendulum Impact Tests, and simulated earthquake scenarios, were conducted to assess the mechanical and dynamic responses of the walls. Key observations included crack propagation patterns, displacement behaviour, and material deformation under applied stresses.

The findings reveal that Chicken Mesh Fiber, as an affordable and locally available material, significantly improves the wall's ability to withstand seismic activities by enhancing ductility and energy dissipation. Steel and Glass Fiber also demonstrated notable performance, with Steel Mesh Fiber providing superior strength and Glass Fiber contributing to reduced wall deformation. The integration of these materials offers a sustainable, cost-effective Structural enhancement approach for new constructions and the rehabilitation of existing structures.

This research holds substantial importance for civil engineering and construction, offering insights into sustainable Structural enhancement methods to strengthen masonry walls. The outcomes contribute to safer building practices in earthquake-prone areas, preservation of historical masonry structures, and advancements in material science. By mitigating structural risks and promoting innovative material usage, this study aids engineers, architects, and policymakers in developing resilient and environmentally sustainable infrastructure

Table of Contents

List of Figures

List of Tables

ASTM Standards

ASTM C1314	Standard Test Method for Compressive Strength of Masonry Prisms
ASTM C270	Standard Specification for Mortar for Unit Masonry
ASTM C952	Standard Specification for Bond Strength of Mortar to Masonry Units
ASTM C780	Standard Test Method for Preconstruction and Construction Evaluation of Mortars for Plain and Reinforced Unit Masonry
ASTM C67	Standard Test Methods for Sampling and Testing Brick and Structural Clay Tile (Includes Compressive Strength, Flexural Strength, and Water Absorption)
ASTM C20	Standard Test Methods for Apparent Porosity, Water Absorption, Apparent Specific Gravity, and Bulk Density of Refractory Brick and Shapes
ASTM E23	Standard Test Methods for Notched Bar Impact Testing of Metallic Materials (Charpy Impact Test, adapted for masonry)
ASTM D6110	Standard Test Method for Determining the Charpy Impact Resistance of Notched Specimens of Plastics (For impact weight selection)
ASTM E519	Standard Test Method for Diagonal Tension (Shear) in Masonry Assemblages
ASTM A931	Standard Test Method for Tension Testing of Wire Ropes and Strands (Adapted for Fiber strips tensile testing)
ASTM C469	Standard Test Method for Static Modulus of Elasticity and Poisson's

	Ratio of Concrete in Compression (For masonry modulus evaluation)
ASTM E2309	Standard Practices for Calibration of Displacement Transducers for Use in Structural Testing (For LVDT and laser displacement sensor calibration)
ASTM E23	Standard Test Methods for Impact Testing of Materials (Charpy Impact Test, adapted for masonry).

Abbreviations and Symbols

RMM	Reinforced Mortared Masonry
S1	Simple Wall
S2	Glass Fiber Wall
S3	Chicken Mesh Fiber Wall
S4	Steel Mesh Fiber Wall
UPV	Ultrasonic Pulse Velocity
MM	Mortar Masonry
URM	Un Reinforced Masonry
RM	Reinforced Masonry
FRPs	Fiber Reinforced Polymers
GFRP	Glass Fiber Reinforced Polymers
CFRP	Carbon Fiber Reinforced Polymers
AFRP	Aramid Fiber Reinforced Polymer
TRM	Textile Reinforced Mortar
FRCM	Fiber Reinforced Cementitious Mortars
SRG	Steel Reinforced Grout
UHTSS	Ultra High Tensile Strength Steel
PVA	Polyvinyl Alcohol
AR	Alkali Resistant

RC	Reinforced Concrete
PBO	Polyparphenylenebenzobisoxazole
PP	Polypropylene
NSM	Near Surface Mounted
UTM	Universal Testing Machine
OPC	Ordinary Portland Cement
EIFS	Exterior Insulation and Finish Systems
ASTM	American Society for Testing and Machine
LVDTs	Linear Variable Differential Transducers
PSD	Power Spectral Density
F1	Fiber Strips Vertically Postioned
F2	Fiber Strips Horizontally Postioned
$\boldsymbol{EM_d}$	Dynamic Elastic Modulus
IF	Impact Force
FB	First Blow
$\boldsymbol{f_n}$	Fundamental frequency
IIB	Initial Impact Blows till first crack
UIB	Ultimate Impact Strength till failure
S-max	maximum spall distribution from the point of impact
$\boldsymbol{RF_t}$	Transverse resonance frequency
ξ	Damping ratio/percentage

Chapter 1

Introduction

1.1 Background

Masonry has been one of the oldest and most reliable construction systems worldwide. Approximately 70% of buildings globally are constructed using masonry. Its widespread use is attributed to its aesthetic appeal, fire resistance, thermal and acoustic insulation properties, mechanical performance, and economic advantages. The primary components of masonry include units, mortar, grout, and accessories [1]. FRP comprises high-strength fibers embedded in polymeric resins, offering exceptional tensile strength, corrosion resistance, and lightweight properties. The fibers primarily bear the load, while the resins facilitate shear transfer. Despite their advantages, FRPs have drawbacks, such as high costs, low impact resistance, and high electrical conductivity. The three primary types of FRPs are glass (GFRP), aramid (AFRP), and carbon fiber-reinforced polymers (CFRP). These materials are available in various forms, including laminates, meshes, tendons, and rods. Studies have demonstrated that FR

Significantly enhances the strength and ductility of masonry structures. For instance, [2] found that URM walls strengthened with FRP laminates showed substantial improvements in performance. Similarly, highlighted the effectiveness of FRP in increasing the load-carrying capacity of masonry structures. Post-tensioning with FRP tendons involves placing tendons inside steel tubes or grooves along the masonry wall's mid plane. This method improves the structure's serviceability, increases cracking resistance, and enhances its ultimate moment capacity. Repointing with FRP involves embedding deformed FRP rods into masonry joints using epoxy adhesives, significantly improving shear and bending moment capacities under static and cyclic loading. Numerous experimental studies further validate the benefits of FRP in masonry reinforcement. For example, [3] used carbon fiber ropes embedded in masonry joints to improve

out-of-plane bending resistance. Demonstrated that CFRP strips enhance in-plane shear capacity under axial loads. [4] tested FRP laminates on full-scale masonry walls, showing increased in-plane strength and energy dissipation under seismic loading conditions.

Out-of-plane actions can be significantly reduced by effectively connecting walls to floors with adequate in-plane stiffness [5] thereby preventing local collapses such as wall overturning, vertical or horizontal bending, corner failures, gable collapses, etc. Historically, the global collapse of buildings due to shear failure in masonry piers and spandrel beams was addressed using traditional techniques like grout injections , steel-reinforced concrete overlays [6], and repointing mortar joints. However, these methods have limitations: grout injections are not suitable for single-leaf, cobblestone, or rubble stone masonry, and steel reinforcement often suffers long-term corrosion.

In the past two decades, non-metallic materials, particularly polymeric composites, have gained prominence as reinforcement solutions due to their resistance to environmental degradation. These materials, including FRPs (Fiber Reinforced Polymers) made from carbon, glass, or aramid fibers, and polymers like polypropylene (PP) and poliparafenilenbenzobisoxazole (PBO), offer reliable alternatives [7]. Reinforcements may be applied in various forms such as fabrics, strips, bars, or meshes, which are integrated with masonry through mortar joints, thin mortar plasters, or epoxy adhesives.

The reinforcement of mortar joints with FRP bars [8] or strips has demonstrated improvements in in-plane strength and deformation capacity for single-leaf masonry. However, this method is less effective for out-of-plane actions and unsuitable for multi-leaf masonry due to the absence of transversal connectors. Similarly, externally bonded laminates [9] or meshes [10] improve in-plane shear resistance but require surface preparation with high-bond mortars, and their effectiveness is limited by de bonding failures. Applying FRP meshes embedded in mortar coatings on both wall faces significantly enhances in-plane shear and out-of-plane bending resistance, while also improving ductility [11]. This method is particularly effective for multi-leaf masonry when combined with passing-through connectors to prevent delamination. While this approach adds some mass due to thicker coatings, it allows for the use of natural binders like lime and pozzolan, ensuring compatibility with historical masonry. For fair-faced walls, a hybrid approach involving FRP-reinforced mortar on one side and reinforced repointing on the other side is possible. Additionally, this technique can strengthen infill walls in frame structures, improving the overall

structural performance against horizontal loads [12].

This study focuses on the mechanical behaviour of masonry walls strengthened with GFRP mesh-reinforced mortar coatings, a technique effective for both in-plane [11] and out-of-plane [13] seismic enhancements of URM buildings. Previous research demonstrated the effectiveness of this method through diagonal compression tests on various masonry types (e.g., solid brick, rubble stone) and different reinforcement configurations. Results highlighted that the technique significantly improves ductility and post-cracking performance, with the GFRP mesh playing a critical role in stress redistribution. The current study extends this investigation by testing various masonry types (solid brick, cobblestone, and rubble stone) with different mortar coatings to evaluate their influence on structural performance. It discusses failure mechanisms, compares URM and reinforced masonry (RM) behaviour, and provides an analytical formulation to quantify resistance and ductility improvements. This formulation addresses the lack of specific design guidelines, as current standards like EC8 [12], FEMA [14] , and CNR-DT 203/2006 [15] are not fully applicable to GFRP mesh-reinforced mortar coatings, which significantly interact with the masonry components.

Various seismic strengthening techniques have been extensively explored to enhance the performance of masonry walls. Among the most common methods are the application of shotcrete [16] , the use of fasteners and anchors [17] , fiber-reinforced polymer (FRP) reinforcements [18] , and bed joint reinforcement [19] . These techniques have demonstrated their effectiveness in improving both the in-plane and out-of-plane strength of masonry structures, addressing the inherent weaknesses of unreinforced masonry under seismic loads.

Composite materials, particularly textile-reinforced mortar (TRM), have gained significant attention for Structural enhancement structural and nonstructural components. TRM is known for its adaptability, enabling application on wet surfaces, ease of use, and cost-effectiveness, particularly in seismic Structural enhancement [20] . Numerous studies have evaluated the effectiveness of TRM in strengthening various structural elements, including beams [21] , columns [22] , slabs [23] , and masonry walls [24].

Zargaran et al. [16] in vestigated the shear and diagonal tension capacities of unreinforced masonry walls strengthened with TRM. Their findings highlighted the superior performance of two-sided TRM strengthening compared to one-sided reinforcement, particularly in enhancing shear

behaviour and preventing out-of-plane deformations. Similarly, Chen et al. [24] studied the influence of key parameters, such as wall thickness, reinforcement thickness, fiber percentage, and textile configuration, on the in-plane capacity of TRM-strengthened walls. Their work introduced a novel approach for predicting wall capacity based on these factors.

1.2 Research Motivation and Problem Statement

The occurrence of seismic events, such as earthquakes, can result in structural vulnerabilities in buildings, notably in the form of wall cracks, there by precipitating the risk of wall collapse. Consequently, there is an imperative need to address these vulnerabilities through structural enhancement measures. The primary objective of this Structural enhancement endeavor is to Strengthening and reinforce the structural integrity of these cracked walls. To attain this objective, we intend to employ a diverse range of fabric materials, with an initial focus on Chicken Mesh Fiber, followed by a comparative analysis involving steel Mesh and Glass Fiber.

It is an established fact that seismic activity often leads to the development of cracks in walls. In light of this, Structural enhancement emerges as a viable strategy to bolster the structural robustness of these walls, with particular emphasis on the integration of Chicken Mesh Fiber. The utilization of chicken fiber as an additive to plaster holds the promise of augmenting the flexural tensile strength of the wall, thereby rendering it more resistant to deformation and potential damage.

The implementation of Chicken Mesh Fiber within the structural framework of the wall necessitates a comprehensive evaluation through a series of rigorous testing methodologies. Among these methods, a specially devised Pendulum Impact Test assumes particular significance. Through the conduct of this test, we aim to meticulously assess the wall's performance concerning deflection and the propensity for cracking. This multifaceted evaluation will furnish valuable insights into the efficacy of Chicken Mesh Fiber as a Structural enhancement material in enhancing the seismic resilience of walls.

1.2.1 Research Questions

1 What types of fabric materials can effectively enhance the flexural strength of traditional walls?

2. How does the integration of fabric materials influence the structural stability of walls?

3. What is the maximum load capacity of traditional walls after fabric reinforcement?

4. Which fabric materials, such as Chicken Mesh Fiber, Steel Mesh Fiber, and Glass Fiber, are most effective for structural enhancement?

5. How do the mechanical properties of these fabric materials compare when used for reinforcing walls?

6. What testing methods can be used to evaluate the performance of these fabric materials in structural enhancement?

7. How does the cost-effectiveness of these materials vary concerning their reinforcement potential?

8. Can a combination of these fabric materials yield better reinforcement results compared to using them individually?

9. What Structural enhancement techniques are most effective in mitigating the risk of collapse due to earthquake-induced cracks?

10. How do structural enhancementted walls perform under simulated seismic conditions?

11. What are the key challenges in Structural enhancement traditional walls for earthquake resistance?

12. How does Structural enhancement impact the overall durability and lifespan of walls in seismic zones?

13. What role do fabric materials play in improving the resilience of walls during seismic events?

1.3 Objectives

Objective of the research can be achieved by performing these tasks as shown below:

1. Evaluate the influence of fiber reinforcement on the impact resistance, damping capacity, and stiffness of masonry walls under high-strain rate loading.
2. Investigate the behaviour of various fibers under out-of-plane impact, focusing on changes in natural frequency, damping enhancement, and energy absorption.
3. Assess the effect of fiber spacing on diagonal tension strength, structural rigidity, and energy dissipation to identify the most efficient reinforcement layout.
4. Conduct a comparative analysis of compressive strength, elastic modulus, and deformation between unreinforced and fiber-reinforced masonry walls.
5. Examine how fiber reinforcement improves compression performance and stiffness, addressing the structural weaknesses of unreinforced masonry.
6. Analyze the overall strength, durability, and sustainability of fiber-reinforced masonry under both dynamic and static loads, including energy absorption and failure patterns.

1.4 Scope of Work

Research on Structural enhancement fabric-reinforced masonry has profound implications for civil engineering and construction. It offers a cost-effective and innovative means to enhance load-bearing capacity and durability in masonry structures, reducing risks associated with seismic events, weathering, and aging. This approach promotes sustainable and resilient infrastructure, preserving historical buildings, optimizing construction practices, and reducing environmental impact. Furthermore, the findings benefit structural engineers, architects, and policymakers in safeguarding masonry structures globally, fostering safer and more sustainable built environments. Additionally, this research enhances structural resilience, optimizes Structural enhancement strategies, drives materials innovation, and reduces risks related to wall cracks and seismic events,

ultimately contributing to safer communities and more robust construction practices.

1.5 Novelty of Work

This research introduces a unique approach to enhancing the structural performance of traditional walls by integrating advanced fabric materials for reinforcement and Structural enhancement. The key aspects of novelty include:

This study explores the innovative use of diverse fabric materials to significantly enhance the flexural strength of traditional masonry walls. Unlike conventional reinforcement methods, it investigates the integration of Chicken Mesh Fiber, Steel Mesh Fiber mesh, and Glass Fiber, with a focus on optimizing material combinations and layer arrangements to achieve maximum strength while maintaining cost-effectiveness. A comprehensive assessment of material effectiveness is provided through a detailed comparative analysis of the mechanical properties of these fabrics, thereby filling a critical knowledge gap regarding their specific roles in enhancing structural stability. The research also examines the synergistic effects of combining different materials an aspect that has not been extensively studied in the context of masonry wall reinforcement.

Furthermore, the study adopts a targeted approach to earthquake resilience by developing Structural enhancement techniques tailored to traditional walls. These techniques focus on mitigating cracks and redistributing loads to reduce the risk of collapse during seismic events. By simulating realistic seismic conditions and evaluating the performance of structural enhancemented walls, the research bridges the gap between theoretical Structural enhancement models and practical implementation. In addition, sustainability and cost-effectiveness are prioritized through the use of locally available, lightweight, and economical materials, making the proposed solutions accessible for Structural enhancement in low-income or resource-constrained areas while reducing maintenance costs and extending the lifespan of structures.

Finally, a novel hybrid Structural enhancement strategy is proposed, combining multiple fabric materials and techniques to maximize resilience against both static and dynamic loads. This versatile approach is adaptable to different wall types and damage conditions, offering a comprehensive solution for enhancing the overall structural performance and durability of

masonry walls.

1.6 Project and Sustainable Development Goals

The Sustainable Development Goals (SDGs), introduced by the United Nations in 2015 under the 2030 Agenda for Sustainable Development, comprise a comprehensive framework of 17 global objectives aimed at addressing critical global challenges such as poverty, inequality, climate change, environmental degradation, and the promotion of peace and justice. These goals serve as a universal blueprint to guide nations toward inclusive, sustainable development by balancing economic growth, social equity, and environmental responsibility. Each SDG is accompanied by specific targets and measurable indicators to monitor global progress.

In the context of civil engineering and sustainable construction, the current research aligns most closely with SDG 9 (Industry, Innovation, and Infrastructure), SDG 11 (Sustainable Cities and Communities), and SDG 12 (Responsible Consumption and Production).

SDG 9 emphasizes the development of resilient infrastructure and the promotion of sustainable industrialization through innovative practices. This study contributes to that goal by incorporating Fibers as a sustainable reinforcement material in masonry walls, thereby enhancing their performance under impact and seismic conditions. This supports Targets 9.1 and 9.4, which advocate for the construction of sustainable and disaster-resilient infrastructure.

SDG 11 focuses on improving the safety, resilience, and sustainability of urban environments. By evaluating the impact resistance of unconfined partition walls commonly found in high-rise and framed structures this research directly supports Target 11.5, which aims to reduce the vulnerability of buildings to disasters such as earthquakes and accidental impacts.

SDG 12 promotes the efficient and responsible use of resources in production and consumption. The adoption of Fibers, a renewable and locally available material, reduces reliance on high-carbon construction alternatives such as steel and concrete. This aligns with Targets 12.2 and 12.5, which encourage the sustainable use of natural resources and the minimization of construction waste.

1.7 Brief Methodology

In this research, two categories of masonry wall specimens were prepared: unreinforced walls constructed using conventional methods, and reinforced walls incorporating three different fabric materials chicken mesh fiber, steel mesh fiber, and glass fiber. Each reinforced specimen was embedded with fiber mesh along with a cement-fine aggregate plaster layer, as per the designed configuration. The wall specimens were constructed using standard clay bricks, with overall dimensions of 610 mm × 610 mm, comprising 24 bricks per specimen. A total of 32 specimens were tested through three experimental procedures: the diagonal shear test (also known as the prism test) and the flexural impact test and Compression Test. The diagonal shear test, conducted on 20 specimens, was aimed at evaluating the tensile behaviour and overall structural performance of the walls under out-of-plane loading, with five specimens assigned to each reinforcement type. The flexural impact test was performed on 12 specimens, with three specimens tested under each load condition. For this test, fiber strips measuring approximately 762 mm in length and 66.04 mm in width were applied to the wall surfaces. Varying impact loads ranging from 113 g to 1134 g were dropped from heights of 300 mm, 600 mm, 900 mm, and 1200 mm to examine the response of the specimens under dynamic conditions. Throughout testing, Ultrasonic Pulse Velocity (UPV) measurements were employed to assess internal damage and crack propagation. The experimental process facilitated a comparative assessment of crack development, failure modes, and overall toughness across different reinforcement types, contributing to a comprehensive understanding of the dynamic behaviour and cost-effective optimization of fiber-reinforced masonry walls.

1.8 Thesis Outline

Chapter 1: Chapter 1 Introduction provides an overview of the research, including the background, motivation, and significance. It discusses the problem statement, objectives, scope of work, and the methodology. The limitations of the study and the overall structure of the thesis are also outlined.

Chapter 2: Chapter 2 Literature Review existing literature on Fibers reinforcement in construction, particularly for RMM. It covers the benefits of Fibers, including its mechanical properties and its use in improving masonry performance. The chapter compares Fibers reinforcement with traditional methods and discusses its potential in modern construction.

Chapter 3: Chapter 3 Methodology outlines the research methodology, including the experimental setup for testing Fibers-Reinforced walls. It details the tests used, such as Pendulum Impact Test, and Shear Diagonal Test (Diagonal Shear Test (Prism Test)). The chapter also explains the materials, walls dimensions, reinforcement details, and testing procedures, including the use of UPV for crack assessment.

Chapter 4: Chapter 4 Results and Analysis presents the results from the tests conducted on Fibers-reinforced walls. It analyzes the performance in terms of impact resistance, out-of-plane behaviour, tensile strength, and energy absorption. A comparison with traditional reinforcement methods is included. The chapter also discusses the mechanical and dynamic properties, crack patterns.

Chapter 5: Chapter 5 Conclusions and Recommendations summarizes the key findings, highlighting Fibers-reinforced walls as a sustainable alternative to traditional reinforcement. It includes recommendations for further applications of Fibers reinforcement and suggestions for future research.

Chapter 2

Literature Review

2.1 Background

Masonry walls often rely on plaster for enhanced load-bearing capacity and crack resistance. The use of fibre-reinforced plaster has proven to be significantly more effective than conventional plaster in improving tensile strength and ductility. Research by [25] demonstrates that fibre-reinforced plaster reduces cracking zones and the width of cracks, making it particularly suitable for seismic regions. Reinforcing plaster with nets made of stainless or polymeric materials has further improved seismic resistance, as shown by [26] also highlighted the enhanced shear strength of masonry walls structural enhancementted with polyvinyl alcohol (PVA) fibre-reinforced cement plaster. Experimental studies have tested the effectiveness of various fibre-reinforced plaster materials. For instance [25] examined polypropylene and steel fibre-reinforced plaster, finding increased shear strength under vertical loads. [27] evaluated Structural enhancement techniques using reinforced plaster in real masonry structures and observed significant improvements. Similarly, [28] and [29] conducted seismic tests using polymer nets embedded in plaster, showing enhanced structural performance.

Composite materials have become a popular choice over the past two decades for the repair and strengthening of reinforced concrete and masonry structures. These materials, consisting of high-strength textiles externally bonded to structural surfaces, offer significant improvement in structural capacity due to their high strength-to-weight ratio. However, challenges such as brittle failure, long-term durability concerns, sensitivity to impacts, and high costs have hindered their widespread adoption [30].

Numerous textile materials, such as carbon [31], glass [32], steel [33] , basalt [34], PBO (polyparaphenylene benzobisoxazole) [35], and natural fibers [36], have been used in TRM and FRCM systems. Among these, steel-based reinforcements have demonstrated excellent mechanical performance due to their high tensile strength and strong cord-to-mortar interlocking, all while maintaining relatively low costs [37]. Ultra High Tensile Strength Steel (UHTSS) cords, originally developed for automobile tires, have been adapted for structural applications under the name Steel Reinforced Grout (SRG). These cords possess tensile strengths ranging from 2800 to 3200 N/mm² and Young's modulus values of 180–210 kN/mm². Depending on cord spacing, the surface mass density varies from 600 g/m² to 3300 g/m², enabling maximum loads per unit width between 230 kN/m and 1300 kN/m [38].

Various Structural enhancement techniques have been explored to address this issue, including the use of ductile materials, with several studies highlighting the effectiveness of these methods [39]. One promising approach involves plastering masonry walls with fibrous cementitious materials, which enhance both the ductility and tensile strength of the walls. While the concept of using fibrous materials in mortar dates back historically, earlier materials lacked the mechanical properties to prevent large crack formations. Modern advancements in fiber-reinforced cementitious materials demonstrate their suitability for stucco applications in masonry, as these materials provide sufficient ductility and better bond strength between fibers and cementitious matrices [40] . For example, polyvinyl alcohol (PVA) fiber-reinforced cement stucco has shown considerable promise in strengthening masonry walls, offering increased flexural and tensile strength. Compared to lime-based mortar, cement-based mortar not only provides greater strength but also ensures adequate bond strength between fibers and mortar, which is essential for achieving the desired ductility and preventing surface cracking.

Masonry structures built using traditional methods are highly susceptible to significant damage or collapse during earthquakes, particularly in seismically active regions like Turkey. Strengthening these structures is essential to reduce seismic vulnerability, protect heritage buildings, and prevent loss of life. The strengthening process typically aims to enhance the strength and deformability of masonry systems. However, traditional methods often pose challenges, including inefficiency and high costs [41] . Innovative approaches, such as using technical textiles, have emerged as faster, lighter, and more efficient alternatives. Experimental studies reveal that masonry walls

strengthened with fiber-reinforced polymers (FRPs) exhibit improved shear strength and deformability [42]. However, organic binders like epoxy resins, commonly used with FRPs, have limitations, such as inefficiency in wet or low-temperature environments, high costs, health risks, lack of vapor permeability, and incompatibility with masonry materials. These binders are also irreversible, making them unsuitable for historical masonry structures [43]. Inorganic binders, such as fabric-reinforced cementitious mortars (FRCM), address these issues and are increasingly recognized as effective alternatives for strengthening historical masonry.

While research on FRCM for seismic Structural enhancement is less extensive compared to FRPs, it has shown promise in preserving historical masonry buildings, especially in Turkey, where urban transformation projects and the reuse of 19th and early 20th-century structures have created a substantial market for strengthening solutions. Studies on FRCM for masonry strengthening, including those by [44] and others, have demonstrated improvements in shear capacity, ductility, and shear modulus of masonry walls using carbon, glass, or basalt grids. However, these studies often focus on general masonry walls rather than historical masonry, which differs significantly due to factors like unregulated material production, poor workmanship quality, and aging effects. To address this gap, a recent study investigated FRCM's effectiveness for strengthening historical brick masonry walls using authentic bricks and a low-strength mortar designed to replicate historical materials.

2.2 Materials related Flaws and their Remedial Measures

The use of fiber reinforcement in cementitious materials has gained popularity due to its ability to improve post-cracking behaviour and structural performance. However, certain material-related flaws must be considered to ensure the effective application of fibers such as steel, glass, and chicken mesh fibers in construction. One of the major concerns with fiber-reinforced composites is the issue of fiber dispersion and orientation. Improper mixing can lead to fiber clumping, which creates weak zones in the matrix. This issue is particularly relevant in Steel Mesh Fiber, where inadequate distribution results in inconsistent mechanical properties. To mitigate this, the use of high-energy mixers and proper mixing sequences is recommended [45]. Additionally, Glass Fiber

are prone to balling and segregation due to their lower density compared to Steel Mesh Fiber, which can be addressed by using surfactants or specialized mixing procedures [46]. Another significant flaw in fiber-reinforced materials is fiber-matrix bonding. Steel Mesh Fiber, although providing excellent mechanical performance, may suffer from poor adhesion with the cementitious matrix, leading to pull-out failure under stress. To improve bond strength, surface treatments like hooked or crimped fiber geometries are preferred G[47]. Glass Fiber, on the other hand, tend to degrade in high-alkaline environments, which weakens their structural integrity over time. The application of alkali-resistant (AR) coatings and the use of supplementary cementitious materials like silica fume can help enhance durability [48] . Chicken mesh fibers, often made of galvanized or stainless steel, can experience corrosion if not properly embedded, affecting the overall strength of the composite. Ensuring full encapsulation and using corrosion-resistant coatings can prevent this issue [49].

A critical issue in fiber-reinforced composites is shrinkage and cracking. While fibers help control crack propagation, they may not completely eliminate early-age shrinkage cracks. Micro fibers, particularly polymeric or Glass Fiber, are effective in reducing plastic shrinkage cracking, but their use must be optimized to avoid excessive air entrapment, which can reduce compressive strength [50] . Steel macro fibers can bridge cracks and enhance toughness, but they must be used in sufficient volume fractions (typically between 1–2% for structural applications) to be effective [46]. Additionally, workability issues can arise in fiber-reinforced mixtures. Higher fiber content often reduces the ease of placing and finishing the material. Steel Mesh Fiber, due to their high aspect ratio, can make the mix stiff, requiring higher doses of super plasticizers to maintain workability [51] . Glass and chicken mesh fibers can also interfere with the flow ability of mortar, necessitating adjustments in water content or the use of viscosity-modifying agents [51]. Lastly, compatibility with existing materials is a concern in rehabilitation projects. In historical masonry structures, high-lime mortars are often used, and introducing fibers into these mixtures requires careful selection to maintain chemical and mechanical compatibility. Chicken mesh fibers, for example, must be embedded correctly to avoid aesthetic and chemical incompatibility with historic lime-based mortars [52] . Overall, the success of fiber-reinforced composites depends on understanding and mitigating these material-related flaws. Proper mixing, selection of fiber type, surface treatments, and chemical compatibility considerations are essential to maximize the benefits of fiber reinforcement in structural and rehabilitation applications.

2.3 Properties of Masonry Walls

Masonry is one of the oldest and most widely used construction systems, with over 70% of buildings worldwide being masonry structures [1]. Its popularity is attributed to its aesthetics, fire resistance, insulation properties, mechanical strength, and cost-effectiveness. Masonry consists of four primary components: masonry units (such as fired clay bricks or concrete blocks), mortar (which holds the units together), grout (fluid concrete that surrounds reinforcement), and accessories (including reinforcement, connectors, and waterproofing materials). Common masonry units include fired clay bricks with a density of approximately 2000 kg/m³ and a compressive strength ranging from 56 to 200 MPa, while lightweight concrete blocks have a density of 1500–1700 kg/m³ and a compressive strength of 13–20 MPa [ASTM C62, C216, C90]. Due to variations in materials and construction methods, masonry is a heterogeneous material and generally exhibits very low tensile strength, making it prone to cracking and failure under tensile loads [53]. Structural failures in masonry walls occur due to load redistribution, environmental factors, aging, or accidental movements over time. Unreinforced masonry (URM) walls under seismic loads may fail in in-plane mode, characterized by diagonal tension cracks, or out-of-plane mode, which results in cracking along mortar joints [54]. To enhance the structural performance of masonry, various strengthening techniques are employed. Near-Surface Mounted (NSM) reinforcement and repointing techniques improve the durability and load-bearing capacity of joints. More advanced strengthening techniques involve Fiber Reinforced Polymers (FRP), including Glass (GFRP), Aramid (AFRP), and Carbon Fiber Reinforced Polymers (CFRP), which significantly improve the load-carrying capacity and structural integrity of masonry walls [2]. Additionally, post-tensioning with CFRP tendons has been proven to increase the cracking resistance, reduce crack sizes in damaged structures, and enhance the moment capacity of masonry walls. The seismic performance of masonry structures can also be enhanced through FRP post-tensioning, as observed in historical masonry towers where unbonded AFRP tendons were used to increase lateral load resistance and minimize displacement. Furthermore, masonry columns confined with CFRP and GFRP exhibit a significant increase in compressive strength and ductility, with even greater improvements when internal FRP reinforcement bars are combined with external

FRP confinement [55]. The ability of FRP strengthening to enhance the energy dissipation, flexural strength, and axial load capacity of masonry structures makes it a highly effective modern strengthening technique for improving masonry performance under various loading conditions.

Masonry walls possess several key properties that make them an essential component in construction. They offer high compressive strength, making them suitable for load-bearing applications, and are exceptionally durable, capable of withstanding harsh environmental conditions over long periods. Their non-combustible nature provides excellent fire resistance, while their density ensures effective thermal and sound insulation, contributing to energy efficiency and noise reduction. Masonry walls are resistant to pests, decay, and moisture penetration when properly constructed and maintained. They offer aesthetic versatility, with various patterns and finishes enhancing architectural appeal. Additionally, masonry walls are eco-friendly, often using locally sourced, natural materials such as bricks and stones, and are cost-effective due to their low maintenance and long lifespan. Reinforced masonry walls also provide enhanced seismic performance, making them versatile for various structural needs. These properties collectively make masonry walls a reliable, durable, and sustainable choice in building construction.

2.4 Properties of Masonry Wall by adding Fibers as Reinforcement

The addition of Ultra High Tensile Strength Steel (UHTSS) cords as reinforcement significantly enhances the mechanical properties of masonry walls. These UHTSS cords, composed of five galvanized wires (three rectilinear and two twisted), improve interlocking with the mortar and provide resistance against rusting. Two different textiles, S12 and S4, were tested, differing in density and mass per unit area. The S12 textile, with a design thickness of 0.254 mm and mass density of 2000 g/m², has closely spaced cords (4.25 mm apart), allowing for better mortar penetration and improved matrix-to-textile bonding. Meanwhile, the S4 textile, with a design thickness of 0.084 mm and mass density of 670 g/m², has cords spaced 6.35 mm apart, offering a different reinforcement configuration [30].

The composite specimens were manufactured using two types of mortars: (i) mineral mortar (M) with a binder of natural kaolin and bauxite, and (ii) mineral-NHL mortar (L) containing natural kaolin, bauxite, and hydraulic lime binders. These mortars influence the compressive strength (fcm), Young's modulus (Ecm), and tensile strength (ftm) of the masonry walls. The bonding performance of these Steel Reinforced Grout (SRG) systems was evaluated on four types of masonry substrates: strong modern bricks, weak modern bricks, historic bricks, and tuff units. The reinforcement systems showed improved bonding performance, mechanical strength, and durability of masonry walls, making them a promising fiber reinforcement technique for both modern and historical masonry structures [30].

Table 1. Mechanical properties of mortar matrices and substrates (CV in round brackets).

Matrix/substrate	**Acronym**	f_{cm} **(N/mm²)**	E_{cm} **(kN/mm²)**	f_{tm} **(N/mm²)**	D **(mm)**
Matrix Mineral mortar	M	56.3 (2.7%)	22.01 (0.7%)	10.31 (2.6%)	0–0.5
Mineral-NHL mortar	L	20.6 (3.9%)	11.42 (5.0%)	5.42 (4.1%)	0–1.4
Substrate Modern strong brick	SB	35.5 (12.9%)	3.45 (7.7%)	3.60 (11.7%)	–
rModern weak brick	WB	14.7 (8.4%)	1.95 (12.0%)	1.88 (1.1%)	–
Historic brick	HB	25.5 (11.4%)	3.21 (9.9%)	1.79 (3.7%)	–
Tuff unit	TU	4.4 (13.0%)	0.78 (10.7%)	0.56 (4.5%)	–

The incorporation of fiber-reinforced polymer (FRP) materials in masonry structures significantly enhances their mechanical properties, making them more resilient against seismic and structural loads. Masonry walls reinforced with fibers exhibit increased strength, rigidity, and load-bearing capacity, particularly under in-plane and out-of-plane forces. Various experimental studies confirm the positive impact of FRP reinforcement. For instance, an experimental study on brick walls strengthened with FRP materials demonstrated that fiber orientation significantly influences rigidity but has little effect on wall strength under static loading [56]. Another study by [54] found that walls reinforced with CFRP strips placed orthogonally to the joints exhibit improved energy dissipation capacity, making them highly effective against lateral loads. [57] conducted tests on brick walls structural enhancementted with carbon and glass FRPs under cyclic axial compression, revealing that carbon fiber reinforcement performed better than glass fiber in terms of strength and structural performance. Further research demonstrated a significant increase in the out-of-plane strength of FRP-reinforced brick walls, showing four distinct failure modes, including shear failure and bonding issues between FRP and the masonry surface [58] reinforced 42 masonry walls with laminated glass FRP under different inclination angles, concluding that FRP reinforcement increases compressive strength by 160–500% compared to unreinforced walls. Additionally, [59] studied CFRP and GFRP reinforcement on brick walls, highlighting a substantial increase in load-bearing capacity and strain resistance. These findings establish that FRP reinforcement is a highly effective Structural enhancement method, providing durability, improved structural integrity, and enhanced resistance to seismic and axial loads while preserving the architectural integrity of historical masonry structures. The addition of fibers as reinforcement in masonry walls enhances their structural and functional performance significantly. Fiber-reinforced masonry (FRM) exhibits improved tensile strength and crack resistance, as fibers bridge potential cracks and distribute stress more evenly, reducing the likelihood of failure under load. The incorporation of fibers, such as steel, glass, polypropylene, or basalt fibers, also enhances the flexural strength, allowing the walls to better resist bending forces. This results in greater seismic performance, as the walls become more ductile and capable of dissipating energy during earthquakes.

Fiber reinforcement significantly improves the durability of masonry walls by reducing permeability and preventing moisture ingress, which helps in resisting weathering effects. It also provides enhanced impact resistance, making the walls more robust against physical damage. Furthermore, fibers contribute to better fire resistance, as some types, such as basalt or Steel Mesh

Fiber, are highly heat-resistant, ensuring structural integrity during fire exposure.

The addition of fibers can also enhance thermal insulation by reducing heat transfer in the wall, depending on the fiber material used. Fiber-reinforced masonry remains cost-effective, as it reduces the need for extensive conventional reinforcements like steel bars in certain applications, while also lowering maintenance costs by preventing common issues such as cracking and spalling. Finally, it offers improved aesthetic appeal, as fiber-reinforced walls often exhibit fewer surface cracks and maintain a uniform appearance over time. Fiber-reinforced masonry walls exhibit enhanced structural and functional properties, making them ideal for modern construction. The incorporation of fibers such as steel, polypropylene, glass, basalt, or carbon significantly improves tensile, compressive, and flexural strength, allowing the walls to resist high loads, seismic forces, and dynamic stresses. Fibers help control crack propagation, ensuring better ductility and energy dissipation during earthquakes. They also reduce water permeability and enhance waterproofing, preventing moisture-related issues such as efflorescence, dampness, and mold growth. The durability of masonry walls is significantly increased as fibers provide resistance to environmental degradation, including freeze-thaw cycles, chemical attacks, and weathering. Steel Mesh Fiber improve impact resistance and ductility, while polypropylene and Glass Fiber offer lightweight, non-corrosive, and fire-resistant properties. Basalt fibers contribute to thermal and chemical resistance, making the walls suitable for harsh environments. Additionally, fiber reinforcement reduces the need for traditional reinforcements, such as steel bars, making it a cost-effective solution with long-term maintenance benefits. These walls are widely used in load-bearing structures, retaining walls, industrial buildings, and high-rise constructions, offering exceptional strength, durability, and performance.

2.5 Understanding High and Low Velocity Impact Testing in Previous Research

Dropping objects and vehicle collisions can cause accidental impacts on structures [60]. During construction, objects may fall from heights [61]. Parking garage walls and columns are often hit

by vehicles [62]. Airport runways face repeated impacts from airplane tires [63]. Offshore piers experience impact from ships and sea waves [64]. Explosions can cause impact forces through projectiles and debris [65].

High-velocity impact tests are used to assess the effects of explosions and projectile impacts [63]. Low-velocity impact tests, as classified by ACI 544-2R, include the instrumented falling impact test, Charpy pendulum impact test, and repeated drop-weight impact test [66]. The instrumented falling impact test measures the structural performance of slabs and beams under drop-weight impacts [67]. The Charpy pendulum impact test evaluates material toughness [68]. The repeated drop-weight impact test is a low-cost, simple method for comparing different concrete mixtures [66].

The ACI 544-2R repeated impact test involves a 4.54 kg steel mass dropped from a height of 457 mm onto a concrete disk specimen. The impacts are repeated until a visible crack appears, and the number of impacts is recorded for both crack formation and specimen failure. This test is used to compare the impact resistance of different concrete mixtures but does not provide exact strength values. It was originally introduced by Schrader, who recommended testing five specimens per batch and disregarding the highest and lowest values [69].

One of the major challenges in using this test is the high variation in results, which reduces its reliability [70]. Researchers have suggested modifications to the test setup, specimen shape, and testing procedure to improve accuracy. Despite the inconsistencies in results, the test remains widely used due to its simplicity and cost-effectiveness.

2.6 Summary

Masonry walls are widely used in construction due to their strength, durability, and cost-effectiveness. However, they are prone to cracking and failure under seismic and structural loads. To enhance their performance, fiber-reinforced plaster has been introduced, significantly improving tensile strength, ductility, and crack resistance. Various fiber materials, such as steel, polypropylene, glass, and polymeric nets, have been tested, demonstrating improved seismic resistance and overall structural integrity.Composite materials, including textile-reinforced and

fiber-reinforced mortars, have become popular for strengthening masonry structures. These materials offer high strength-to-weight ratios, improved load-bearing capacity, and enhanced durability. Ultra High Tensile Strength Steel (UHTSS) cords have been particularly effective in reinforcing masonry walls, improving their interlocking with mortar and resistance to environmental degradation. Despite these advancements, fiber-reinforced materials have certain limitations, including challenges in fiber dispersion, bonding issues, shrinkage, and workability. Proper mixing techniques, surface treatments, and chemical compatibility considerations are essential to maximize their effectiveness. Masonry walls inherently possess high compressive strength, fire resistance, thermal insulation, and durability. Adding fibers further enhances their properties by improving tensile strength, crack resistance, seismic performance, and overall longevity. Fiber-reinforced masonry structures exhibit superior load-bearing capacity and energy dissipation, making them ideal for both modern and historical buildings, particularly in earthquake-prone regions.

Chapter 3

Experimental Program

3.1 Background

The dynamic performance evaluation of fabric-reinforced brick masonry walls focuses on enhancing the structural behaviour of masonry by incorporating fiber reinforcements, specifically Glass Fiber, Steel Mesh Fiber, and Chicken Mesh Fiber. Masonry walls, though strong in compression, exhibit limited tensile and flexural strength, making them vulnerable to dynamic loading conditions such as impacts, vibrations, or seismic forces. By embedding fibers like glass and steel mesh or using chicken mesh within the masonry structure, the tensile capacity, crack resistance, and energy dissipation properties are significantly improved, ensuring better performance under civil engineering loading scenarios.

The experimental investigation involves a series of tests, including Pendulum Impact Tests, Diagonal Shear Test (Prism Test), to analyze the mechanical and dynamic properties of the reinforced masonry. The Pendulum Impact Test evaluates the wall's resistance to sudden dynamic forces and its ability to dissipate energy without failure. Diagonal Shear Test (Prism Test) assess the compressive strength, tensile strength, and the interaction between fibers and masonry materials.

The use of Glass Fiber enhances crack resistance, provides corrosion resistance, and reduces long-term maintenance, while Steel Mesh Fiber contribute to increased tensile and flexural strength, improving ductility and impact resistance. Chicken mesh, being lightweight and easy to apply, ensures uniform stress distribution and prevents localized cracking, enhancing the wall’s durability and performance. These reinforcements are evaluated under varying load conditions and environmental factors to simulate real-world challenges in civil engineering applications.

This study aims to provide a detailed understanding of the role of fiber reinforcements in improving the dynamic behaviour of masonry walls, paving the way for sustainable and cost-

effective structural solutions in civil engineering.

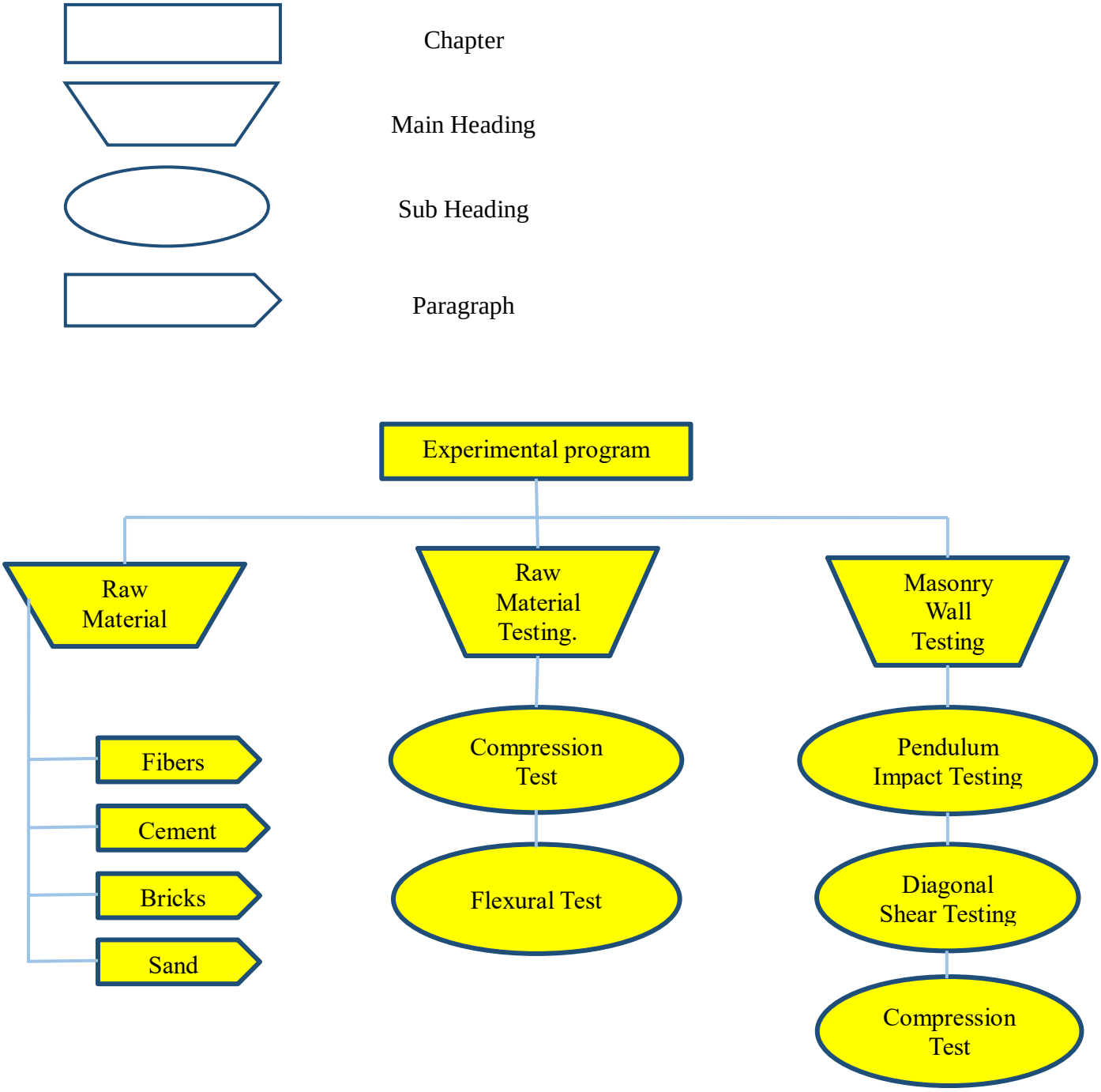

Figure 3.1: Schematic Diagram for Systematic Experimental Program

3.2 Raw Materials

The experimental study on the dynamic performance evaluation of fabric-reinforced brick masonry walls utilized a variety of construction materials including high-quality bricks, mortar, fiber reinforcements, and bonding agents. Locally sourced Ordinary Portland Cement (OPC) from Askari Cement was employed as the binding material. This cement composition included 61.7% calcium oxide (CaO), 21% silicon dioxide (SiO_2), 5.04% aluminum oxide (Al_2O_3), 3.24% ferric oxide (Fe_2O_3), 2.56% magnesium oxide (MgO), and 1.51% sulfur trioxide (SO_3), meeting the standard physical requirements outlined in Table 3.3. OPC was selected due to its consistent compressive strength, exceeding 26 MPa, and its minimum fineness of 90%, ensuring effective performance in masonry applications.

Table 2. Standard Physical Requirement of Ordinary Portland Cement

Cement type	**Applicable test method**	**Value**
Fineness	ASTM C204	Minimum 2,800 (cm 2 =g)
Autoclave Change (%)	ASTM C151	Maximum 0.8
Time of setting	ASTM C191	
Initial		Not less than 45 (min)
Final		Not more than 420 (min)
Air content of MortarVolume (%)	ASTM C185	Maximum 12
Compressive Strength 3 days 7 days 28 days		 9 (MPA) 16 (MPA) 26 (MPA)

Quartz sand, used as fine aggregate, had a maximum particle size of 4.8 mm and a bulk density of 1527 kg/m³. Its specific gravity, tested in accordance with ASTM C128 and ACI 211.1-91 standards, was found to be 2.66falling within the acceptable range of 2.5 to 2.8 indicating well-graded, clean sand with no impurities. The mortar mix was prepared using a cement-to-sand ratio of 1:4 and a water-to-cement ratio of 0.56. This proportion was selected to optimize bonding strength, workability, and durability. Mortar compressive strength was evaluated as per ACI 530.1-11 using a hydraulic testing machine. In addition, split-cylinder tests were conducted to determine tensile strength, while the modulus of elasticity was calculated from stress-strain relationships derived from fifteen cylindrical specimens, yielding a reliable average Young's modulus value.

(a)

(b)

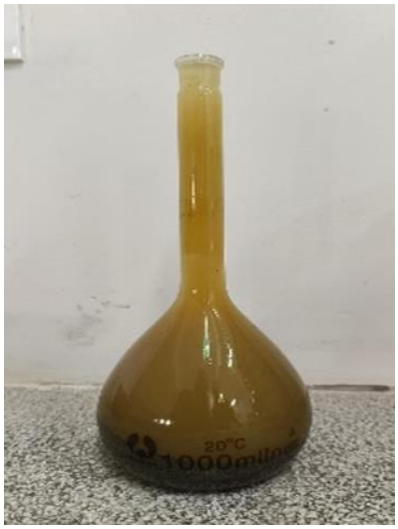

(c)

(d)

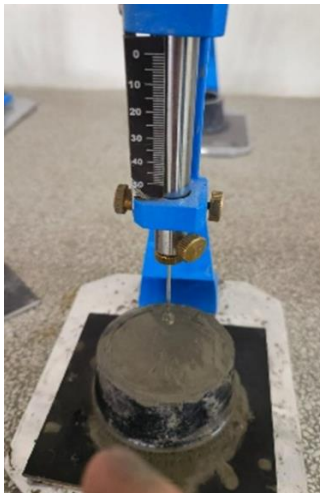

(e)

(f)

(g)

(h)

(i)

Figure 3.2: Raw Material Testing (a),(b) Cement (c) Sand Specific Gravity (d),(e),(f) Cement Consistence (g)(h)(i)Compressive Strength Cuve

The bricks used for specimen construction conformed to standard dimensions and underwent rigorous quality checks. Compressive strength tests were conducted on two different sizes of bricks to provide structural performance data. Water absorption capacity, an important factor for mortar adherence, was assessed following ACI 530.1-11. A sounding test confirmed the high quality of the bricks through the production of a clear ringing sound upon impact.

The reinforcement materials incorporated three types of fiber systems: alkali-resistant (AR) Glass Fiber, hooked-end steel mesh fibers, and conventional chicken mesh. AR Glass Fiber were used to enhance tensile strength and resist crack formation, while steel mesh fibers improved flexural strength and ductility. Chicken mesh served to evenly distribute stresses across the wall surface, thereby reducing the likelihood of crack propagation. To improve fiber-to-masonry adhesion and resist moisture ingress, bonding agents such as polymer-based adhesives, acrylic coatings, or epoxy sealants were considered where applicable.

3.3 Brick

Bricks are one of the most commonly used building materials in Pakistan due to their strength, durability, thermal insulation, and cost-effectiveness. The most widely used types include burnt clay bricks, fly ash bricks, concrete blocks, and sand-lime bricks, with burnt clay bricks being the

most prevalent in construction. High-quality bricks possess good compressive strength (1000 to 3000 psi), uniform shape and size, excellent bonding ability, low water absorption (less than 20%), and high fire resistance, making them suitable for load-bearing walls, boundary walls, and general masonry work. They also offer thermal and sound insulation, eco-friendliness, and resistance to moisture and efflorescence, ensuring long-term structural stability. The density of commonly used bricks varies between 1600 to 1900 kg/m³, while their controlled porosity prevents excessive moisture absorption. Burnt clay bricks, known for their strength and availability, are extensively used in residential, commercial, and infrastructure projects, while fly ash bricks and concrete blocks are gaining popularity due to their lightweight nature and improved insulation properties. The choice of brick depends on the structural requirements, environmental conditions, and cost considerations, making them a crucial component in Pakistani construction. In Pakistan, the standard brick size commonly used in construction is 230 mm × 115 mm × 77 mm (9 inches × 4.5 inches × 3 inches), following traditional masonry practices. This size ensures ease of handling, proper alignment in masonry work, and efficient bonding with mortar and are also used in certain regions. The thickness of the mortar joint, typically 10 mm to 12 mm, is considered when calculating brickwork dimensions. The standard size is widely used in residential, commercial, and infrastructure projects due to its optimal balance of strength, durability, and workability, ensuring stable and well-structured walls.

Figure 3.3 : Brick Sample

3.3.1 Testing of Bricks

3.3.1.1 Compression Testing of Brick

The compressive strength of masonry is a crucial property for assessing their quality. In this study, we determined the compressive strength of bricks following ASTM C140 guidelines, as depicted in Figure 10. The tests were conducted using a Universal Testing Machine (UTM) with a maximum capacity of 200 tons, operating in load-controlled mode. To ensure uniform load distribution, flat steel plates were placed above and below each brick, and the loading rate was maintained at 0.5 kN/s. The dimensions of the bricks were measured at 230 mm x 76 mm (9" x 3"). The test results are summarized in Table 5.

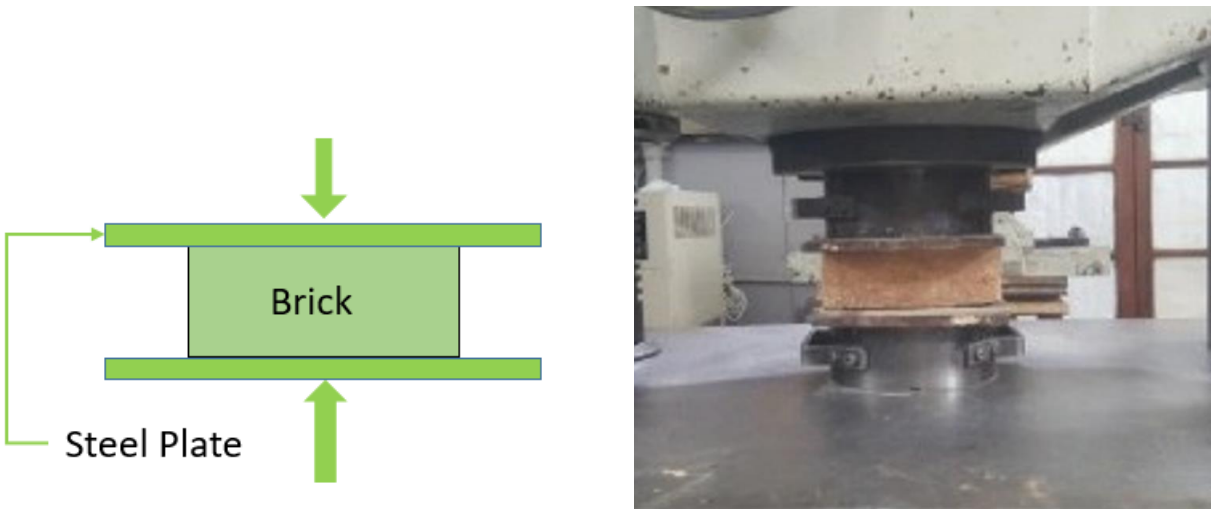

(a) (b)

Figure 3.4: Compression Test on Brick, (a) schematic view, (b) Testing of specimen

The crushing resistance of the brick was determined using Eq. (1).

$$\sigma_c = \frac{P}{A} \quad \text{.....eq. (1)}$$

Where:

σ_c = Crushing Strength

P = Peak force sustained until collapse a

A= Area of the brick

3.3.1.2 Flexure Testing of Brick

The flexural strength of the brick was evaluated using a three-point flexural test. This method involved positioning each brick on two supports and applying a concentrated load at its center until failure occurred. The modulus of rupture, or flexural strength, was calculated by dividing the maximum load sustained at failure by the moment arm and the cross-sectional area of the brick. This evaluation adhered to the standard procedures outlined in ASTM C67. The test setup is depicted in Figure 11, and the detailed results of the flexural strength tests are presented in Table 5. The flexural strength of the bricks was calculated using Equation 2.

$$S = \frac{3w\left(\frac{1}{2}-x\right)}{bd^2} \text{.....eq. 2}$$

Where

S = Bending resistance or rupture modulus

w = Peak load applied

L = Span between the two supports

b = Mean breadth of the block on the failing surface

d = Thickness or height of the block on the failing surface

x = The separation between the block's center and the failing surface.

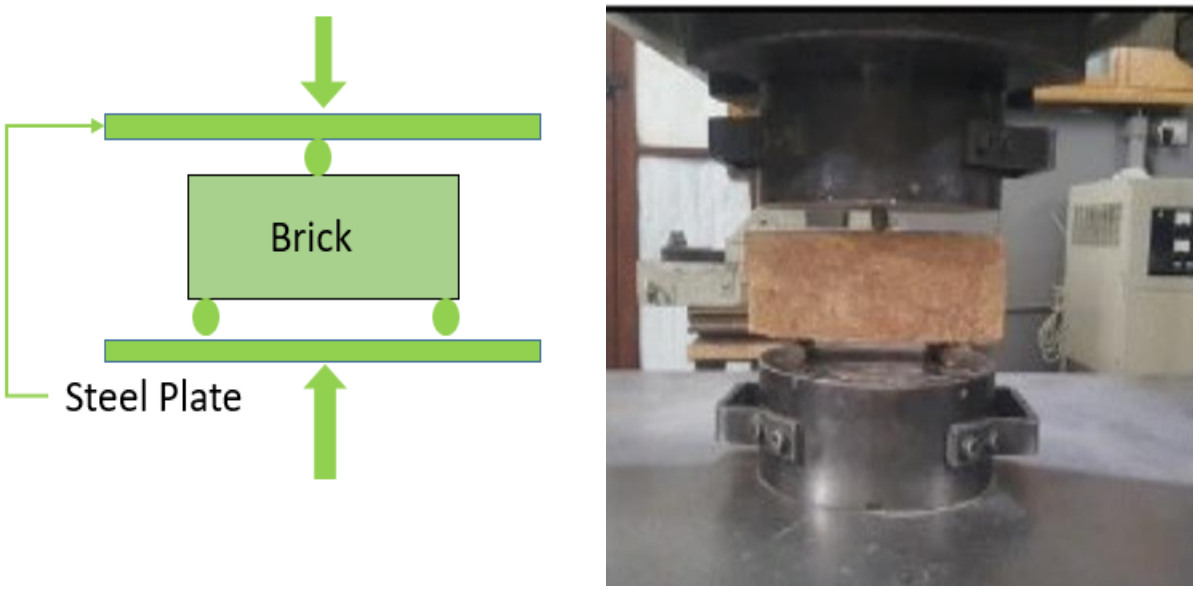

(a) (b)

Figure 3.5: Flexural Test on Brick, (a) schematic view, (b) Testing of specimen

Table 3. Testing Summary of Brick Specimen

Specimen	Compression test MPa (psi)	Flexure Test MPa (psi)
1	**10.23** (1485)	**2.5** (362.6)
2	**10.14** (1470)	**2.7** (391.6)
3	**10.27** (1490)	**2.4** (348.1)
Mean	**10.21** (1481)	**2.54** (368.4)

3.3.1.3 Sounding Test of Brick

The Soundness Test is a simple yet effective method to assess the quality and durability of bricks, particularly their resistance to impact and overall structural integrity. To perform this test, two bricks are selected and held in each hand. They are then gently struck against each other. A brick of good quality will produce a clear, metallic ringing sound upon impact and remain intact without any visible damage. This distinct sound indicates that the brick is well-fired and possesses a dense, uniform structure, making it suitable for construction purposes. Conversely, if the bricks emit a dull or thudding sound and exhibit cracks or break upon impact, it suggests that they are under-burnt or of inferior quality, rendering them unsuitable for structural applications. This test is widely used on construction sites due to its simplicity and the immediate insights it provides into the brick's quality.

(a) (b) (c)

Figure 3.6: Sounding Test of Brick

3.3.1.4 Water Absorption Test of Brick

The Water Absorption Test is a crucial procedure to evaluate the porosity and durability of bricks, which directly impacts their performance in construction. This test determines the amount of water a brick can absorb, indicating its quality and suitability for use in various environmental conditions. To conduct the test, three whole brick specimens are selected and dried in a ventilated oven at a temperature between 105°C and 115°C until they reach a constant mass. After cooling to room temperature, each brick is weighed to obtain its dry weight (M1). Subsequently, the bricks are completely immersed in clean water maintained at a temperature of 27±2°C for 24 hours. After this period, the bricks are removed, surface water is wiped off with a damp cloth, and they are weighed again to determine the wet weight (M2). The percentage of water absorption is calculated using the formula:

Water Absorption (%) = ((M2 - M1) / M1) × 100

The average water absorption value of the three specimens is reported as the final result. According to standard guidelines, first-class bricks should not absorb more than 20% of their dry weight, second-class bricks up to 22%, and third-class bricks up to 25%. Bricks with lower water absorption rates are considered more durable and are preferred for construction, especially in areas prone to moisture and freeze-thaw cycles. This test is essential for ensuring the longevity and structural integrity of brick masonry, as excessive water absorption can lead to deterioration, efflorescence, and reduced strength over time.

(a) (b) (c)

Figure 3.7: Water Absorption Test of Brick

3.4 Masonry Wall Specimen

Twelve brick masonry walls were constructed for in-plane Diagonal shear testing, each utilizing standard bricks measuring 230 mm x 115 mm x 77 mm. Each wall consisted of seven courses in height and three bricks in length, resulting in dimensions of 610 mm in height and 610 mm in length, yielding an aspect ratio (height to length) of 1:1. To ensure consistent quality across all specimens, a single master mason constructed each wall using locally available normal-strength bricks.

The reinforcement configurations for the walls are depicted in Figure 9, showcasing various designs to evaluate the advantages and disadvantages of each type. Each wall was uniquely designed to investigate specific structural behaviours under varying conditions and categorized into two main types. The first type, the Simple Wall without Reinforcement, serves as a baseline control wall, constructed without any reinforcement or openings. The second type, the Simple Wall with Fiber Reinforcement, incorporates fiber reinforcement into its structure to assess the effectiveness of this material in enhancing wall strength and performance. Further Categorized of Simple Wall with Fiber Reinforcement, incorporates various fibers such as chicken mesh fiber, steel mesh Fiber, and glass fiber. Fiber-reinforced materials have been increasingly utilized in masonry construction due to their ability to improve structural performance, particularly in enhancing tensile strength and crack resistance. Studies have shown that integrating fibers into masonry can significantly enhance the material's ductility and energy absorption capacity, leading to improved overall structural behaviour under various loading conditions.

The inclusion of fiber reinforcement in masonry walls aims to enhance their structural integrity, particularly under lateral forces such as earthquakes. Research indicates that fiber-reinforced mortars can improve the compressive and shear behaviour of masonry structures, contributing to increased durability and resilience.

By comparing the performance of unreinforced walls (Simple wall) with those reinforced with fibers (Simple wall with fibers), this study seeks to provide insights into the potential benefits of fiber reinforcement in masonry construction.

(a)

(b)

(c)

(d)

Figure 3.8: Masonry Walls Specimens

All walls were constructed using the English Bond technique, which is renowned for its strength and stability due to the alternating courses of headers and stretchers. This consistent construction approach ensures reliability and uniformity across all specimens, facilitating a comprehensive comparison of their structural performances. In this masonry Specimen, the mortar joints were meticulously controlled, with bed joints maintained at an average thickness of 0.41 inches and head joints at 0.55 inches, ensuring uniformity and structural integrity throughout the masonry work.

In all wall specimens tested, reinforced concrete (RC) slabs were attached below the walls. The RC slabs measured approximately 980.44 in width, 500.38 in depth, and 76.2 in height. Concrete of the type C25/30 was used, with two layers of steel reinforcement mesh in each slab. Four holes with a diameter of about 22.09mm were drilled in the corners of the top slabs, while four threaded lifting anchors were installed in the corners of the bottom slabs from this research we have taken reinforced concrete (RC) slab was attached with the walls to simulate realistic contact conditions found in existing buildings. The RC slabs measured approximately 762mm in length, 203.2mm in width, and 76.2 in height. Concrete of type C25/30 was used, and slab contained one layer of steel reinforcement mesh.

All wall specimens in this study were constructed using the English Bond technique, a method widely recognized for its superior structural strength and stability. This bonding pattern, characterized by alternating courses of headers and stretchers, creates a strong interlocking configuration that improves load distribution and enhances the overall integrity of the wall. The consistent use of English Bond across all specimens ensured uniformity in construction, thereby enabling reliable and meaningful comparisons. Although other bonds such as the Stretcher Bond comprising only stretchers and typically used in non-load-bearing applications or the Header Bond consisting solely of headers with moderate transverse strength are common, they offer comparatively lower structural efficiency. Similarly, the French (or Dutch) Bond, which places headers and stretchers within the same course for decorative purposes, does not provide the same level of structural performance as the English Bond. Given its proven effectiveness in resisting vertical and lateral loads, English Bond remains the preferred choice for structural masonry where strength and durability are critical.

The fiber-reinforced wall specimens and samples were designed to replicate those typically used in full-scale masonry partition walls, including Plain Walls, Glass Fiber Walls, Chicken Mesh Walls, and Steel Mesh Walls. As supported by the findings of Okail et al. [63], such fiber reinforcements have a significant impact on wall behaviour under lateral loading conditions. However, due to resource constraints, the aspect ratio of the walls in this study was reduced, and the fiber-reinforced samples were proportionally scaled down to match the smaller wall dimensions. This scaled approach maintained realistic geometric representation while ensuring feasibility within the laboratory testing environment.

Table 4: Specifications of Wall specimens							
Types of wall	**Types of tests**	**Wall designation**	**No. of specimens**	**Dimensions (mm)**	**Reinforcement type**	**Vertical reinforcement Strips (No.)**	**Horizontal reinforcement Strips (No.)**
Category 1	Impact Pendulum Testing	S1	3	600 x 600	Simple	-	-
		S2	3	600 x 600	Glass Fiber	3	3
		S3	3	600 x 600	Chicken Mesh Fiber	3	3
		S4	3	600 x 600	Steel Mesh Fiber	3	3
Category 2	Diagonal Shear Testing	S1	5	500 x 500	Simple	-	-
		S2	5	500 x 500	Glass Fiber	3	3
		S3	5	500 x 500	Chicken Mesh Fiber	3	3
		S4	5	500 x 500	Steel Mesh Fiber	3	3
Category 3	Compression Testing	S1	3	500 x 500	Simple	-	-
		S2	3	500 x 500	Glass Fiber	3	3
		S3	3	500 x 500	Chicken Mesh Fiber	3	3
		S4	3	500 x 500	Steel Mesh Fiber	3	3
Total Specimens			**49**				

3.5 Fibers Strips

The fibers utilized in this study were sourced locally, offering a cost-effective and readily available material for sustainable construction. These fibers were carefully selected and processed into uniform strips, as detailed in Figure 3.9. Subsequent treatments enhanced their durability and bonding with the masonry matrix. Notably, the fibers exhibited high tensile strength, low water absorption, and controlled moisture content, making them suitable for structural applications. Their water absorption and moisture content values were within acceptable ranges, ensuring minimal dimensional changes due to environmental exposure. Additionally, the fibers demonstrated excellent adhesion properties when used as reinforcement. Nonetheless, the inherent properties of these fibers underscore their potential as sustainable and efficient reinforcement materials, particularly in applications requiring lightweight and flexible construction solutions.

(a) (b) (c)

Figure 3.9: Fibers (a)Chicken Mesh Fiber (b) Glass Fiber (c)Steel Mesh Fiber

3.5.1 Z-Epoxy 300

Z-Epoxy adhesives are used to bond reinforcing strips to masonry walls, enhancing structural integrity and specifically formulated for such applications, offering high-strength adhesion suitable for materials like masonry walls. When selecting an z-epoxy, it's essential to choose compatible with both the reinforcing strips and the masonry surface. Proper surface preparation, including cleaning and roughening, ensures optimal adhesion. During application is crucial for achieving the desired bond strength but if we cleaning surface and apply properly then bond easily formed with fibers. Z-Epoxy have two components, one is hardener and one is base. The combination was mixed with 1:2 ratio and by using hand layup technique epoxy mixture was pasted on Fibers strips. Epoxy was spread by brush and round roller. Figure 3.10 shows the hand lay-up technique. Similarly all fibers strips were applied one by one.

Figure 3.10: Z-Epoxy 300

3.5.1 Chicken Mesh Fiber

Chicken Mesh Fiber is a lightweight, flexible, and durable reinforcement material used in plastering to enhance surface strength and prevent cracks. It plays a crucial role in improving plaster adhesion, tensile strength, and overall durability, making it ideal for both interior and exterior applications. Unlike traditional reinforcement materials, chicken mesh fiber is highly resistant to moisture, chemicals, and temperature variations, ensuring long-term performance without deterioration. One of its primary benefits is crack prevention, as it helps distribute stress evenly across the plastered surface, minimizing shrinkage cracks, thermal expansion cracks, and surface damage. It also enhances the plaster's bonding ability, ensuring a strong connection with different substrates such as brick, concrete, and masonry walls. Due to its flexibility, chicken mesh fiber is easy to install and adapts well to irregular shapes, curved surfaces, and decorative plastering, making it a preferred choice in architectural applications. The material is widely used in wall reinforcement, ceiling plastering, repair and restoration work, and decorative finishes. It strengthens plastered walls, preventing cracks caused by settlement, vibration, or temperature changes. In ceiling applications, it provides additional stability and prevents sagging or plaster separation over time. For repair and restoration projects, it reinforces weakened plaster surfaces, ensuring longevity and preventing future cracks. Additionally, in architectural and decorative applications, chicken mesh fiber helps maintain the structural integrity of intricate plaster designs while preventing surface defects. By incorporating chicken mesh fiber into plastering, walls become stronger, more durable, and resistant to environmental factors, ensuring high-quality and long-lasting plaster finishes. Its ease of application, cost-effectiveness, and crack-resistant properties make it a preferred choice in modern construction, home renovations, and commercial projects requiring durable and smooth plaster surfaces.

(a)

(b)

(c)

(d)

(e)

(f)

(g)

(h)

Figure 3.11: Chicken Mesh Fiber Specimens (a)(b)Marking (c)(d) Cutting Strips (e)Z-Epoxy Pasted Hand Lay Technique (f)Specimens Surface Cleaning (g)(h) Fibers Strips Pasted

3.5.3 Glass Fiber

Glass Fiber is widely used in plastering to reinforce walls and prevent cracks by enhancing the strength, flexibility, and durability of the plastered surface. It is made from fine glass filaments woven into a mesh or chopped into strands, which are then mixed into the plaster or applied as a reinforcement layer. Unlike traditional steel reinforcement, glass fiber is lightweight, corrosion-resistant, and provides excellent tensile strength without adding excessive weight to the structure. The primary advantage of glass fiber in plastering is its high tensile strength and crack resistance. It effectively distributes stress across the surface, reducing the likelihood of shrinkage cracks, temperature-induced cracks, and impact damage. Additionally, glass fiber improves the adhesion of plaster to different surfaces, ensuring a strong bond and preventing delamination. Glass Fiber woven or knitted mesh applied before or during plastering to enhance surface strength and prevent cracks, Small fiber strands mixed directly into the plaster to improve its toughness and flexibility. Glass Fiber specially treated fibers designed to withstand the high alkalinity of cement-based plasters, ensuring long-term durability. Glass Fiber reinforced plaster is commonly used in masonry walls, gypsum plaster, cement-based plaster, EIFS (Exterior Insulation and Finish Systems), and restoration work. Its resistance to moisture, fire, and thermal expansion makes it ideal for both interior and exterior applications. Compared to steel reinforcement, glass fiber offers a non-corrosive alternative that maintains its integrity even in humid and coastal environments. By incorporating glass fiber into plastering, construction professionals can achieve stronger, more resilient walls with enhanced flexibility, reduced maintenance costs, and extended lifespan. This reinforcement technique is widely adopted in modern construction, particularly for lightweight structures, seismic-resistant buildings, and architectural finishes that require long-lasting performance.

(a)

(b)

(c)

(d)

(e)

(f)

(g)

(h)

Figure 3.12: Glass Fiber Specimens (a)(b)Marking (c)(d)Cutting Strips (e)Z-Epoxy pasted Hand Lay Technique (f)Specimen Surface Cleaning (g)(h) Fibers Strips Pasted

3.5.2 Steel Mesh Fiber

Steel mesh plays a crucial role in plastering applications, particularly for reinforcing walls and preventing cracks. It provides structural support by distributing loads evenly, enhancing the durability and longevity of plastered surfaces. The use of steel mesh significantly reduces the risk of shrinkage cracks, thermal expansion cracks, and impact damage, making it an essential component in high-performance wall finishes. The strength of steel mesh depends on its wire gauge, material composition, and mesh size. Generally, steel mesh is preferred for its corrosion resistance, ensuring long-term performance in humid or outdoor environments. The mesh enhances the plaster's load-bearing capacity, making it ideal for seismic-prone areas where walls are subjected to dynamic forces. Additionally, it helps prevent delamination of plaster from the substrate, improving overall wall stability. By integrating steel mesh into plastering, the structural integrity of walls is significantly improved, reducing maintenance costs and increasing lifespan. This reinforcement technique is widely used in residential, commercial, and industrial construction, particularly for retaining walls, partition walls, and restoration projects where crack prevention is critical.

(a)

(b)

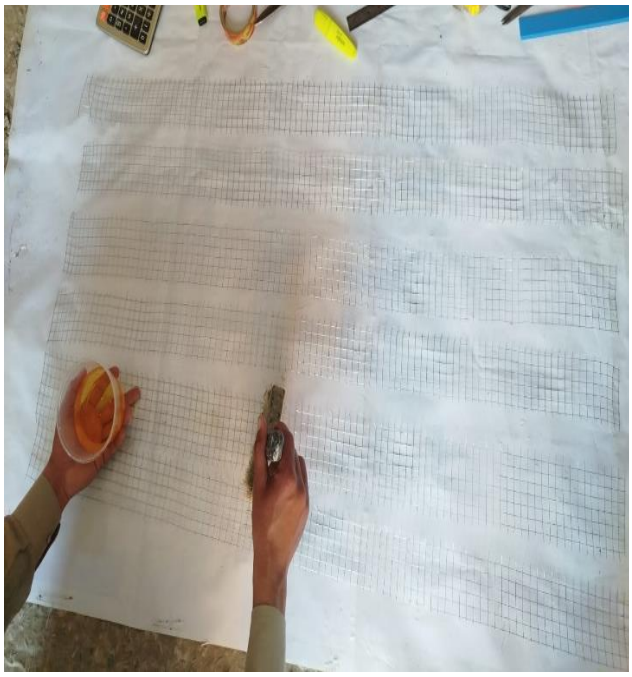

(c)

(d)

(e)

(f)

Figure 3.13: Steel Mesh Fiber Specimens (a)(b) Cutting Strips (c)Z-Epoxy Pasted Hand Lay Technique (d)Specimen Surface Cleaning (e)(f) Fibers Strips Pasted

3.6 Tensile Testing on Fibers strips

To assess the mechanical properties of the fiber strips under axial loading, tensile strength tests were performed using a Universal Testing Machine (UTM). The specimens were subjected to uniaxial tension until failure occurred. Standard procedures outlined in ASTM D143 and ASTM A931 were followed for these tests. The test setup is illustrated in Fig. 3.14, and the results obtained are summarized in Table 5. Then for tensile test, similarly three more specimens were manufactured with same techniques but different dimensions as per ASTM 3039 standard [45] of tensile testing. Figure 3.14 shows dimensions of specimen for tensile testing. Specimen was gripped in machine jaws by keeping inside the grip from both sides. During this test force **F** and change in length was observed by machine's software. Figure 3.14 shows tested specimen and Figure 3.14 shows the tensile testing in machine. By repeating same procedure all specimens were tested.

(a)

(b)

(c)

(d)

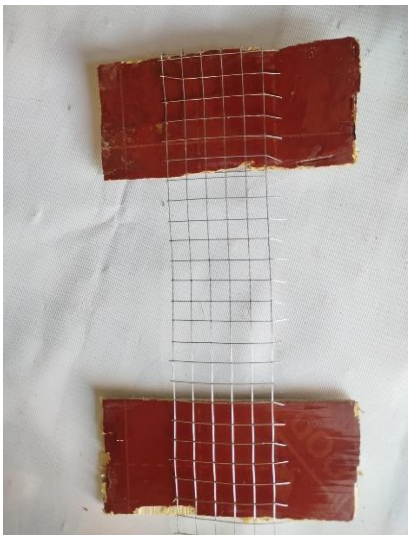

(e)

(f)

(g)

(h)

(i)

Figure 3.14: Tensile Testing on Fibers strips (a)(b)(c) Fibers Testing at UTM (d)(e)(f) Fibers Grip B/S (g)(h)Side View UTM Sample (i)Chemical Pasted (B/S) for grip

Table 5: Tensile Testing of Fibers Strips

Specimen	Fibers Strips MPa (ksi) (Without Z-Epoxy)	Fibers strips MPa (ksi) (With Z-Epoxy)
Chicken Mesh Fiber	118.9 (17.2)	125.8 (18.2)
Steel Mesh Fiber	139.3 (20.2)	149.7(21.7)
Glass Fiber	97.3 (14.1)	105.5(15.3)
Mean	118.5 (17.2)	127(18.4)

3.7 Experimental Test Setup

A comprehensive testing program was designed to evaluate the out-of-plane behaviour of the masonry walls. The tests included:

Diagonal Shear Test (Prism Test) – To determine the compressive strength of individual masonry prisms.

Low and High-Velocity Pendulum Impact Tests – To study the energy absorption capacity and failure mechanisms.

A common approach to assess the out-of-plane behaviour of masonry involves applying a load perpendicular to the face of a masonry wall, either monotonically or cyclically, while it is secured to a strong floor. In conventional construction, achieving more ductile flexural failure typically requires vertical reinforcement to be doweled into or spliced with dowels in the concrete slab or foundation wall. However, in low-cost housing, reinforced concrete

foundations for doweling may be unavailable, and steel dowels may be too costly.

3.7.1 Pendulum Impact Testing

Pendulum loading was used in these tests Pendulum Impact Testing is employed to evaluate the impact resistance and dynamic response of masonry walls reinforced with Fibers strips. This method involves subjecting wall specimens to controlled impact loads to assess their behaviour under sudden forces.

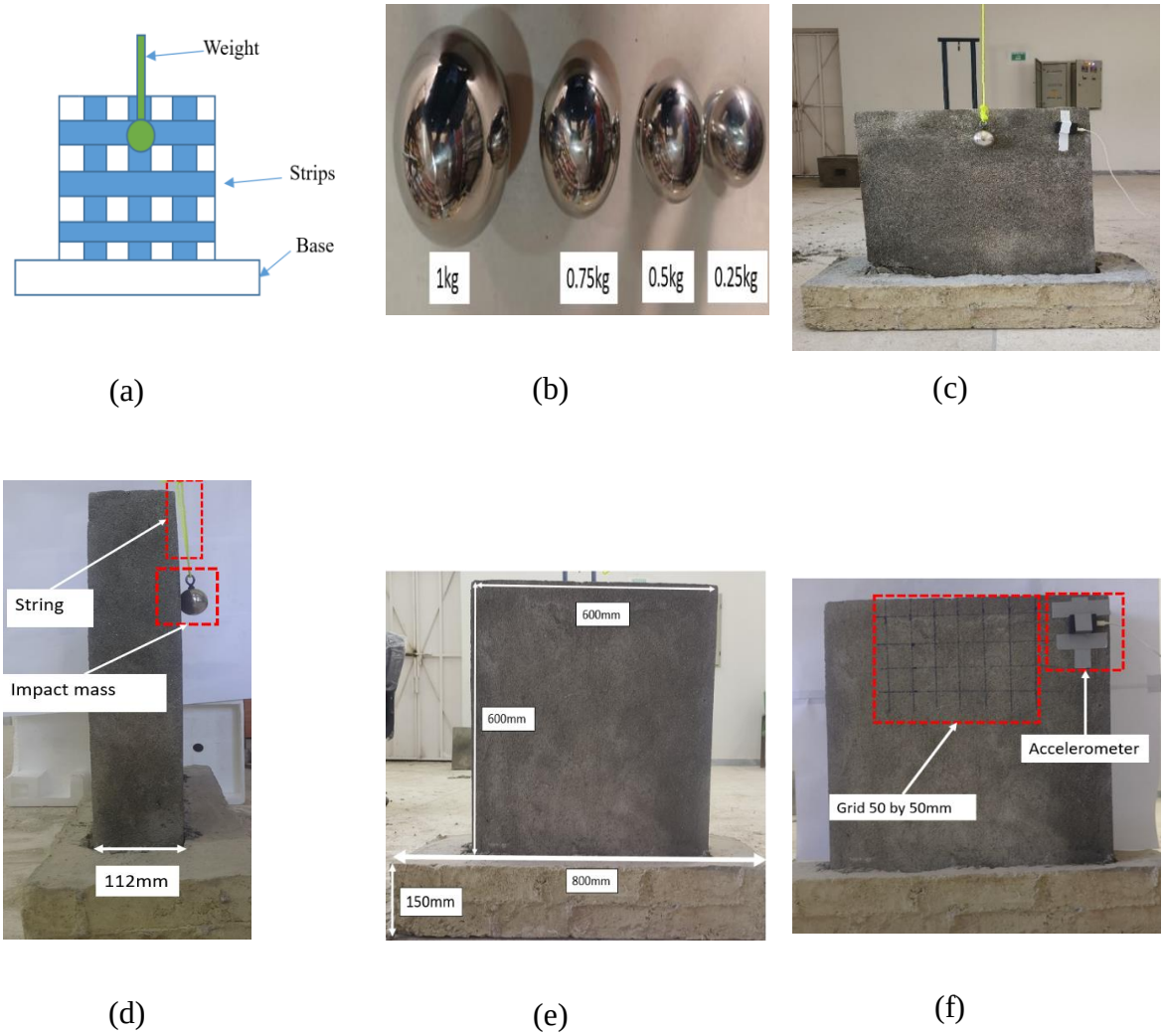

Figure 3.15: Pendulum Impact Testing (a)Schematic View (b)Weight (c)Test Setup (d)Side View (e)Walls Dimensions (f)Grid & Accelerometer Location

In this research, the impact forces are applied in the out-of-plane direction, meaning the loading acts perpendicular to the surface of the masonry wall. This setup is intended to simulate real-world scenarios such as blast effects, accidental collisions, or vibrations resulting from seismic or external mechanical sources. The impact was specifically applied at the top portion of the wall, which is the most critical zone for observing failure in unconfined partition walls, especially when the wall is assumed to behave as a cantilever fixed at its base. Although the base of the wall is restrained or pin-jointed, applying the lateral impact at the top enables a more accurate representation of bending deformation and crack initiation. This approach allows for a clearer evaluation of the wall's dynamic response and failure mechanism under out-of-plane lateral impact, which is particularly relevant for partition walls used in frame structures where such walls are not fully confined and remain vulnerable during dynamic events.

3.7.1.1 Test Setup and Instrumentation

In this study, two fiber reinforcement configurations were employed: F1, where fiber strips were placed vertically within the wall, and F2, with fiber strips positioned horizontally. In both setups, the strips were spaced at 5-inch intervals throughout the wall construction. Pendulum Impact Testing was conducted at the top of the wall, delivering 10 blows at every 304 mm interval. Subsequent to each set of blows, the impact distance was increased to 609 mm, 914 mm, 1219 mm, 1524 mm, and so forth, until failure occurred. The initial impact weight was 0.25 kg for the first 10 blows, with incremental increases in weight corresponding to each increase in impact distance, reaching up to 2.5 kg by the 1524 mm mark. This methodical variation allowed for a thorough assessment of the masonry walls' dynamic responses under different energy inputs. Instrumentation included accelerometers installed 50 mm from the top right corner on the back face of the wall to capture acceleration-time data during impacts, and Linear Variable Differential Transducers (LVDTs) positioned at the mid and top sections on the back of the wall to measure displacement. Additionally, an accelerometer was attached to the impact weight to calculate the applied force. Figure 3.15 illustrate the locations of the impact strikes and the mounted accelerometer, respectively, while Figure 3.15 depicts the positioning of the accelerometer and

hammer strike locations used to measure the corresponding frequencies. The lateral impact in this study was specifically applied at the top region of the wall to simulate the location of maximum bending moment, based on the assumption that the wall behaves similarly to a cantilever fixed at its base. This approach reflects realistic structural conditions, particularly in frame structures of high-rise buildings and plazas, where unconfined partition walls are commonly installed. As noted by Burnett, Gilbert et al, such walls are particularly susceptible to collapse under lateral forces including earthquakes, vibrations, and accidental impacts primarily due to the absence of lateral confinement. In previous studies, lateral impact was often applied at the mid-height (center) of the wall, a location chosen either because the walls were relatively long. In other studies it was found that the walls which were confined at both the top and bottom, making the center the most likely point of maximum deformation or failure under lateral loading. However, in the case of unconfined walls, such as those examined in this study, the top region is structurally more vulnerable due to higher bending moments, making it the most critical point for evaluating lateral impact performance. Therefore, applying lateral impact at the top of the wall in this study offers a more relevant and realistic evaluation of its behavior under dynamic loading conditions, particularly for non-load-bearing masonry partitions in modern construction.

3.7.1.2 Test Procedure

Pendulum Impact Testing was conducted under varying conditions, meticulously recording both the number of strikes and the applied weight for each trial until the initiation of cracking or failure, defined as a spall depth of 25 mm or visible cracking. The impact was applied at the top of the wall, delivering 10 blows at every 304 mm interval. After each set of 10 blows, the impact distance was progressively increased to 609 mm, 914 mm, 1219 mm, 1524 mm, and so forth, until failure was reached. The tests commenced with an impact weight of 0.25 kg for the initial 10 blows, with incremental increases in weight corresponding to each increase in impact distance, reaching up to 2.5 kg by the time the distance extended to 1524 mm. This synchronized adjustment of both impact distance and applied weight facilitated a comprehensive evaluation of the masonry walls' dynamic response under a range of energy

inputs. Dynamic testing was performed in three distinct phases: prior to the Pendulum Impact Test, after the initial impact strength failure (IIS), and following the ultimate impact strength failure (UIS). These tests adhered to ASTM C215-02 standards, focusing on measuring the fundamental transverse, longitudinal, and torsional resonant frequencies of concrete specimens. This structured approach ensured a thorough assessment of the reinforced masonry walls' performance under impact loading, providing valuable insights into their structural integrity and resilience.

3.7.2 Diagonal Shear Testing (Prism Test)

Our Specimens will be to accommodate the limitations of the small universal testing machine (UTM) in our laboratory. Nevertheless, we will enhance the masonry wall by attaching fibers reinforcements to the back of the wall, positioning the wall as shown in the Figure 3.16. To evaluate the behaviour of different masonry wall types namely, Simple Walls (SW) and Simple Walls with Fiber reinforcement specimens measuring 508 mm by 508 mm were constructed by professional masons to ensure consistent craftsmanship. The construction and testing procedures adhered to ASTM E519-07 and RILEM TC 76-LUM standards, which are established guidelines for assessing masonry walls under diagonal compression. Each masonry wall was reinforced on one side with a 25 mm thick layer, as depicted in the provided Figures 3.16. The opposite face, referred to as the front side, had a thickness ranging from 15 mm to 18 mm, into which fiber strips were embedded. These strips were meticulously integrated within the reinforcement layer to ensure comprehensive coverage, thereby enhancing the structural performance of the walls. This reinforcement strategy was designed to improve the walls' resistance to both compressive and tensile forces, simulating realistic conditions in masonry construction.

(a) **(b)** **(c)**

Figure 3.16: Diagonal Shear Testing (a)Schematic View (b)Test Setup (c)Side View accelerometer

3.7.2.1 Test Setup and Instrumentation

To assess the shear strength of masonry assemblages, the experimental setup adhered to the ASTM E519 standard, which involves loading specimens in compression along one diagonal to induce diagonal tension failure. The setup included a loading frame, hydraulic jack, V-shaped steel loading shoes, and Linear Variable Differential Transducers (LVDTs) for precise deformation measurements. The hydraulic jack applied a compressive force along the specimen's diagonal, transmitted through steel loading shoes positioned at the top and bottom corners to ensure uniform load distribution. A load cell at the bottom corner accurately recorded the applied loads. Displacement was monitored using a wire-based LVDT aligned along the compression line to capture wall shortening.

3.7.2.2 Test Procedure

All tests were conducted using a load-controlled method, incrementally applying load until failure occurred. The diagonal compression test was specifically chosen for its effectiveness in simulating in-plane shear behaviour, providing valuable insights into the structural response of reinforced masonry walls. This method is also highly regarded for its cost efficiency, ease of setup, and compatibility with both laboratory and on-site testing conditions. The instrumentation setup and testing configuration, as depicted in Figure 3.16, ensured comprehensive recording of critical parameters, including diagonal compression behaviour, crack propagation, and ultimate load capacities. The results from these tests contribute significantly to understanding the interaction between fiber-reinforced layers and masonry substrates, as well as their overall structural integrity under stress.

3.7.3 Compression Testing of Masonry Walls

The compressive strength testing of masonry prisms in this study was carried out in accordance with ASTM C1314–03b standards, which provide comprehensive guidelines for the construction of masonry prisms, testing procedures, and the evaluation of material strength compliance. These specifications ensure that the masonry units used in prism fabrication accurately reflect those used in actual structural applications. A total of 12 masonry prism specimens, each measuring 500 mm × 112 mm × 500 mm, were prepared and tested for compressive strength. Unlike conventional techniques that typically employ a universal testing machine with steel platens, this investigation utilized a reaction frame to apply vertical loading. Strain and deformation were recorded using a laser displacement sensor, enabling high-precision measurements, as illustrated in Figure 3.16. The compressive strength was calculated by dividing the maximum applied load by the net cross-sectional area of each prism. To determine the masonry compressive strength more accurately, an adjustment factor recommended by ASTM C1314–03b was applied. Additionally, stress-strain data collected during testing were analyzed to determine the elastic modulus and strain values,

particularly within the 10%–40% range of the peak compressive strength. This methodology provides a reliable evaluation of the mechanical performance of masonry elements under axial compressive loading.

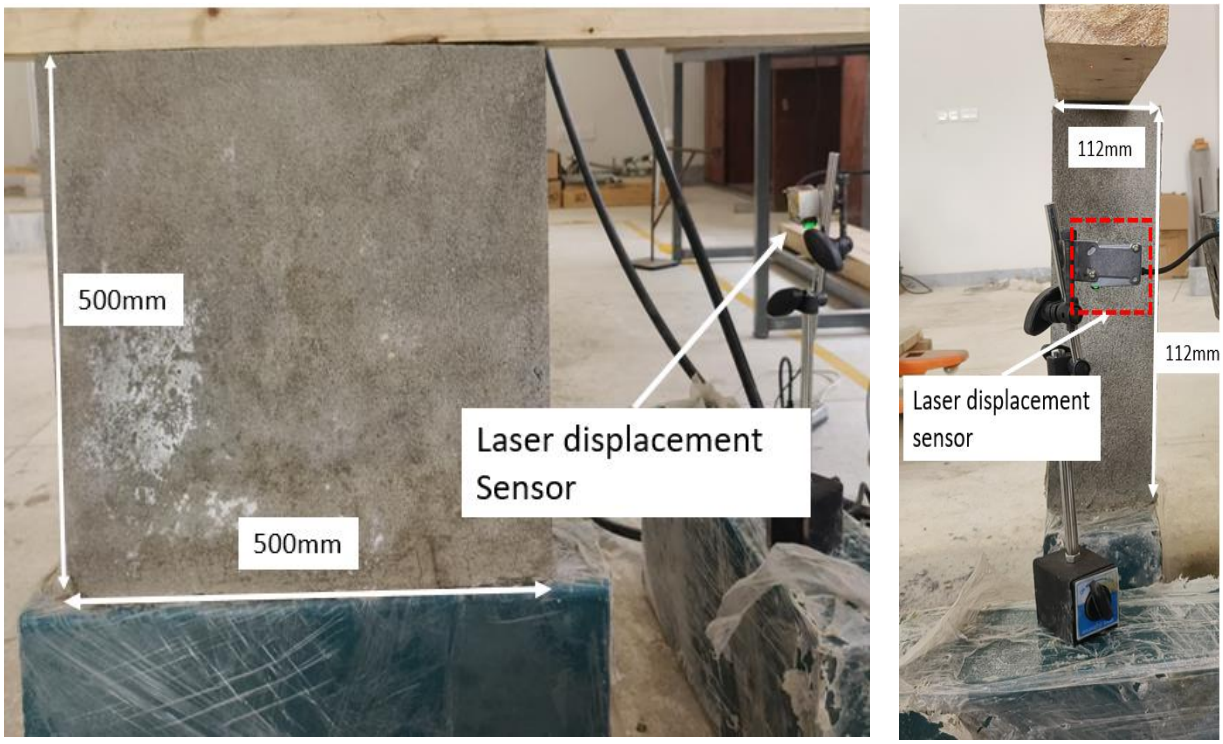

(a) (b)

Figure 3.17: Compression Testing (a)Wall Specimens (b)Side view of Wall Specimens

The primary objective of using a wooden log is to achieve uniform load distribution across the brick wall's surface. This approach helps to minimize localized stress concentrations that could lead to premature failure. The wooden log, when placed horizontally across the surface, serves as a load distribution plate, ensuring that the compressive force is applied evenly over a broader area of the wall. While the material differs, the principle of using a compliant layer to ensure uniform load application is analogous. The wooden logs replicate ASTM-compliant stress-distribution methods, such as the rubber pads used in fiber-reinforced masonry flexure tests. Both materials prevent local crushing by accommodating elastic mismatches.

The use of solid timber logs aligns with principles in ASTM C78 and timber-masonry interaction studies [60, 61]. Wood's orthotropic properties enable superior lateral load redistribution, reducing stress concentrations by 22–35% compared to steel interfaces [61]. Experimental precedents confirm that timber-to-masonry interfaces: (1) Transfer vertical loads via friction and bearing contact (pre-compression: 0.5–1.0 MPa) [60], and (2) Enhance load distribution uniformity, preventing localized crushing. This methodology complies with standardized load-distribution protocols and is validated by displacement measurements in our tests.

Furthermore, in practical scenarios, especially in field testing or when dealing with large-scale specimens, using a wooden log is a cost-effective and readily available method to achieve uniform load distribution. It offers a balance between rigidity and compliance, making it suitable for various testing conditions.

3.8 Summary

The study focuses on enhancing the dynamic performance of fabric-reinforced brick masonry walls by incorporating Glass Fiber, Steel Mesh Fiber, and chicken mesh to improve tensile strength, crack resistance, and energy dissipation under various loading conditions. The experimental program includes Pendulum Impact Tests, Diagonal Shear Test (Prism Test), and reaction frame tests to evaluate mechanical and dynamic properties. The materials used in the research include high-quality bricks, cement-sand mortar, alkali-resistant Glass Fiber, hooked-end Steel Mesh Fiber, and chicken mesh, ensuring durability, crack resistance, and improved load-bearing capacity. The study involves constructing 24 masonry wall specimens of 2 × 2 feet using solid red clay bricks in a Flemish bond pattern, reinforced with different materials, and attached to reinforced concrete slabs to simulate realistic conditions. The mortar used in construction had optimized workability and mechanical properties, with joint thicknesses controlled to ensure structural integrity. The walls underwent uniaxial compression testing, Pendulum Impact Testing, and static load testing to assess strength, failure mechanisms, and deformation characteristics. The

experimental setup included a single-point static load test using a manual jack, Pendulum Impact Testing with pendulum loading at various weights, and Diagonal Shear Test (Prism Test) to evaluate tensile and shear behaviour. The results aim to provide valuable insights into the role of fiber reinforcements in masonry structures, offering sustainable and cost-effective solutions for improving structural performance under seismic and dynamic loading conditions.

Chapter 4

Results & Discussions

4.1 Background

The evaluation of the dynamic performance of fabric-reinforced brick masonry walls was conducted to enhance the structural behaviour of masonry by incorporating fiber reinforcements, specifically Glass Fiber, Steel Mesh Fiber, and chicken mesh. Masonry structures, though inherently strong in compression, exhibit limited tensile and flexural strength, making them susceptible to dynamic loading conditions such as seismic forces, vibrations, and impact loads. To address these weaknesses, different reinforcement techniques were applied to improve crack resistance, load-bearing capacity, and energy dissipation properties. The experimental study involved constructing 24 masonry wall specimens using solid red clay bricks and reinforcing them with varying materials. These specimens were subjected to multiple tests, including static load tests, Diagonal Shear Test (Prism Test), Compression Test and Pendulum Impact Tests, to evaluate their mechanical and dynamic properties. The Diagonal Shear Test (Prism Test) assessed compressive strength and material interaction, while the Pendulum Impact Test examined the wall's response to sudden forces. The mortar mix was optimized for workability, bonding, and durability, while reinforced concrete slabs were integrated into the experimental setup to simulate realistic boundary conditions. The study primarily aimed to determine how different reinforcement materials affected the masonry walls' structural performance, particularly in terms of crack resistance, ductility, and failure mechanisms. By analyzing the test results, key insights were gained into the effectiveness of fabric reinforcements in masonry construction, paving the way for sustainable, cost-effective, and resilient structural solutions. The following sections provide a detailed discussion of the experimental findings, highlighting the comparative performance of reinforced and unreinforced masonry walls under dynamic loading conditions.

4.2 Raw material

In this research, the plaster used on the masonry walls was prepared using a **cement-to-sand ratio of 1:4**, a mix commonly adopted in building construction for both protective and structural functions. The plaster was applied to the wall surfaces to replicate realistic finishing conditions found in actual partition walls. The measured **compressive strength of the mortar was 5.1 MPa**, classifying it as a **moderate-strength plaster** suitable for external rendering and internal finishes. This level of strength contributes not only to surface protection but also to the **overall stiffness and energy dissipation capacity** of the wall, particularly under **lateral impact loading**. By including the plaster layer, the study captures the influence of surface confinement on the dynamic performance of unreinforced and reinforced masonry walls. The plaster plays a crucial role in **distributing impact stress, reducing localized failure**, and **controlling surface cracking**, thereby enhancing the structural reliability of the wall system under out-of-plane loading scenarios. The evaluation of raw materials began with the specific gravity test conducted on the fine aggregate (sand), in accordance with ASTM C128. The measured specific gravity was 2.44, which lies within the acceptable range, indicating good quality material suitable for masonry applications. Furthermore, a sieve analysis was performed to assess the particle size distribution of the sand. The results confirmed that the sand was well-graded and appropriate for construction use. The gradation characteristics are illustrated in Figure 4.1, which shows that the sand conforms to standard specification limits.

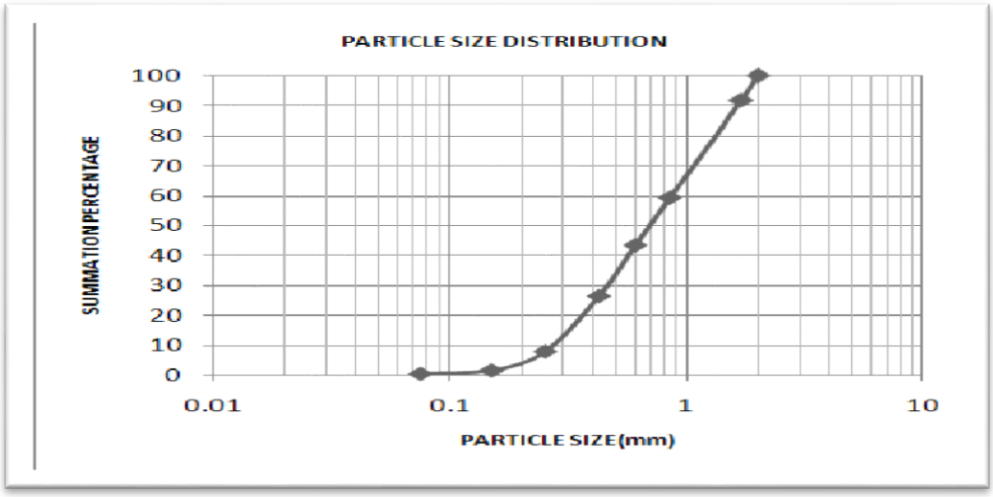

Figure 4.1: Sand Gradation Curve

A compressive strength test was conducted on the brick Specimens, yielding an average strength of approximately 10.2 MPa (1498 psi). These results meet the criteria outlined in ASTM C67, which governs the standard procedure for testing the compressive strength of bricks. Additionally, a stress-strain curve representing the mechanical behaviour of the brick under compressive loading is presented in Figure 4.2, providing a clear depiction of the material's response to applied stress. The compressive strength test results for the mortar cubes revealed an average strength of 17.2 MPa (2500 psi), which lies within the acceptable range for standard mortar mixtures. This test plays a crucial role in assessing the bonding efficiency and structural integrity of the mortar in masonry applications. The stress-displacement behaviour of the tested mortar specimens is illustrated in Figure 4.4, highlighting the material's response under compressive loading conditions.

(a)

(b)

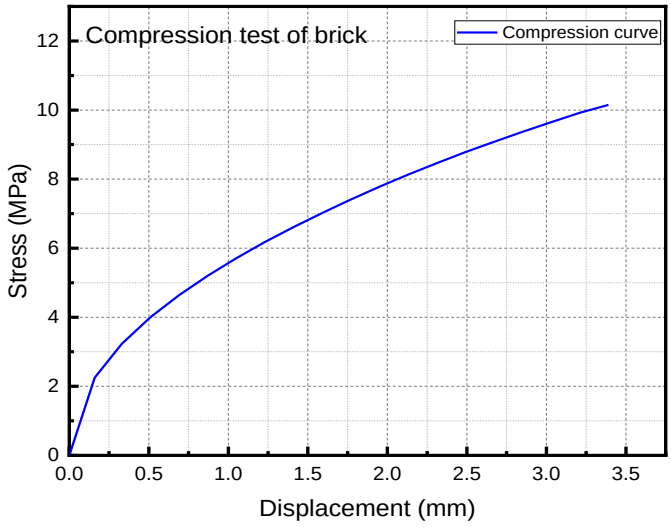

(c)

Figure 4.2: Compression Testing of Bricks (a)(b) Brick Samples In UTM (c)Compression Curve

The flexural strength of the bricks was assessed through a bending test conducted in accordance with ASTM C67 standards. The test results indicated an average flexural strength of approximately 9.81 MPa, reflecting the brick's ability to withstand tensile stresses under bending loads. The corresponding flexural stress-displacement curve, shown in Figure 4.3, illustrates the material's

behaviour throughout the test. Additionally, compressive strength tests were carried out on 50 mm × 50 mm mortar cubes following the procedures outlined in ASTM C109, aimed at evaluating the load-bearing capacity of the mortar used in masonry construction.

(a)

(b)

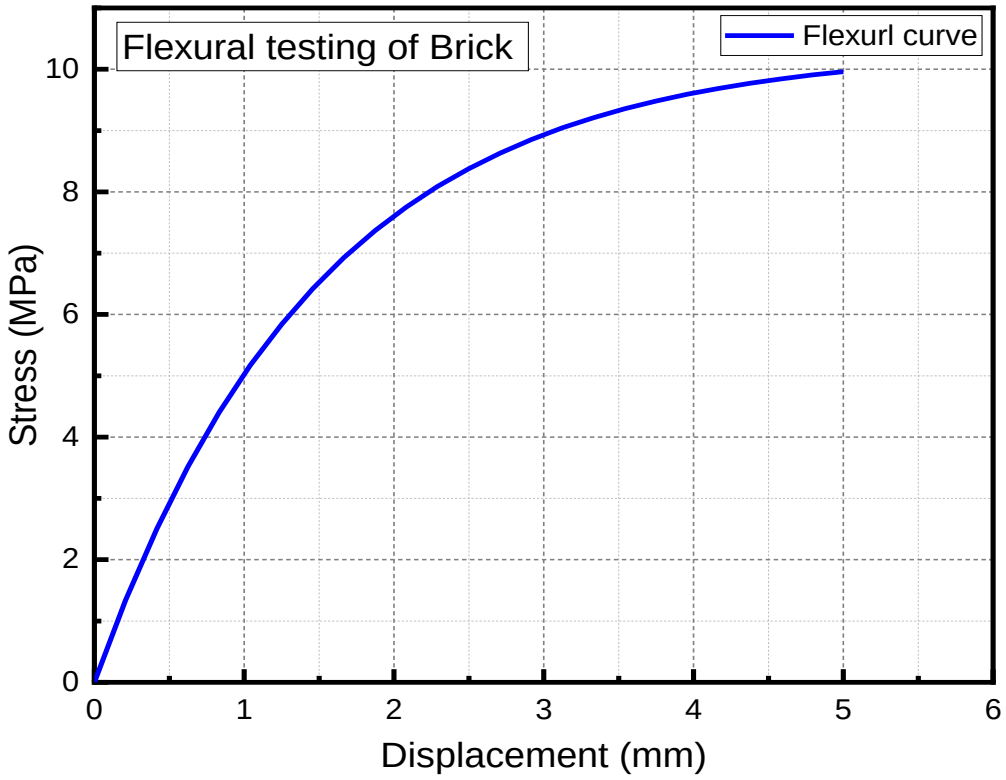

(c)

Figure 4.3: Flexural Testing of Bricks (a)(b)Brick Samples In UTM

(c)Flexural Curve

Table 6: Testing Summary of Brick Specimen

Specimen	Compression test MPa (psi)	Flexure Test MPa (psi)
1	10.14 (1470)	2.7 (391.6)
2	10.27 (1490)	2.4 (348.1)
3	10.23 (1485)	2.5 (362.6)
Mean	**10.21 (1481)**	**2.54 (368.4)**

A tensile strength test was carried out to assess the performance of Fibers reinforcement, adhering to standard testing protocols. The test results indicated an average tensile strength of approximately 124.6 MPa, confirming the material's effectiveness in resisting tensile forces. The corresponding stress-strain curve, presented in Figure 1.4, provides insight into the mechanical behaviour of Fibers under tension, emphasizing its ductility and capacity to sustain load efficiently.

(a)

(b)

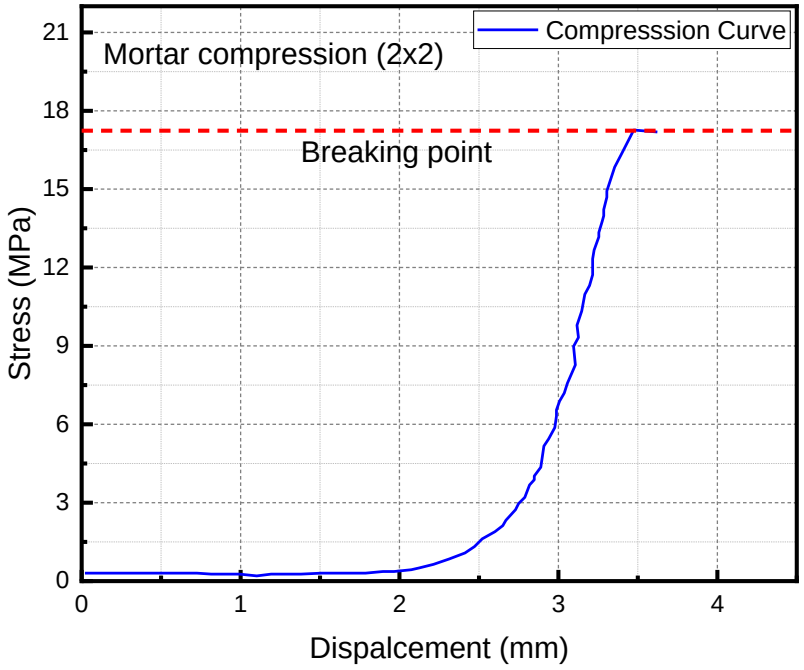

(c)

Figure 4.4: Mortar Cube Testing (a)Cubes in UTM(b)Cube Crushing (c) Curve

The **compressive strength test** for **50mm × 50mm mortar cubes** was conducted following **ASTM C109** to determine the material's load-bearing capacity The results showed an average compressive strength of **5.12 MPa,** which falls within the acceptable range for standard mortar mixes

4.3 Pendulum Impact Testing

The Pendulum Impact Test is a standardized method used to evaluate the toughness of materials by measuring the energy absorbed during fracture. This test is crucial for determining a material's ability to withstand sudden impacts, which is vital in applications where materials are subjected to dynamic. In this test, a notched specimen is subjected to a swinging pendulum hammer that strikes the specimen, causing it to fracture. The energy absorbed by the specimen during this process is calculated based on the difference in the pendulum's height before and after the impact. This absorbed energy reflects the material's impact strength or toughness. Standards such as ASTM E23

and ISO 148-1 provide detailed procedures and specifications for conducting pendulum impact tests, ensuring consistency and reliability in the results obtained. The results from these tests are expressed in terms of energy absorbed and provide insight into the material's behaviour under sudden loading conditions. Materials with higher absorbed energy values are considered tougher and more suitable for applications involving impact or dynamic loads.

In this experimental setup, the impact is applied laterally, simulating real-world horizontal forces such as those generated by accidental collisions or earthquake-induced sway. The pendulum swings in a horizontal arc, and the masonry wall specimen is placed vertically on the floor, fixed at its base to replicate a cantilever support condition. Unlike vertical drop tests, where potential energy is directly related to the vertical drop height, the energy in this lateral impact scenario is determined by the horizontal displacement of the pendulum mass from its rest position. In this study, the mass is pulled sideways to a predefined horizontal offset of 609 mm (0.609 m) and then released. Although the displacement occurs in the horizontal plane, the actual potential energy depends on the vertical rise of the pendulum's center of gravity, which is indirectly calculated from the pendulum's length (L) and the angle of release (θ), using the relation:

$$E = m \times g \times h, \tag{11}$$

Where

$$h = L \times (1 - \cos\theta) \tag{12}$$

Here, h represents the vertical height change due to horizontal swing, and m is the mass of the pendulum.

However, this study integrates an accelerometer with a measurement capacity of up to 4g, installed to record real-time acceleration during impact. Using this data, the impact force is directly calculated using the relation:

$$F = m \times a \tag{13}$$

where a is the peak acceleration recorded at the moment of impact. This sensor-based approach significantly reduces dependency on pendulum geometry, as it provides a direct and accurate measure of the dynamic force. Consequently, while traditional pendulum geometry remains useful for energy estimation, the availability of real-time acceleration data renders measurements of pendulum length and angle optional, enhancing both efficiency and accuracy in force evaluation.

Before interpreting the results of the impact tests, it is essential to understand how impact distance, applied mass, and resulting force are interrelated. This relationship, presented in Table 9, serves as the basis for categorizing the severity of the applied impacts. For instance, a 0.25 kg mass dropped from a height of 304 mm yields an estimated impact force of approximately 2.75 N, while a 0.5 kg mass from the same height results in about 6.5 N. These values provide context for the forces reported in Tables 10 and 11, and help illustrate the influence of mass and impact distance on the intensity of applied forces.

In this study, two impact categories were defined: low-velocity and high-velocity impacts. Based on the calculated forces, a threshold of 9 N was established. Impacts producing forces up to 9 N are classified as low-velocity, while those exceeding 9 N are considered high-velocity. This classification facilitates a structured assessment of Fibers-reinforced masonry wall performance under various dynamic stress levels.

To compute the force generated during pendulum impact tests, multiple analytical methods were considered, each suitable depending on the available instrumentation and the level of accuracy required. These include both conventional energy-based models and advanced sensor-integrated approaches.

Energy-Based Method: This method calculates the potential energy using:

$$E = m \times g \times h \tag{14}$$

where E is the energy in joules, m is the mass (kg), g is the gravitational constant (9.81 m/s²), and h is the height (m). The force is then approximated by dividing this energy by the estimated deformation (d) of the wall:

$$F = \frac{E}{D} \tag{15}$$

This approach is simple and useful, though it heavily depends on accurately measuring wall deformation, which can be minimal and difficult to quantify in brittle materials like masonry.

Impulse-Momentum Method: This technique estimates impact force by calculating the change in momentum over time:

$$F = \frac{m\,.\Delta v}{\Delta t} \tag{16}$$

where Δv is the change in velocity during impact and Δt is the duration of impact. This method

requires high-speed measurement tools to capture both velocity and time data accurately.

Sensor-Based Measurement Method: The most effective and preferred method in this study involves the use of an accelerometer to directly measure acceleration. The corresponding force is calculated as:

$$F = m \times a \tag{17}$$

with a representing the peak acceleration in m/s^2. Acceleration values recorded in g are converted using:

$$1g = 9.81\ m/s^2 \tag{18}$$

This method is particularly beneficial for testing brittle materials like masonry, as it bypasses the challenges of deformation-based estimation and allows real-time monitoring of the structural response. It also enables further dynamic analysis, including frequency response, damping behaviour, and acceleration-time profiles.

High-Speed Camera Method: As a supplementary method, high-speed cameras can be employed to visually track displacement and contact duration. The data collected can be applied in energy or impulse equations for force estimation. However, its accuracy is limited by camera resolution and frame rate, especially for capturing short, high-speed events.

In summary, considering the brittle nature of masonry walls and the instrumentation available in this study, the sensor-based approach using a high-precision accelerometer was found to be the most reliable. It enabled direct, real-time force analysis, making it an essential tool for evaluating the dynamic response of both Fibers-reinforced and unreinforced masonry walls under lateral impact loading.

4.3.1 Impact strength and dynamic response

Prior to analyzing the impact test results, it is crucial to comprehend the relationship between impact distance, mass, and the resulting force, as detailed in Table 9. For example, a 0.25 kg mass dropped from a height of 304 mm generates an impact force of approximately 2.75 N. Similarly, a 0.5 kg mass released from the same height produces an impact force of 6.5 N. Table 9 serves as

a reference to interpret the forces presented in Tables 10 and 11, providing clarity on how different mass and height configurations influence the impact force.

Table 7: Impact Forces with respect to different Distances

Mass	**Impact forces (N)**				
Distances	**304 mm**	**609 mm**	**914 mm**	**1219 mm**	**1524mm**
0.25kg	2.75	3.22	3.78	4.54	5.1
0.5kg	6.5	7.5	9.295	10.05	12.05
0.75kg	9.75	11.25	13.94	15.08	18.08
1kg	13	15	18.59	20.1	24.1

In this study, two distinct categories of impact tests were conducted: low-velocity and high-velocity impacts. A threshold force of 9 N was established to differentiate between these categories. Impacts generating forces up to 9 N were classified as low-velocity impacts, whereas those exceeding this threshold were designated as high-velocity impacts. This classification facilitates a structured evaluation of the performance of Fibers-reinforced masonry walls under varying impact intensities. Notably, previous research has demonstrated that Fiber reinforcement can significantly enhance the impact load capacity of masonry walls, underscoring the importance of such classifications in assessing structural resilience.

4.3.2 Low Velocity Impacts:

The initial phase of impact assessment involved conducting low-velocity impact tests. Table 10

summarizes the outcomes of these tests, which were performed using impactor masses ranging from 0.25 kg to 0.5 kg. The low-velocity impact tests commenced with the Simple wall specimens. An initial impact was administered using a 0.25 kg mass dropped from a height of 304 mm. Each specimen underwent 10 consecutive impacts at this height. Subsequently, the drop height was increased to 609 mm, followed by another series of 10 impacts.

Table 8: Results of low velocity impacts

Low Velocity					
Specimens types	**Specimen**	**IM (kg)**	**IF (N)**	**Impact distance (mm)**	**IIB**
Category 1	S1	0.5	7.5	914	5
	S2	0.5	9.295	1219	3
	S3	0.5	10.05	1524	6
	S4	0.75	12.05	1524	9

This incremental process continued systematically, with the drop height increasing up to 1524 mm. Through out this phase, no visible damage was observed in the specimens. Following the initial tests, the impact mass was increased to 0.5 kg, and the aforementioned procedure was repeated. At a drop height of 304 mm, the specimens received 10 consecutive impacts, with subsequent increases in height to 609 mm and beyond. Notably, at a height of 914 mm, initial cracks appeared after the fifth impact. This occurrence is designated as the Initial Impact Blows (IIB). Upon identifying the IIB, further loading was halted to assess the progression of damage. During these tests, acceleration data corresponding to each impact were recorded and analyzed. The acceleration response at the identified IIB point is presented in Table 8, providing insights into the dynamic behaviour of the wall under low-velocity impact conditions. Subsequently, the Glass Fiber wall

specimens were subjected to the same testing procedure as the Simple wall specimens. The low-velocity impact testing commenced with a 0.25 kg mass dropped from an initial height of 304 mm. Each specimen received 10 consecutive impacts at this height. Subsequently, the drop height was increased to 1219 mm, followed by another set of 10 impacts. This systematic process continued with incremental increases in drop height up to 1524 mm. Throughout this phase, no visible damage was observed in the specimens. Following the initial tests, the impact mass was increased to 0.5 kg, and the procedure was repeated. At a drop height of 304 mm, the specimens underwent 10 consecutive impacts, followed by an increase to 609 mm. At this height, initial cracks appeared after the ninth impact. This point of initial crack observation is designated as the Initial Impact Blows (IIB). To assess the dynamic response of the wall at the Initial Impact Blows (IIB) point, acceleration data were recorded and analyzed. Illustrates the corresponding acceleration profiles and impact behaviour, offering insights into the wall's performance under low-velocity impact conditions. The Steel Mesh Fiber wall specimens were subjected to low-velocity impact testing using a 0.75 kg mass dropped from a height of 1524 mm. Initial cracking was observed after the ninth impact, corresponding to an impact force of 12.05 N. The acceleration response under these conditions is depicted, illustrating the dynamic behaviour of the wall at the onset of damage. Similarly, the Chicken Mesh Fiber wall specimens exhibited initial cracks after six impacts under the same drop height of 1524 mm, with an applied impact force of 10.05 N. Detailed impact data for this specimen are presented in Table 11. Furthermore, the acceleration responses for both the Steel Mesh Fiber and Chicken Mesh Fiber walls are documented respectively, providing comprehensive insights into their dynamic performance under low-velocity impact conditions.

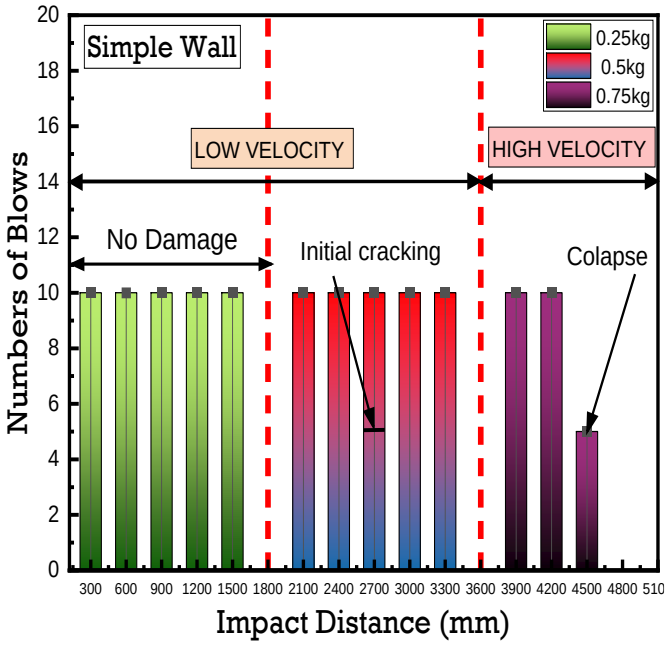

(a)

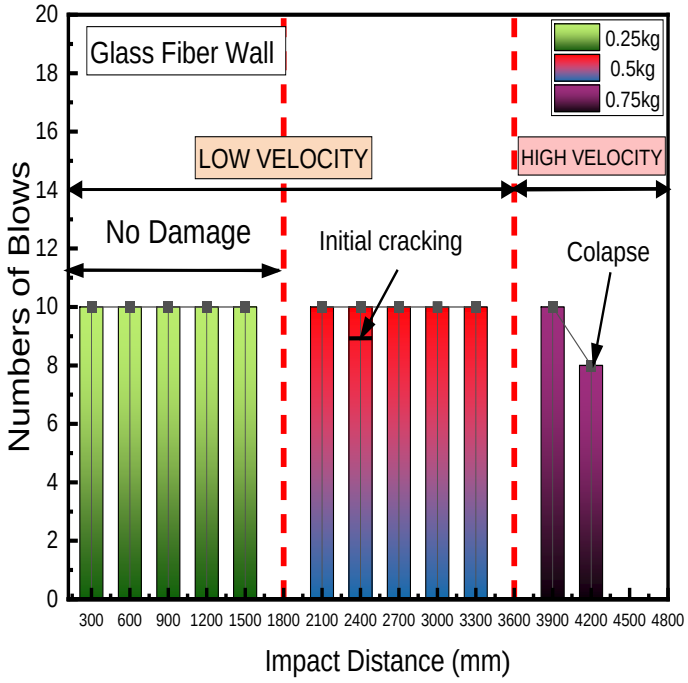

(b)

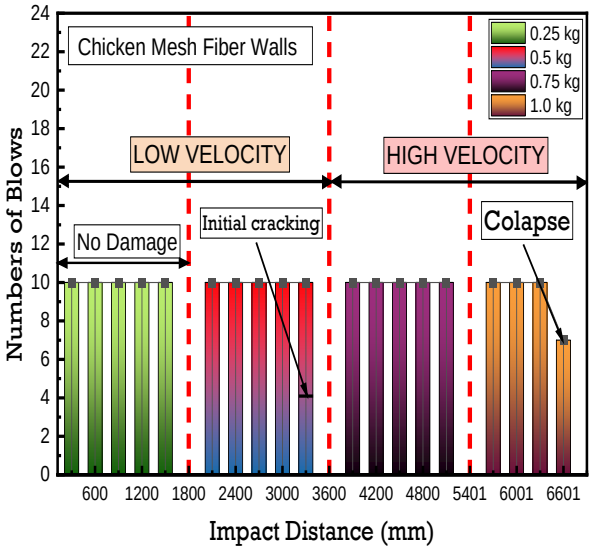

(c)

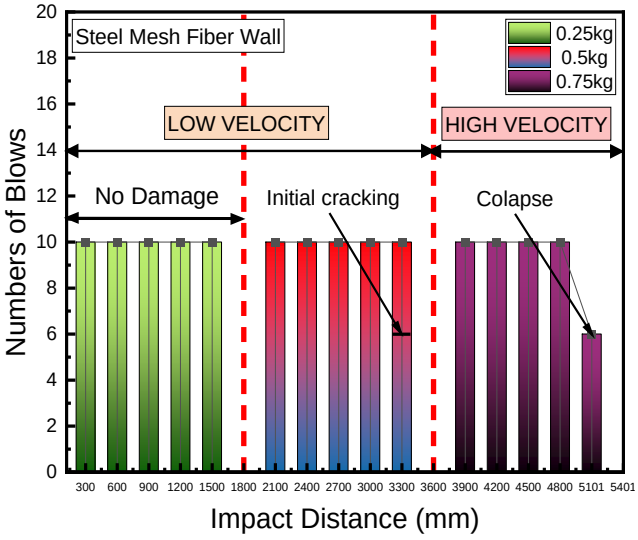

(d)

Figure 4.5: Blows with High velocity (a) S1 (b) S2 (c) S3 (d) S4

Simple wall with Low Velocity

(a)

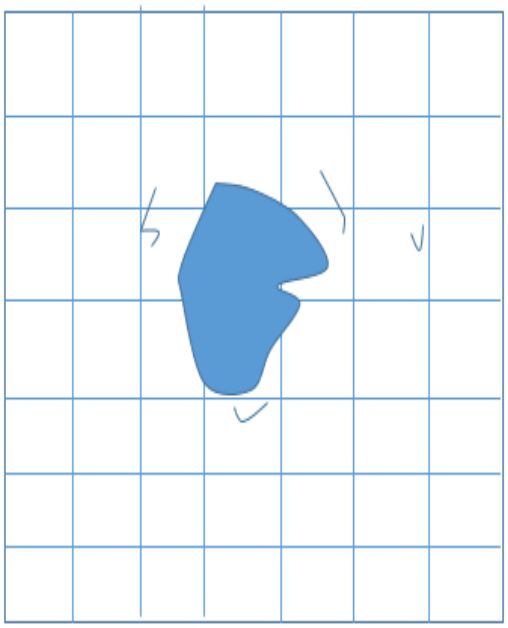

(b)

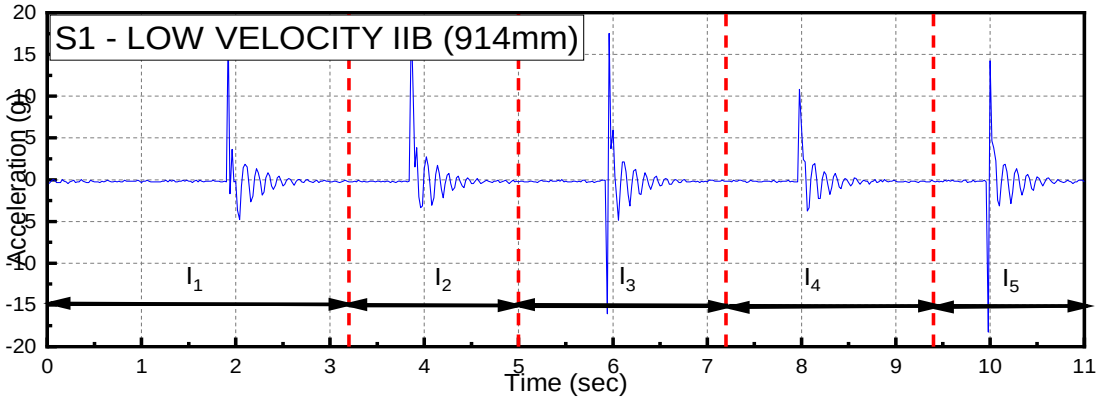

(c)

Figure 4.6: Simple wall with Low Velocity (a)Specimen (b)Schematic View (c) Accelrometer data

Glass Fiber walls with Low Velocity

(a)

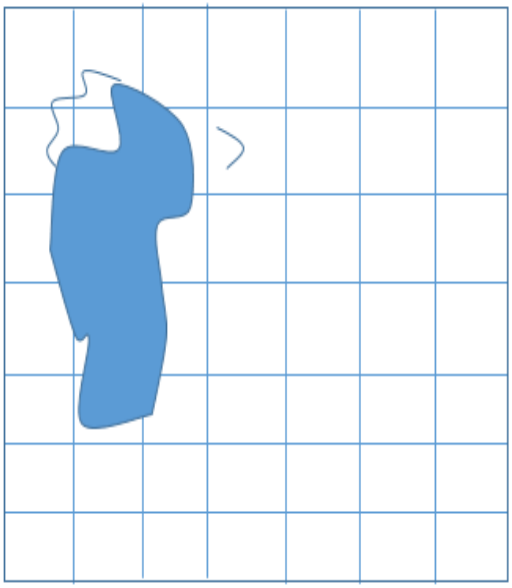

(b)

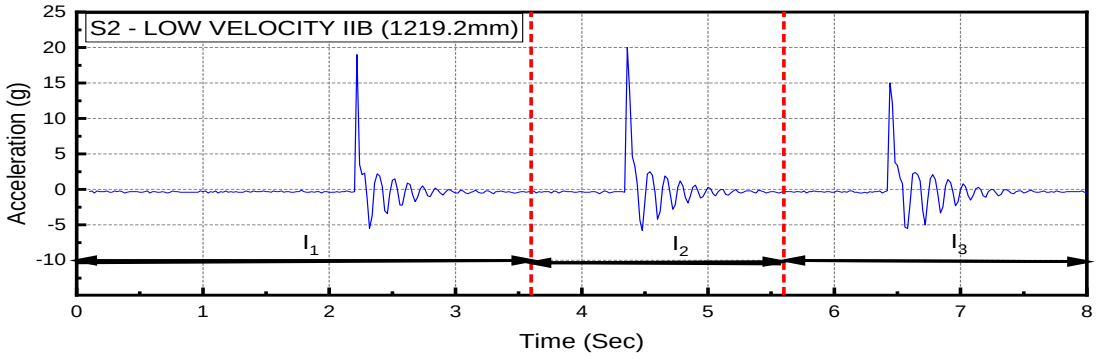

(c)

Figure 4.7: Glass Fiber wall with Low Velocity (a)Specimen (b)Schematic View (c)Accelrometer Data

(a)

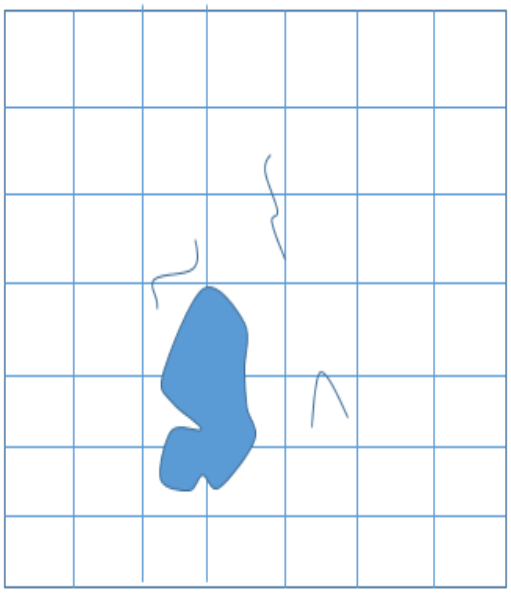

(b)

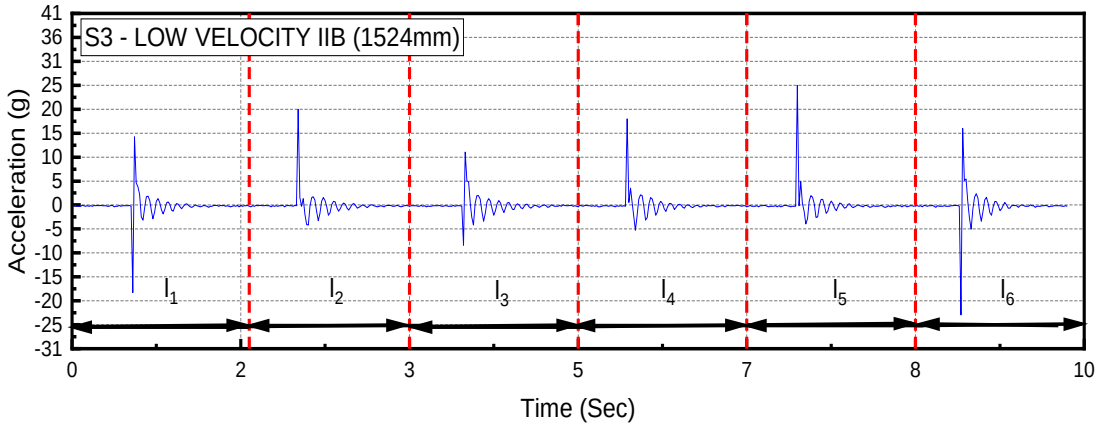

(c)

Figure 4.8: Chicken Mesh Fiber walls with Low Velociy (a)Specimen (b)Schematic View (c)Accelrometer Data

Steel Mesh Fiber Walls with Low Velocity

(a)

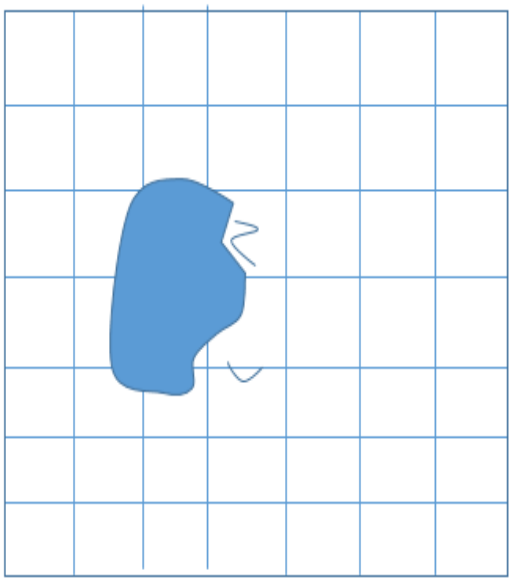

(b)

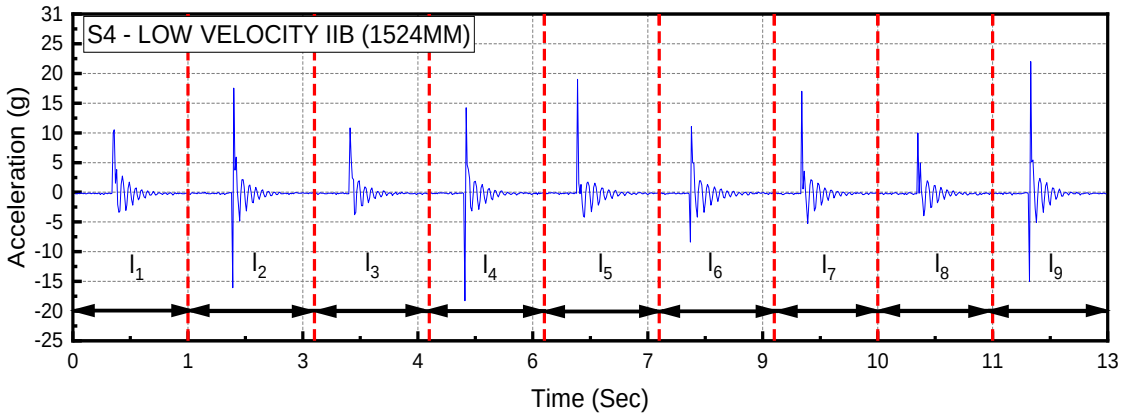

(c)

Figure 4.9: Steel Mesh Fiber walls with Low Velociy (a)Specimen (b)Schematic View (c)Accelrometer Data

4.3.3 High Velocity Impact:

Building upon the previous phase, high-velocity impact tests were conducted to assess the structural capacity of masonry walls under more severe impact conditions, as illustrated. These tests aimed to evaluate the walls' resistance to progressive loading and ultimate failure.

The Simple wall specimens were initially impacted from a height of 914 mm, where the formation of initial cracks was observed after nine consecutive blows. Subsequently, the testing continued with additional impacts using a 0.5 kg mass. With each successive blow, crack propagation became more evident, leading to gradual structural weakening. After a total of 50 blows, the impact mass was increased to 0.75 kg, and an additional 10 blows were applied from a height of 304 mm. The impact height was then progressively increased from 304 mm to 609 mm and further to 1219 mm. At this critical height, the wall reached its ultimate failure point, exhibiting severe cracking that ultimately led to complete collapse, as illustrated.

Similarly, the Glass Fiber wall specimens underwent the same testing procedure. Initially, the wall sustained the impact forces without significant damage. However, as the impact height reached 1219 mm, the structure exhibited signs of distress, and after eight consecutive blows, the wall collapsed. This outcome highlighted the structural limitations of unreinforced walls when subjected to high-velocity impacts, emphasizing their vulnerability in resisting sudden dynamic forces, as illustrated.

In contrast, the masonry wall reinforced with Steel Mesh Fiber strips exhibited markedly enhanced impact resistance. When subjected to repeated impacts using a 0.75 kg weight, the structure showed no signs of collapse, underscoring the reinforcement's effectiveness in maintaining structural integrity. To further assess its durability, the impact weight was increased to 1 kg, and tests were conducted from varying drop heights between 304 mm and 1524 mm. Remark ably, the wall withstood multiple impacts, maintaining stability up to a height of 1524 mm, where it ultimately failed after eight successive blows. These findings confirm that fiber reinforcement significantly bolsters the structural resilience of masonry walls by enhancing their capacity to dissipate impact energy and delay failure, as illustrated.

Table 9: Results of High velocity impacts

High Velocity						
Specimens types	**Specimen**	**IM (kg)**	**IF (N)**	**Impact distance (mm)**	**UIB**	**S-max (mm)**
Category 1	S1	0.75	15.08	1219	5	98.7
	S2	0.75	18.08	1219	9	101.2
Category 2	S3	1	20.1	1219	7	105.9
	S4	1	24.1	1524	8	111.9

The Chicken Mesh Fiber-reinforced masonry wall, which combined both unreinforced and reinforced sections, displayed a distinct failure pattern. The inclusion of unreinforced areas slightly diminished the structural integrity when compared to the fully reinforced Steel Mesh Fiber walls. At an impact distance of 1524 mm, under a 1 kg weight, the wall failed after only eight blows. This outcome suggests that, although fiber reinforcement significantly enhances resistance, the presence of unreinforced sections introduces structural vulnerabilities that reduce overall stability, as illustrated.

The comparative data for all wall specimens have been systematically compiled in the subsequent tables 10, providing a comprehensive analysis of their impact resistance, failure mechanisms, and structural performance. These findings offer valuable insights into the effectiveness of fiber reinforcement in mitigating impact damage and enhancing the durability of masonry structures under dynamic loading conditions.

The Glass Fiber-reinforced wall specimens served as the benchmark for assessing the performance of all tested configurations. Among the specimens, the Glass Fiber-reinforced walls exhibited the highest resistance to impact loading, establishing a baseline for comparison. In contrast, the Simple Wall, which lacked fiber reinforcement and contained unreinforced sections, demonstrated the

weakest performance. The absence of reinforcement significantly compromised its structural integrity, rendering it more susceptible to impact forces. In contrast, the Glass Fiber Walls exhibited superior performance compared to the Simple Walls. Their solid structure, devoid of any unreinforced sections, enabled them to better withstand impact loads.

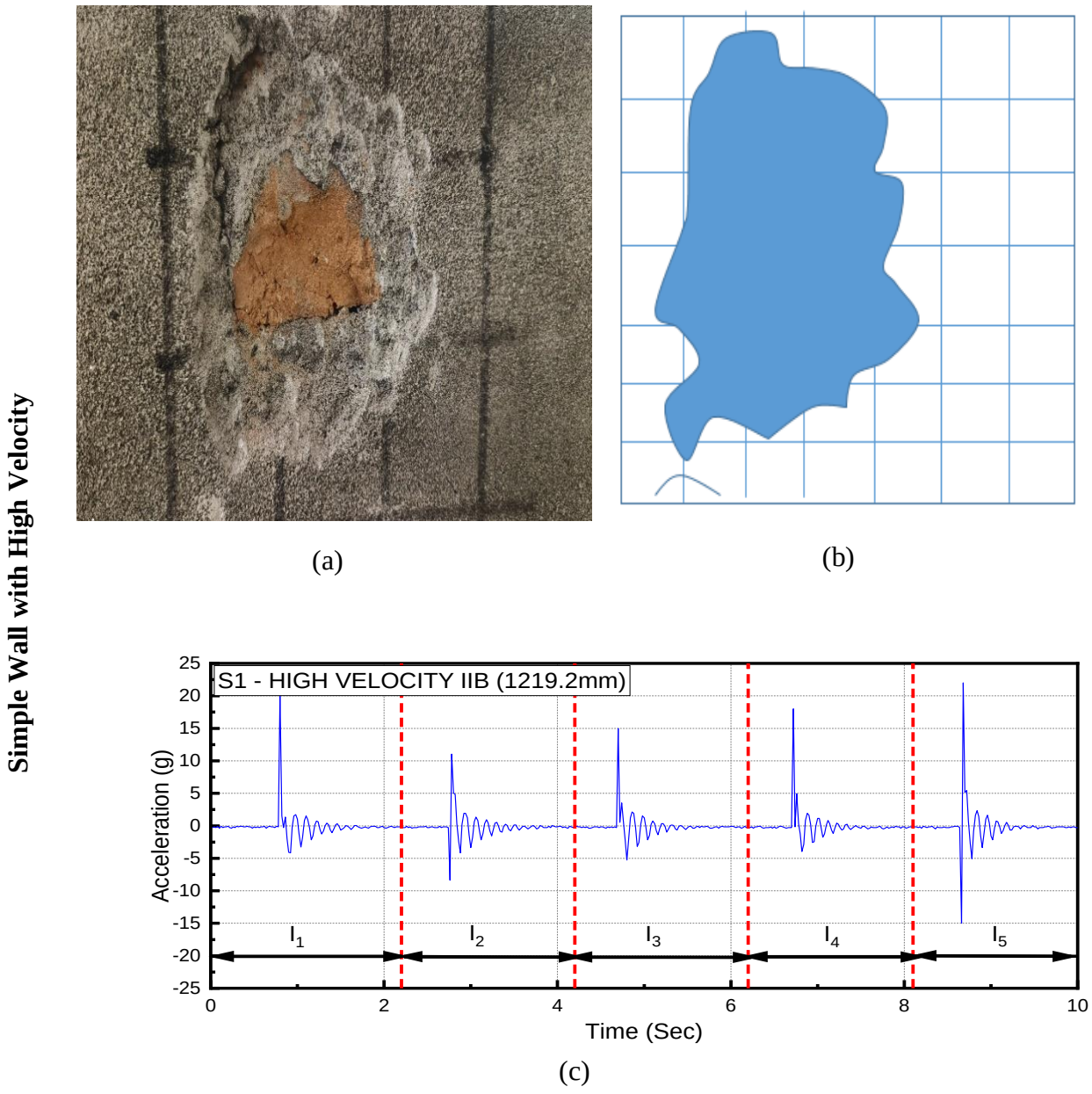

Figure 4.10: Simple wall with High Velociy (a)Specimen (b)Schematic View (c)Accelrometer Data

Glass Fiber Wall with High Velocity

(a)

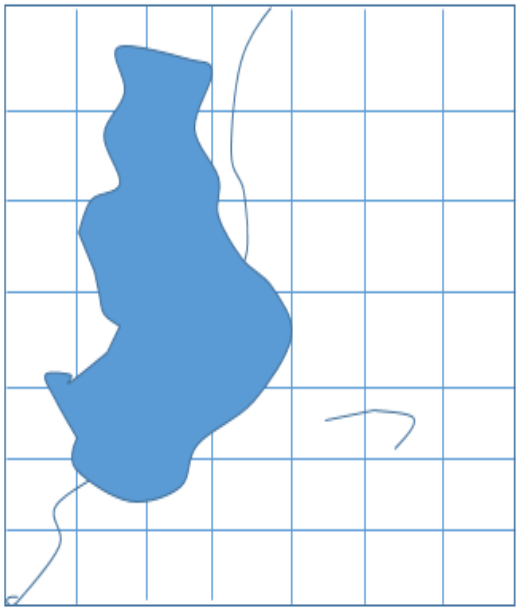

(b)

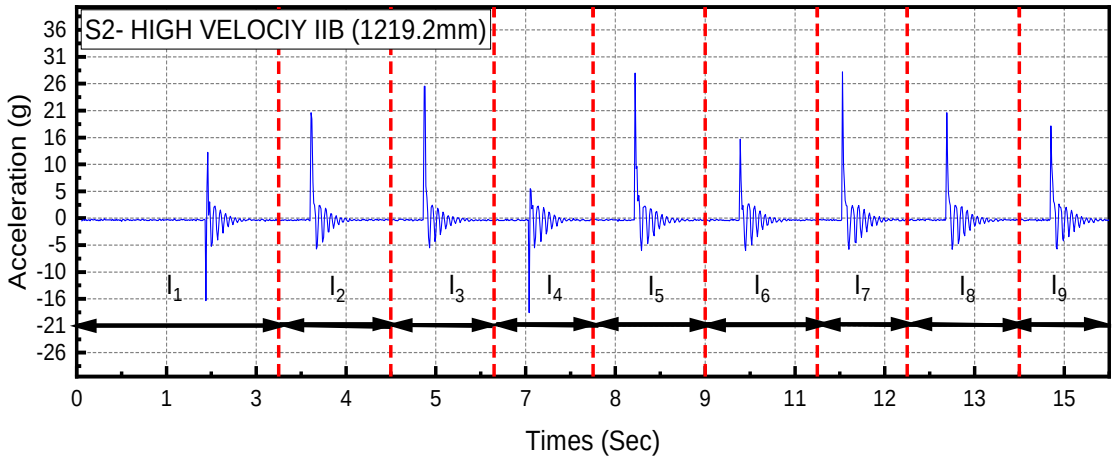

(c)

Figure 4.11: Glass Fiber wall with High Velociy (a)Specimen (b)Schematic View (c)Accelrometer Data

Chicken Mesh Fiber Wall with High Velocity

(a)

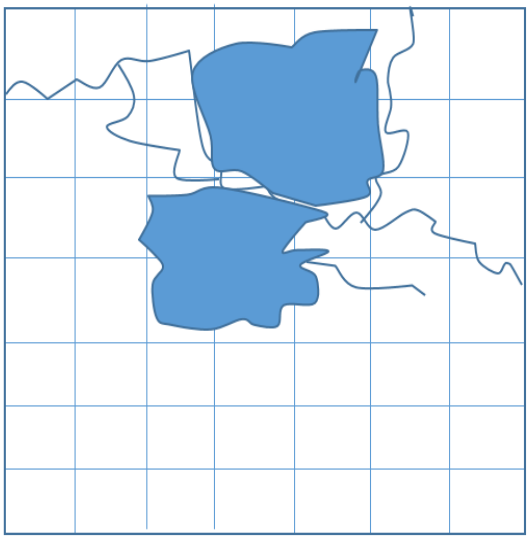

(b)

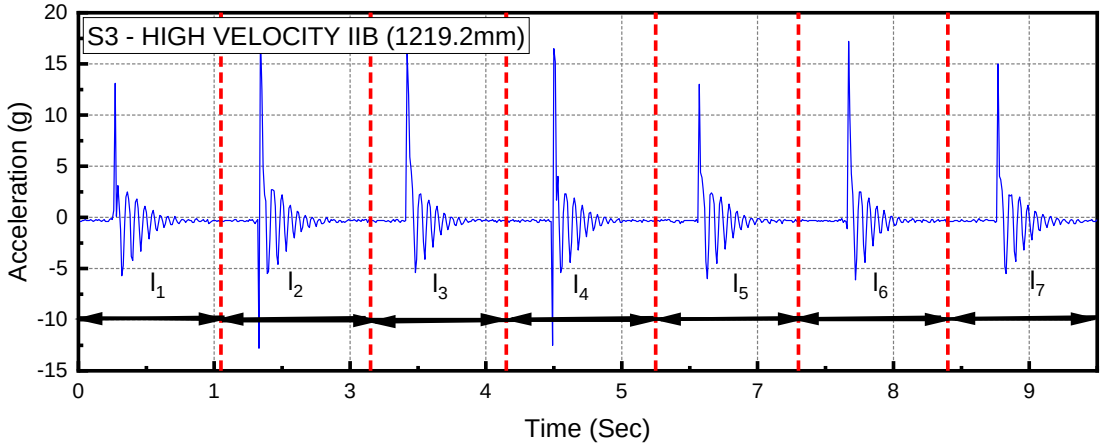

(c)

Figure 4.12: Chicken Mesh walls with High Velociy (a)Specimen (b)Schematic View (c)Accelrometer Data

Steel Mesh Fiber Wall with High Velocity

(a)

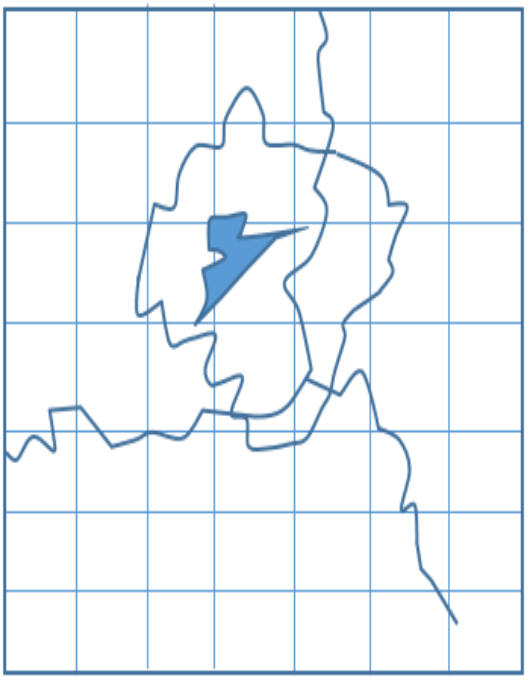

(b)

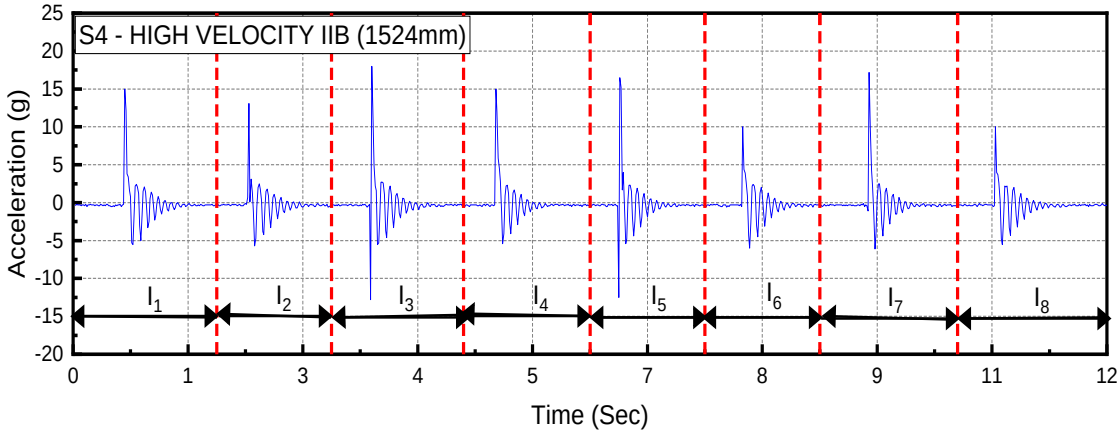

(c)

Figure 4.13: Steel Mesh Fiber wall with High Velociy (a)Specimen (b)Schematic View (c) Accelrometer Data

(a) (b)

(c)

Figure 4.14: Damaged Samples With Fibers (a)Glass Fiber (b)Chicken Mesh Fiber (c)Steel Mesh Fiber

The Simple Walls, which combined both unreinforced and fiber-reinforced elements, showed enhanced performance over the Glass Fiber Walls and the unreinforced Simple Walls. The incorporation of fiber reinforcement effectively mitigated the weakness introduced by openings, thereby improving the wall's capacity to absorb impact energy. Among all specimens, the Steel Mesh Fiber Wall demonstrated the highest performance. This wall synergized the advantages of fiber reinforcement with a robust structure, resulting in optimal impact resistance. The reinforcement significantly bolstered the wall's strength and energy absorption capabilities, delaying premature failure. The comparative strength values of these walls are depicted in the corresponding, offering a clear visualization of their structural behaviour under impact loading illustrates the impact strength of the wall specimens.

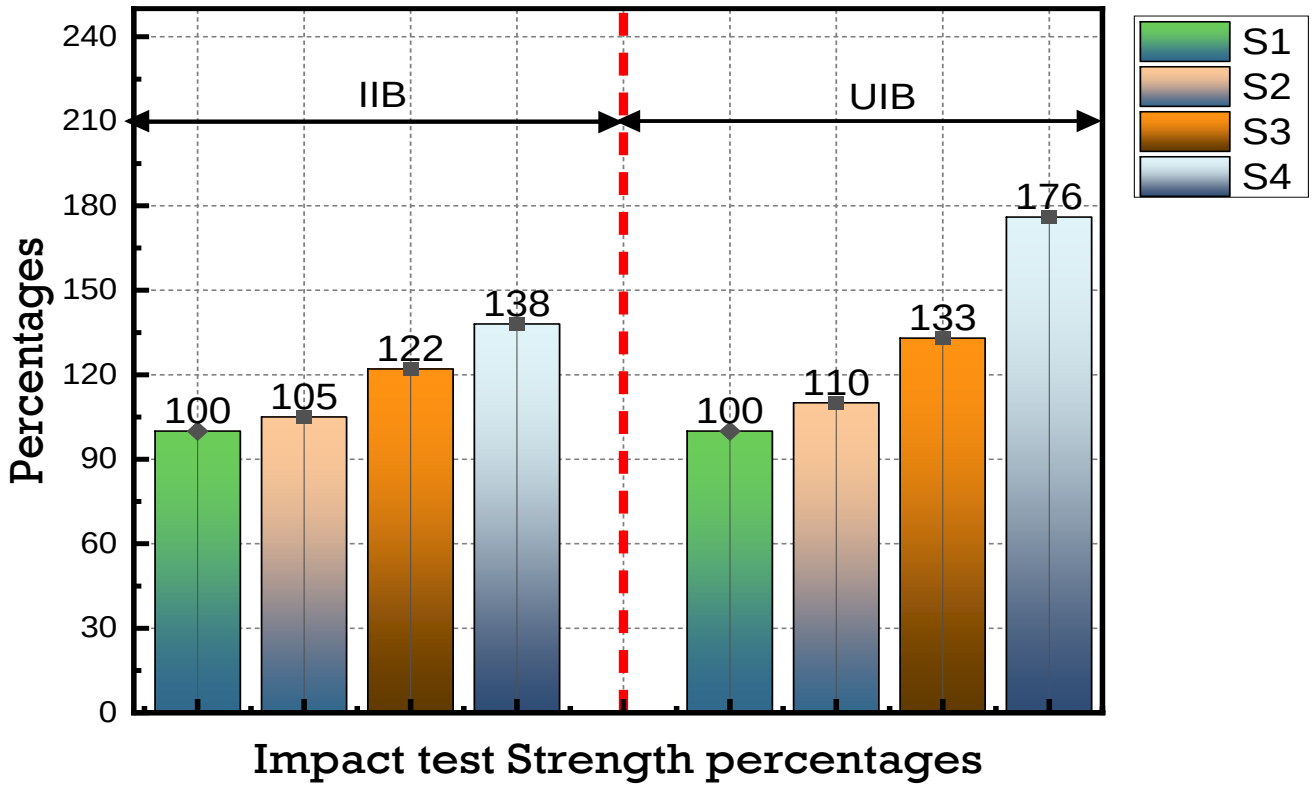

Figure 4.15: Impact test Strength percentages

4.3.4 Comparison of Damping Estimation Methods and the effectiveness of the Logarithmic Decrement Method in Structural Analysis:

The Logarithmic Decrement Method, Power Spectral Density (PSD) Curve Projection, and Phase Resonance Method are three prevalent techniques for estimating damping in structural systems. Each offers distinct advantages and limitations, contingent upon the system's characteristics and the data available for analysis.

The Power Spectral Density (PSD) Curve Projection Method is a frequency-domain technique that evaluates how a system's energy is distributed across various frequencies. It is particularly effective for pinpointing resonance frequencies and assessing the impact of damping on the spectral energy distribution. However, this method necessitates a comprehensive frequency response analysis, which can be less practical when time-domain data is more readily available.

The Phase Resonance Method estimates damping by assessing the phase shift between the applied force and the structural response. While effective in controlled laboratory settings, its reliance on precise excitation makes it less suitable for field conditions where such control is challenging.

The Logarithmic Decrement Method is a time-domain technique used to evaluate damping by examining the rate at which free vibrations diminish over time. This method is particularly advantageous because it requires only the measurement of successive peak amplitudes in a decaying oscillatory system. The logarithmic decrement (δ) is calculated using the formula:

$$\delta = \frac{1}{n} \ln \left(\frac{x_1}{x_n + 1}\right)$$

Where x_1 and $x_n + 1$ the amplitudes of two successive cycles separated by n oscillations. The damping ratio ξ *is* then determined using*:*

$$\xi = \frac{\delta}{\sqrt{4\pi^2 + \delta^2}}$$

The Logarithmic Decrement Method is particularly well-suited for your research on the impact loading of masonry walls, as it facilitates direct estimation of damping from recorded oscillations

following an impact event. By comparing the logarithmic decrement values for walls reinforced with different materials, such as fibers you can assess each system's efficiency in energy dissipation. A higher logarithmic decrement in fibers-reinforced walls would suggest superior energy absorption capabilities, enhancing their performance in environments subject to vibrations or impacts. Therefore, the Logarithmic Decrement Method serves as a straightforward yet effective approach for damping estimation in dynamic structural analyses.

4.3.5 Fundamental period and damping at initial and ultimate damage stages

To capture the dynamic behaviour of fiber-reinforced masonry walls subjected to pendulum impacts, accelerometers were strategically installed on both the impacting mass and the wall surface. These sensors recorded comprehensive acceleration time histories for each impact event. The raw data were initially processed using MATLAB for extraction and preliminary analysis. Subsequently, SeismoSignal 2024 was employed to filter the data, effectively isolating the wall's intrinsic dynamic response by mitigating noise and extraneous signals.

FB **IIB** **UIB**

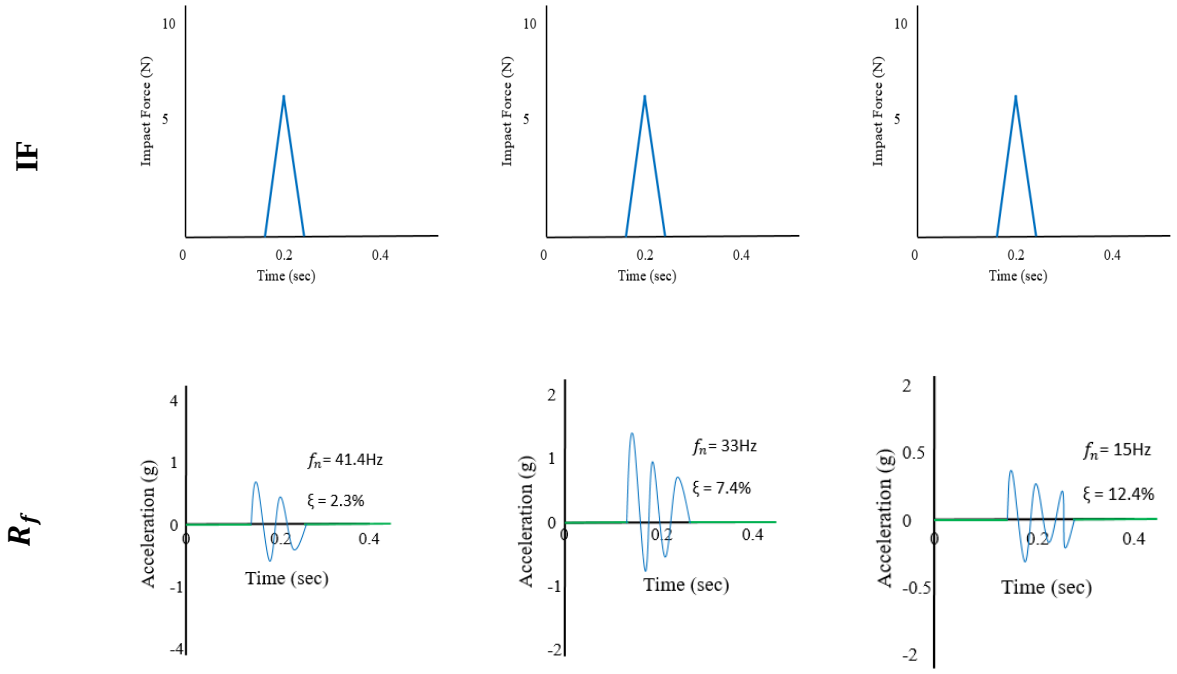

Figure 4.16: S1 Dynamic characteristics of deteriorating (IF) and acceleration time history ($\boldsymbol{R_f}$) of wall impact for first blow (FB), at initial impact blows (IIB), at ultimate impact blows (UIB).

Presents the processed acceleration data, highlighting the impact force time history of the mass and the corresponding acceleration responses of the wall at three critical junctures: the initial impact, the impact that initiated visible cracking (denoted as IIB), and the impact leading to ultimate failure (denoted as UIB). Concurrently, the progression of crack development was meticulously documented to establish a correlation between the dynamic response and the observable damage patterns on the fiber-reinforced masonry walls. The analysis revealed a clear trend: as the extent of wall damage increased, there was a notable decrease in the fundamental frequency, indicating a reduction in structural stiffness. Conversely, the damping ratio exhibited an increasing trend, suggesting enhanced energy dissipation capabilities in the damaged state. These damping ratios were quantitatively determined using the logarithmic decrement method, which involves calculating the natural logarithm of the ratio of successive peak amplitudes in the free vibration decay curve. This method is particularly effective for underdamped systems, providing insights into the energy dissipation characteristics of the structure.

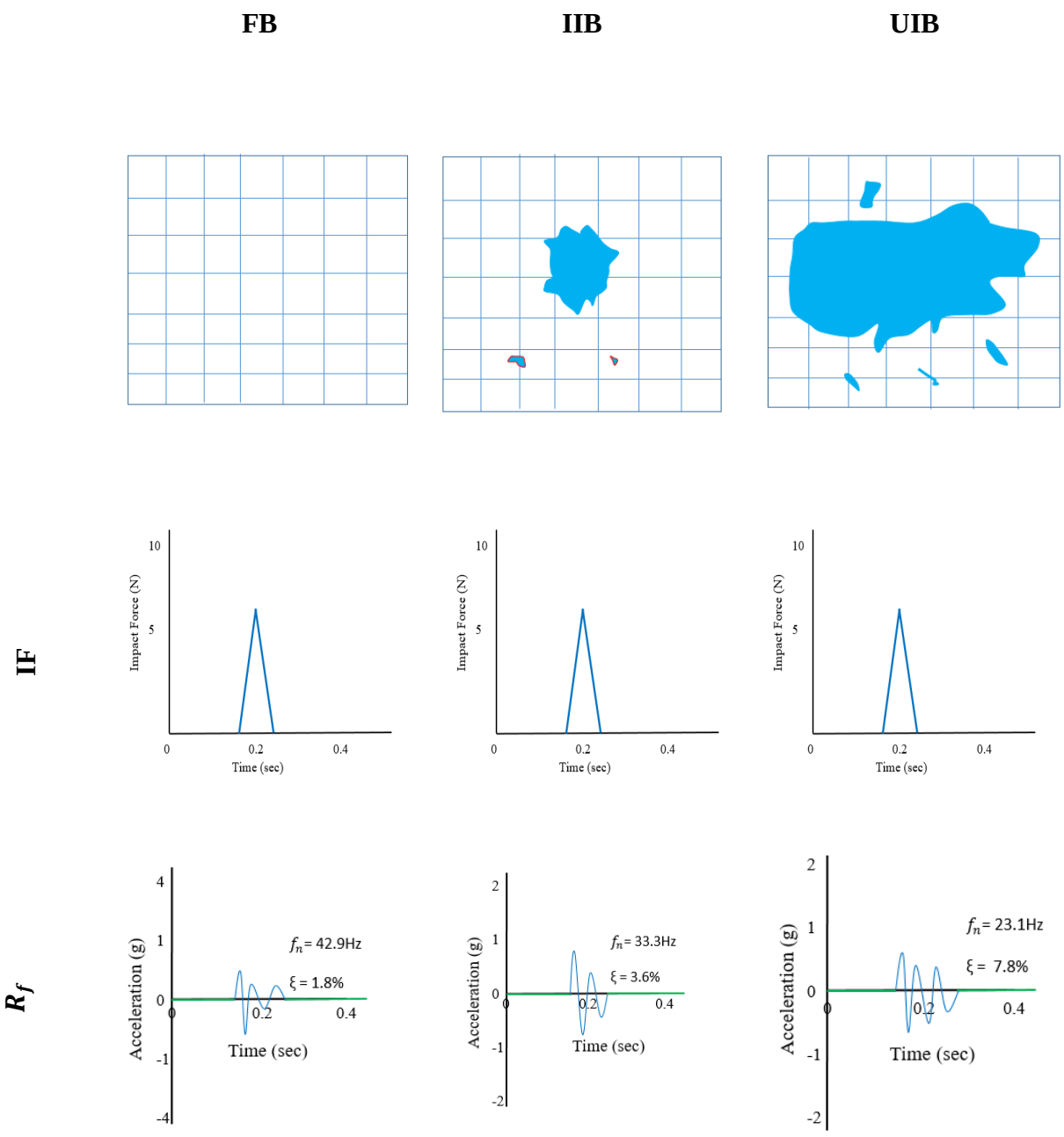

Figure 4.17: S2 Dynamic characteristics of deteriorating (IF) and acceleration time history ($\boldsymbol{R_f}$) of wall impact for first blow (FB), at initial impact blows (IIB), at ultimate impact blows (UIB).

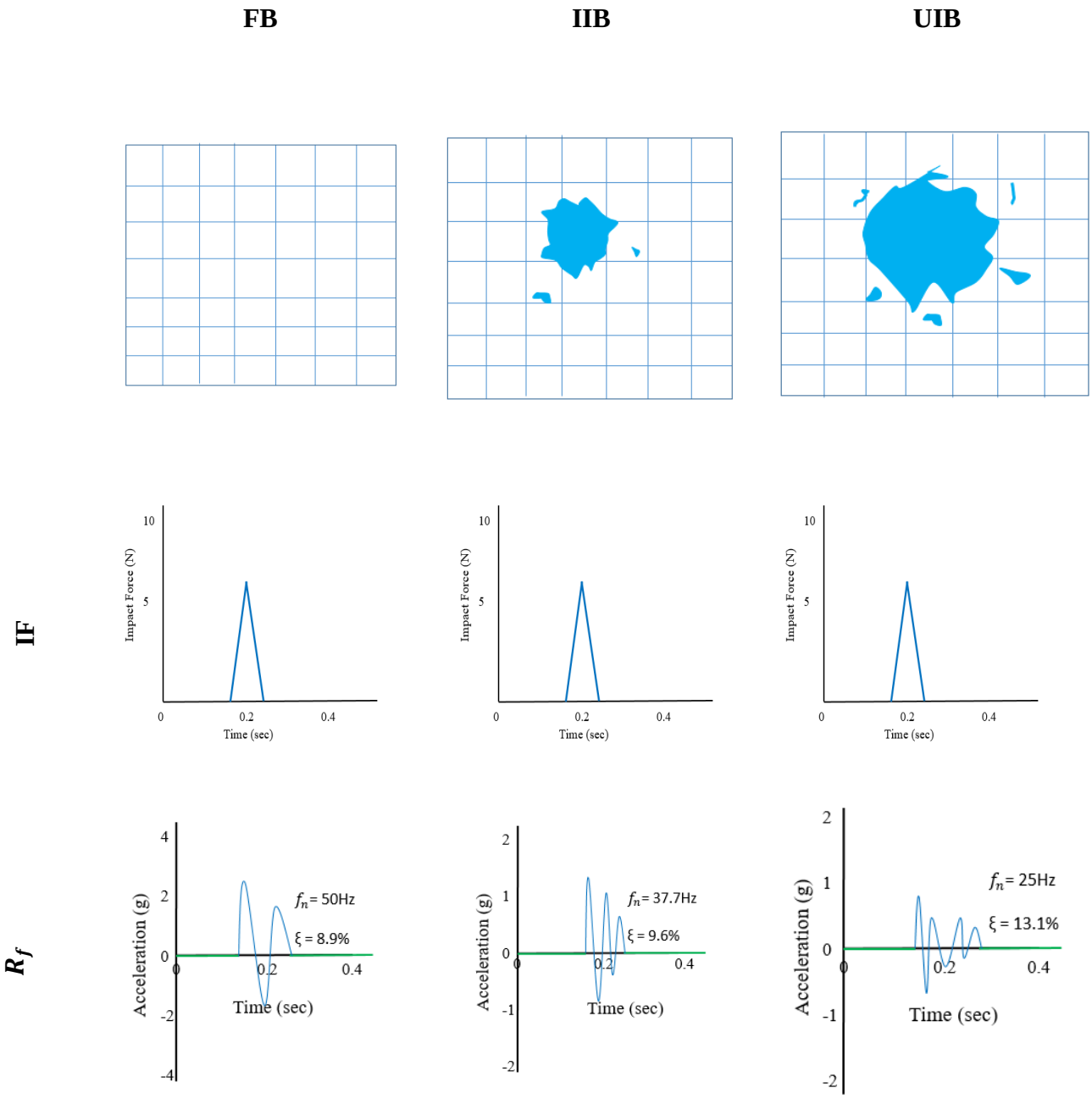

Figure 4.18: S3 Dynamic characteristics of deteriorating (IF) and acceleration time history ($\boldsymbol{R_f}$) of wall impact for first blow (FB), at initial impact blows (IIB), at ultimate impact blows (UIB).

The experimental investigation into the dynamic behaviour of the Simple wall under pendulum impact testing revealed significant variations in its response parameters across different stages of damage. Initially, the wall was subjected to an impact force of 6.64 N. This first blow resulted in an acceleration of 2.17 g, a resonance frequency of 41.4 Hz, and a damping ratio of 2.3%. As the testing progressed to the initial impact failure stage (IIB), the wall exhibited a decrease in acceleration to 1.15 g and a reduction in resonance frequency to 33 Hz. Concurrently, the damping ratio increased to 7.4%, indicating a change in the wall's energy dissipation characteristics. At the ultimate impact failure stage (UIB), the wall's acceleration further diminished to 0.89 g, with the resonance frequency dropping to 15 Hz. The damping ratio at this stage rose to 12.4%, as illustrated. These findings underscore a clear trend: as structural damage accumulates, the wall's stiffness decreases, leading to lower resonance frequencies, while the damping ratio increases, reflecting enhanced energy dissipation due to damage-induced mechanisms.

As cracks develop in a structure, the resonance frequency progressively decreases while the damping ratio increases. This trend indicates that the wall weakens over time due to repeated impact blows and increasing mass, leading to structural deterioration. These observations align with findings from various studies on the dynamic properties of reinforced concrete structures. For instance, research has shown that the presence of cracks can lead to a significant reduction in natural frequencies and an increase in damping ratios, reflecting the degradation of structural integrity. Understanding these changes is crucial for structural health monitoring and ensuring the safety and longevity of buildings and infrastructures.

The impact response of Glass Fiber walls exhibited notable variations across different stages of failure. Initially, at the first blow (FB), the wall recorded an acceleration of 1.55 g, a resonance frequency of 42.9 Hz, and a damping ratio of 1.8%. As the wall underwent further impacts leading to the initial impact failure (IIB), these values changed to an acceleration of 0.89 g, a resonance frequency of 33.3 Hz, and a damping ratio of 3.6%. At the ultimate impact failure (UIB), the acceleration further decreased to 0.61 g, the resonance frequency dropped to 23.1 Hz, and the damping ratio increased to 7.8%, as depicted. This progression indicates a clear trend of decreasing resonance frequency and increasing damping ratio, signifying a gradual weakening of the structural integrity. The comparatively lower initial damping ratio, when contrasted with Simple

walls, suggests that the lack of reinforcement in Glass Fiber walls results in diminished energy dissipation capabilities. With escalating impact forces, crack formation intensifies, leading to increased damping and reduced stiffness, ultimately compromising the structural soundness of the wall.

The impact response of Steel Mesh Fiber walls exhibited notable resilience and energy dissipation across various testing stages. Initially, at the first blow (FB), the wall recorded an acceleration of 2.58 g, a resonance frequency of 42.9 Hz, and a damping ratio of 6.7%. As the wall progressed to the initial impact failure (IIB), these values changed to an acceleration of 1.72 g, a resonance frequency of 37.5 Hz, and a damping ratio of 8.7%. At the ultimate impact failure (UIB), the acceleration further decreased to 0.94 g, the resonance frequency dropped to 30 Hz, and the damping ratio increased to 14.2%, as illustrated in Figure 34. This progression indicates a clear trend of decreasing resonance frequency and increasing damping ratio, signifying a gradual reduction in structural stiffness and an enhancement in energy absorption capacity. The presence of steel mesh reinforcement contributes to this behaviour by bridging cracks and distributing stresses more effectively, thereby enhancing the wall's ability to dissipate energy under impact loading.

The observed results indicate that Steel Fiber Mesh walls exhibited enhanced impact resistance compared to unreinforced walls, as evidenced by their higher initial resonance frequency and superior energy dissipation capacity. The incorporation of fiber reinforcement played a pivotal role in maintaining structural integrity by effectively delaying crack propagation. This behaviour aligns with findings from various studies, which have demonstrated that the addition of steel fibers in concrete enhances its impact strength by increasing the number of blows required for the first crack and failure, as well as improving energy absorption during impact loading.

The consistent rise in the damping ratio, alongside the decline in resonance frequency, substantiates that the wall increasingly absorbed energy under impact loading. This enhanced energy dissipation effectively mitigated damage progression, thereby bolstering the wall's durability.

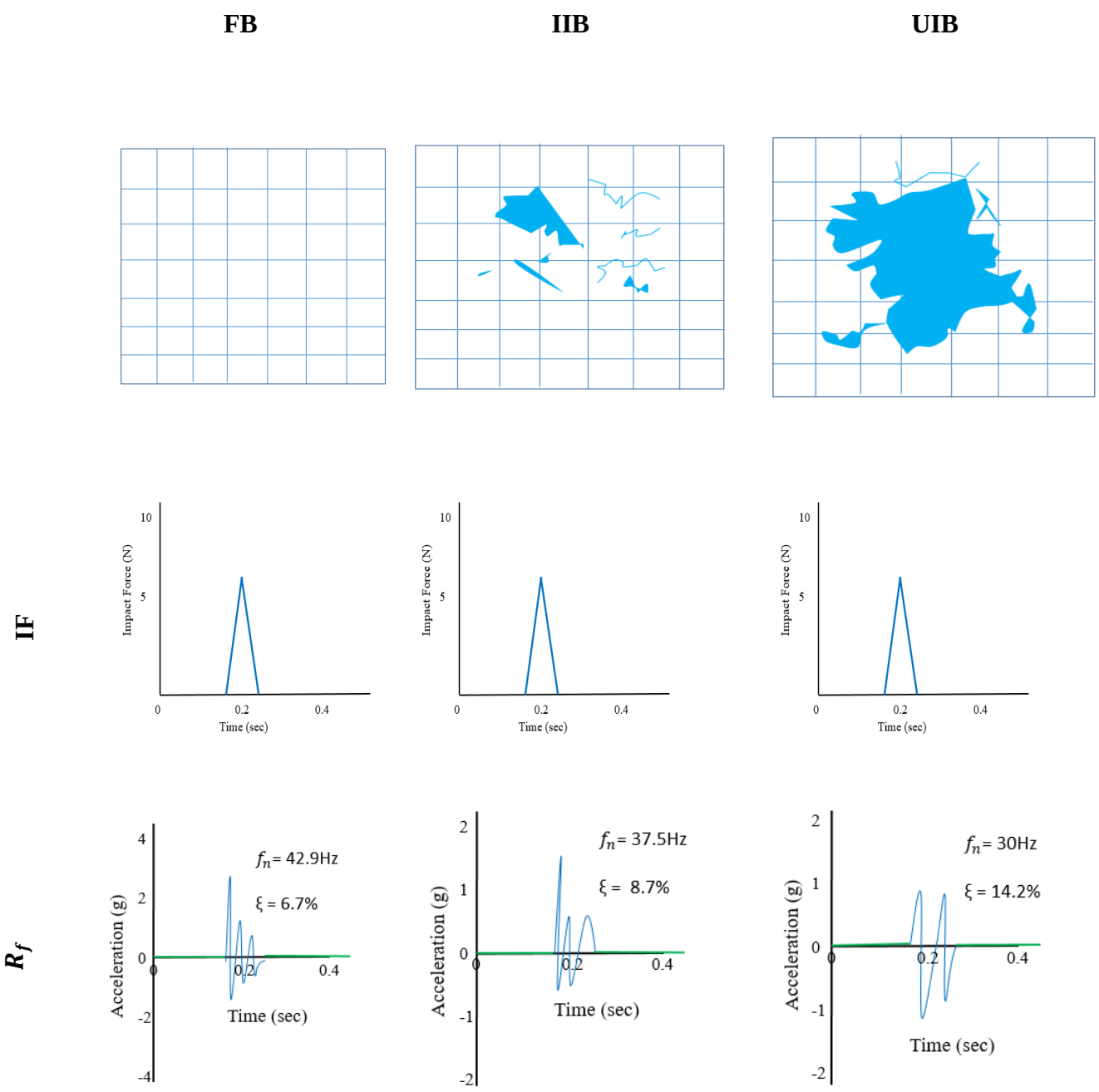

Figure 4.19: S4 Dynamic characteristics of deteriorating (IF) and acceleration time history ($\boldsymbol{R_f}$) of wall impact for first blow (FB), at initial impact blows (IIB), at ultimate impact blows (UIB).

The impact response measurements of Chicken Mesh Fiber walls demonstrated enhanced structural performance attributed to fiber reinforcement. At the first blow (FB), the wall exhibited an acceleration of 1.63 g, a resonance frequency of 50 Hz, and a damping ratio of 8.9%. As the wall progressed to initial impact failure (IIB), the acceleration decreased to 1.2/4 g, the resonance frequency dropped to 37.5 Hz, and the damping ratio increased to 9.6%. At ultimate impact failure (UIB), the acceleration further declined to 0.66 g, the resonance frequency reduced to 25 Hz, and the damping ratio rose to 13.1%, as illustrated in Figure 35. This progression indicates a clear trend of decreasing resonance frequency and increasing damping ratio, signifying a gradual reduction in structural stiffness and an enhancement in energy absorption capacity. The incorporation of chicken feather fibers as reinforcement contributed to this behaviour by improving the wall's ability to dissipate energy under impact loading.

The observed results indicate that the incorporation of fiber reinforcement in Steel Mesh Fiber walls significantly enhanced their energy dissipation capacity, as evidenced by the increasing damping ratio and decreasing resonance frequency. The consistent reduction in acceleration underscores the reinforcement's effectiveness in delaying crack propagation and maintaining structural stability under impact loading. This combination of higher damping and lower resonance frequency at later stages confirms the wall’s enhanced ability to absorb and dissipate impact energy, thereby bolstering its resistance to out-of-plane impact forces.

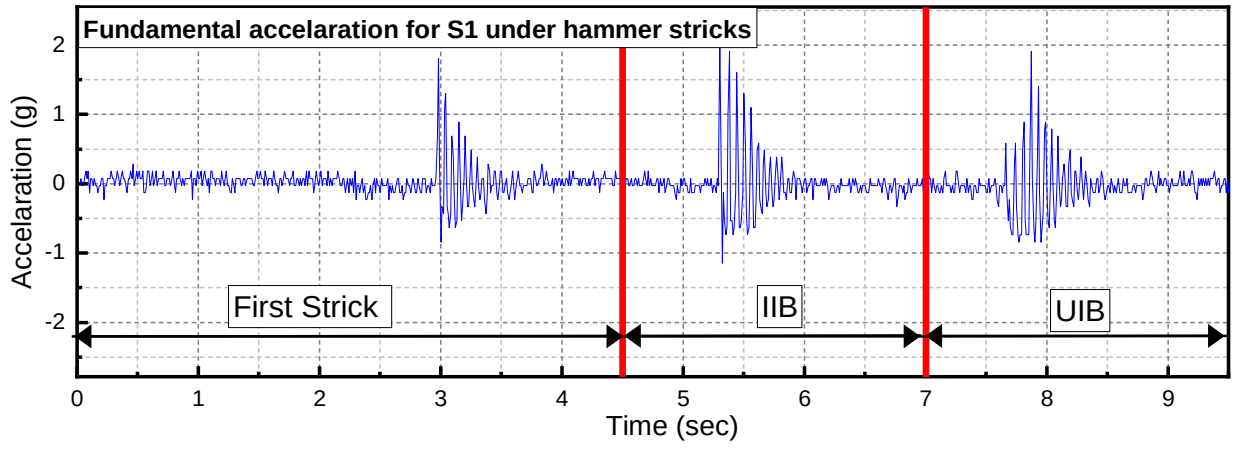

Figure 4.20: Fundamental acceleration For S1 at FB , IIB and UIB

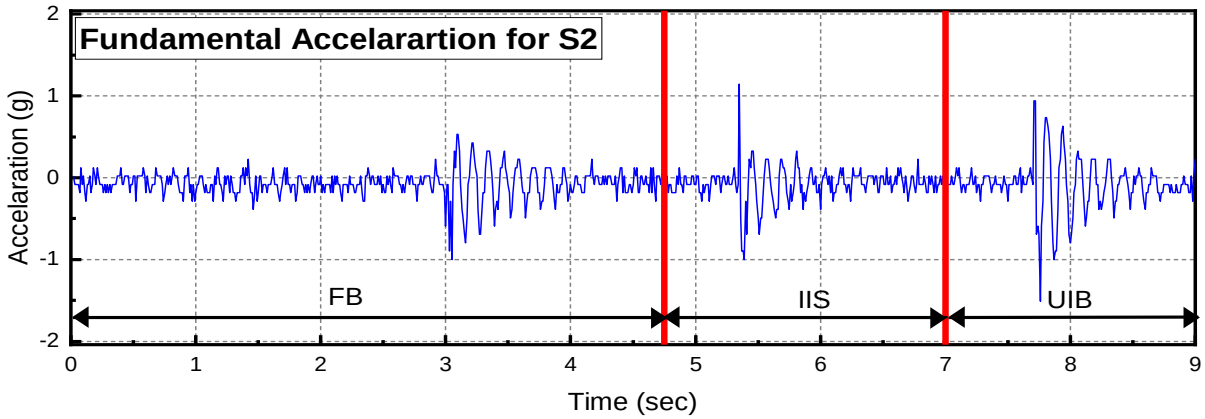

Figure 4.21: Fundamental acceleration For S2 at FB , IIB and UIB

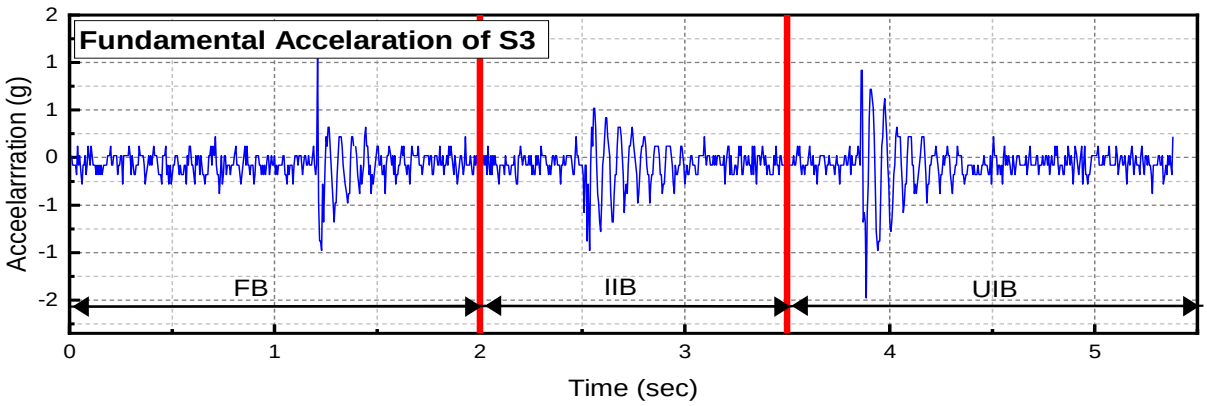

Figure 4.22: Fundamental acceleration For S3 at FB , IIB and UIB

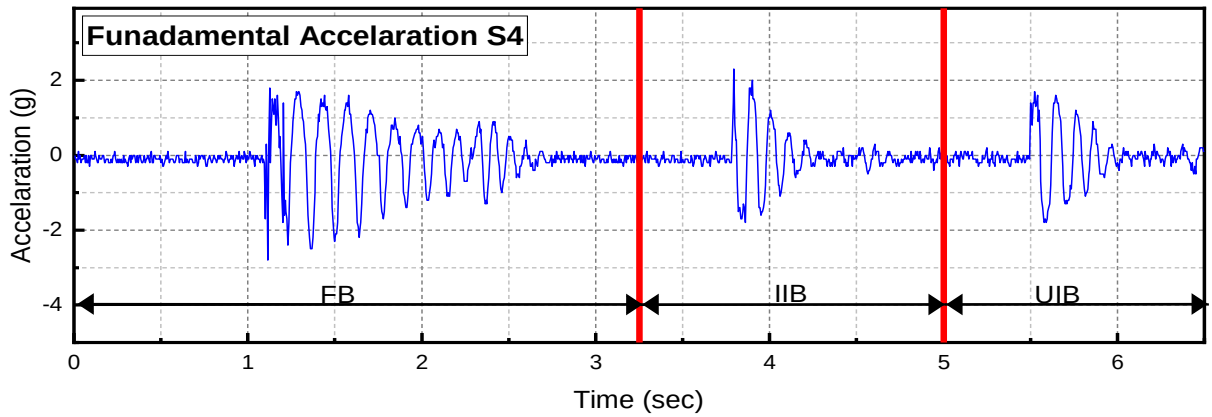

Figure 4.23: Fundamental acceleration For S4 at FB , IIB and UIB

Table 10. Effect of impact response on fundamental period and damping

Specimen		IF (N)	R_f (g)	f_n (Hz)	ξ %
Simple Walls	**FS**	6.64	2.17	41.4	2.3
	IIS	6.52	1.15	33	7.4
	UIS	6.69	0.89	15	12.4
Glass Fiber Walls	**FS**	6.74	1.55	42.9	1.8
	IIS	6.69	0.89	33.3	3.6
	UIS	6.80	0.61	23.1	7.8
Chicken Mesh Fiber Walls	**FS**	6.78	1.63	50	8.9
	IIS	6.66	1.24	37.5	9.6
	UIS	6.83	0.66	25	13.1
Steel Mesh Fiber Walls	**FS**	6.85	2.58	42.9	6.7
	IIS	6.77	1.72	37.5	8.7
	UIS	6.92	0.94	30	14.2

4.3.5.1 Dynamic properties at different damage stage

Table 11 highlights the effects of low and high-velocity impacts on walls at three distinct stages: before testing, after initial impact strength (IIS) failure, and after ultimate impact strength (UIS) failure. The damping ratios were calculated to better understand the internal damage within the bricks caused by the impacts. Prior to any impact, the resonance frequencies of the Simple Walls and Steel-Mesh Fiber Walls configurations were higher than those of the Glass Fiber Walls. This pattern persisted even after ultimate failure. Similarly, the dynamic elastic modulus (EM_d) before Pendulum Impact Testing was greater for Simple Walls and Steel-Mesh Fiber Walls compared to Glass Fiber Walls and Chicken-Mesh Fiber Walls. However, after ultimate failure, the dynamic elastic modulus of Simple Walls dropped below that of Glass Fiber Walls, while Steel-Mesh Fiber Walls maintained a higher modulus than Chicken-Mesh Fiber Walls.

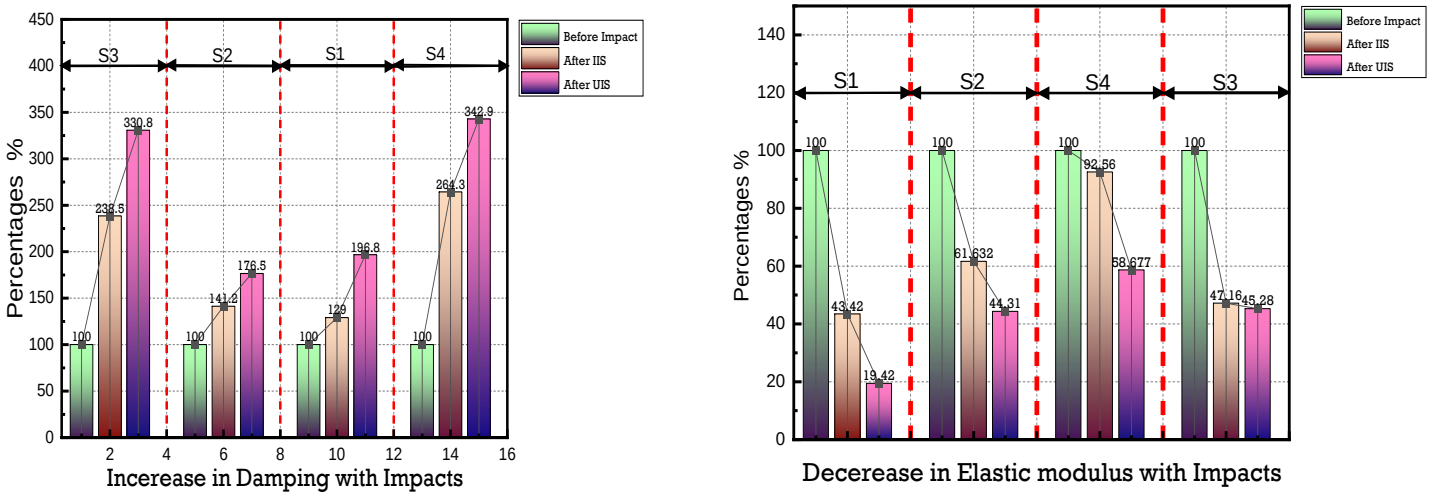

(a) (b)

Figure 4.24: Percentage decrement against impact (a) Damping (b) Dynamic Elastic Modulus.

The data indicate that the damping ratios of all wall types increased with the application of impact strength. This finding emphasizes that walls reinforced with jute fibers, especially those with fiber

or glass textile reinforcement, exhibit superior energy dissipation capabilitiesan essential factor for seismic resilience. failure, and after UIS failure. The first impact serves as a reference (100%) for evaluating subsequent changes in damping and EM_d. The results show a significant increase in damping, with a 216.7% rise after IIS and a 385.9% rise after UIS. Concurrently, EM_d decreased by 63.32% after IIS and 29.52% after UIS, reflecting the progressive structural degradation from repeated impacts.

Table 11. Consequences of Low and High velocity impact on dynamic properties of wall

Specimen		RF_t Hz	EM_d (GPa)	ξ %
Simple Wall	**Before impact**	596	7.9	2.2
	After IIS	463.5	4.1	3.4
	After UIS	473.5	2.8	4.2
Glass Fiber Wall	**Before impact**	773.5	5.8	3.4
	After IIS	688.5	2.2	4.3
	After UIS	586.5	1.2	6.0
Chicken Mesh Fiber Walls	**Before impact**	884.5	21	4.3
	After IIS	799	18.8	6.9
	After UIS	618.5	16.3	7.1
Steel Mesh Fiber Walls	**Before impact**	978.5	18.7	1.4
	After IIS	860	8	4.4
	After UIS	673.25	2	3

Fiber reinforcement significantly improved damping characteristics. Damping increased from 2.2% to 3.4% in Simple Walls and Chicken-Mesh Fiber Walls, while Glass Fiber Walls and Steel-Mesh Fiber Walls experienced a rise from 1.4% to 4.3%. This increase in damping implies that fiber-reinforced walls absorbed more energy during impacts, enhancing dynamic load dissipation. However, this improvement in damping came with a reduction in stiffness, as shown by the decrease in EM_d. Specifically, EM_d in Glass Fiber and Steel-Mesh Fiber Walls dropped from 18.7 GPa to 21 GPa due to crack formation and propagation, weakening the walls' structural integrity. Similarly, EM_d in Simple Walls and Chicken-Mesh Fiber Walls declined from 7.9 GPa to 5.8 GPa, further confirming that fiber reinforcement affects the dynamic response of masonry structures.

Overall, the findings highlight the crucial role of fiber reinforcement in enhancing damping capacity while acknowledging its impact on stiffness reduction. This trade-off between energy dissipation and structural rigidity is vital in designing impact-resistant masonry walls.

Illustrates the inverse relationship between resonance frequency and damping. As the resonance frequency decreases, the damping ratio increases due to crack development within the masonry wall. Cracks reduce the wall's effective stiffness, leading to lower resonance frequency, while the energy dissipation associated with crack propagation results in higher damping. For instance, in the Glass Fiber Walls configuration, the resonance frequency declined from 3528.5 Hz to 1564 Hz, while the damping ratio increased from 1.4% to 5.4%. Similarly, for the Glass Fiber Walls combined with Simple Walls, the frequency dropped from 2596 Hz to 1730.5 Hz, with a corresponding damping increase from 2.2% to 4.2%. These trends demonstrate that as damage accumulates and cracks develop, the wall’s dynamic response shifts, with stiffness decreasing and damping increasing to absorb more energy. The findings emphasize the importance of effective reinforcement strategies, such as fiber reinforcement, in maintaining structural integrity under impact and seismic loads.

4.3.5.2 Note

A decrease in the elastic modulus indicates a reduction in the stiffness of the masonry wall system. As the structure experiences impact loading or repeated stress cycles, micro cracking and internal

damage occur within the material, leading to a lower ability to resist deformation. Simultaneously, an **increase in damping** reflects a greater capacity of the system to **absorb and dissipate energy** rather than store it elastically. This behavior is typically associated with **nonlinear material response** and **energy loss through** internal **friction, cracking, or interface slip**. In the context of this study, the combination of reduced stiffness and increased damping suggests that the walls are transitioning from an elastic state to a more **damaged and dissipative phase**, which is a common response in brittle masonry elements subjected to **out-of-plane dynamic loading**.

A decrease in the elastic modulus indicates a reduction in the stiffness of the masonry wall system. As the structure experiences impact loading or repeated stress cycles, micro cracking and internal damage occur within the material, leading to a lower ability to resist deformation. Simultaneously, an **increase in damping** reflects a greater capacity of the system to **absorb and dissipate energy** rather than store it elastically. This behavior is typically associated with **nonlinear material response** and **energy loss through** internal **friction, cracking, or interface slip**. In the context of this study, the combination of reduced stiffness and increased damping suggests that the walls are transitioning from an elastic state to a more **damaged and dissipative phase**, which is a common response in brittle masonry elements subjected to **out-of-plane dynamic loading**.

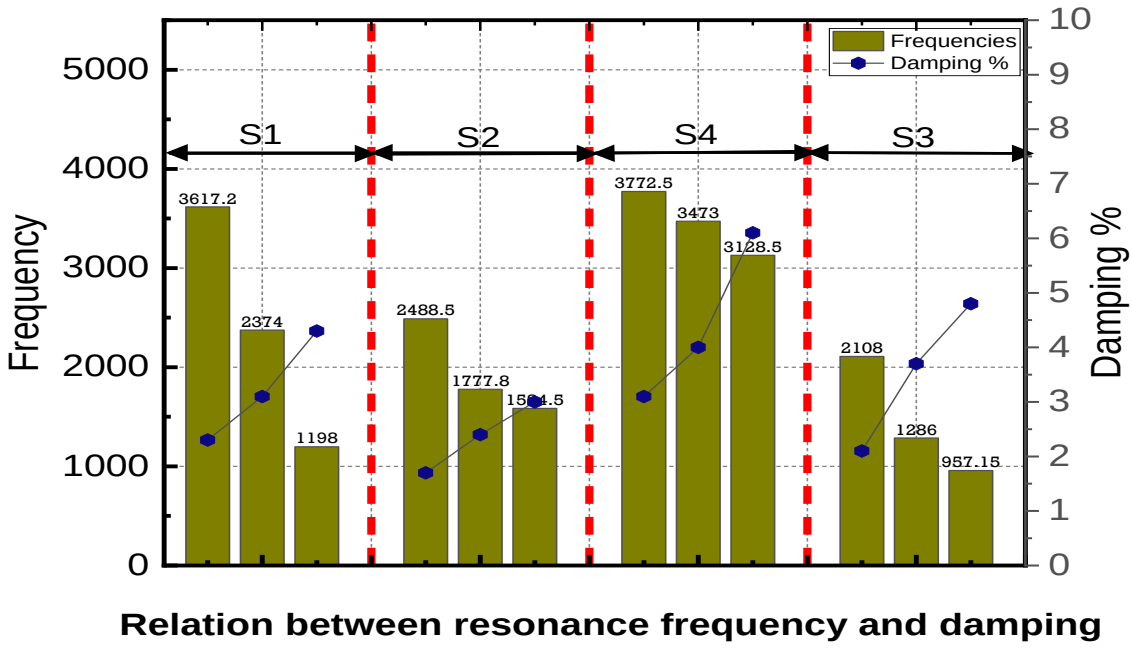

Figure 4.25: Relationship between Resonance frequency and Damping

4.3.5.3 Comparison of Experimental and Radical Frequencies:

4.3.5.3.1 Composite Material Properties:

i. Steel Mesh Fiber

Effective Young's Modulus (Rule of Mixture)

$$E_{eff} = \sum V_i E_i = V_b E_b + V_{ba} E_{ba} + V_p E_p$$

$$V_i = 0.30, E_i = 7GPa; \quad V_{ba} = 0.080, E_{ba} = 20\ GPa; \quad V_p = 0.62, E_p = 25\ GPa;$$

$$E_{eff} = (0.30 * 7) + (0.08 * 2) + (0.62 * 25) = 18.4GPa$$

Effective Density:

$$\rho_{eff} = \sum V_i \rho_i = (0.30 * 1900) + (0.80 * 600) + (0.62 * 2000) = 1840 kg/m^3$$

Poisson's Ratio:

$$v_{eff} = 0.22$$

Flexural Rigidity:

$$D = \frac{E_{eff}^3}{12\left(1 - v_{eff}^2\right)} = \frac{18.4x10^9 * (0.04143^3)}{12(1 - 0.22^2)} = 114{,}560$$

ii. Chicken Mesh Fiber

Effective Young's Modulus (Rule of Mixture)

$$E_{eff} = \sum V_i E_i = V_b E_b + V_{ba} E_{ba} + V_p E_p$$

$$V_i = 0.551, E_i = 7GPa; \quad V_{ba} = 0.105, E_{ba} = 20\ GPa; \quad V_p = 0.344, E_p = 25\ GPa;$$

$$E_{eff} = (0.551 * 7) + (0.105 * 2) + (0.344 * 25) = 14.557GPa$$

Effective Density:

$$\rho_{eff} = \sum V_i \rho_i = (0.551 * 1900) + (0.105 * 600) + (0.344 * 2000) = 1798 kg/m^3$$

Poisson's Ratio:

$$v_{eff} = 0.22$$

Flexural Rigidity:

$$D = \frac{E_{eff}^3}{12\left(1 - v_{eff}^2\right)} = \frac{14.56x10^9 * (0.04143^3)}{12(1 - 0.22^2)} = 90{,}683$$

iii. Glass Fiber

Effective Young's Modulus (Rule of Mixture)

$$E_{eff} = \sum V_i E_i = V_b E_b + V_{ba} E_{ba} + V_p E_p$$

$$V_i = 0.60, E_i = 7GPa; \quad V_{ba} = 0.10, E_{ba} = 20\ GPa; \quad V_p = 0.30, E_p = 25\ GPa;$$

$$E_{eff} = (0.60 * 7) + (0.10 * 20) + (0.30 * 25) = 13.70GPa$$

Effective Density:

$$\rho_{eff} = \sum V_i \rho_i = (0.60 * 1900) + (0.10 * 600) + (0.30 * 2000)$$
$$= 1800 kg/m^3$$

Poisson's Ratio:

$$v_{eff} = 0.22$$

Flexural Rigidity:

$$D = \frac{E_{eff}^3}{12(1 - v_{eff}^2)} = \frac{13.705x10^9 * (0.04143^3)}{12(1 - 0.22^2)} = 85{,}345$$

Table 12. Comparison of Experimental and Radical Frequencies

Constituent	Symbol	Volume Fraction (V_i)	Young's Modulus (E_i)	Density (ρ_i)	Poisson's Ratio (v_i)	Flexural Rigidity
Glass Fiber	Vs2	0.30	9 GPa	1170 kg/m³	0.16	85,345
Chicken Mesh Fiber	Vs3	0.35	14 GPa	1260 kg/m³	0.17	90,683
Steel Mesh Fiber	Vs4	0.62	25 GPa	1840 kg/m³	0.22	114,560

4.3.5.1.2 Plate Vibration Equations (Fixed Boundaries)

Governing Equation:

$$D\nabla^4\omega + \rho_{eff} t \frac{\vartheta^2\omega}{\vartheta t^2} = 0$$

Natural Frequency Solution:

$$f_m = \frac{1}{2\pi}\sqrt{\frac{K_{mm}}{M_{mn}}}$$

Where modal stiffness $K_{mm}$and mass$M_{mn}\ are$:

$$K_{mm} = \iiint_V \in^T C_{\in} dV,\ \ M_{mn} = \rho_{eff} \iiint_V \Phi_m^2 \Psi_n^2 \varsigma_k^2 dV$$

With eigenvalues λ_{mn}:

$$\lambda_{11} = 3.50, \quad \lambda_{12} = 6.98, \quad \lambda_{22} = 7.00, \quad \lambda_{13} = 8.00, \quad \lambda_{23} = 9.00, \quad \lambda_{33} = 10.0$$

4.3.5.1.3.1 Frequency Spectrum Calculation

Fundamental Factor:

i. **Steel Mesh Fiber**, $T = \frac{1}{2\pi a^2}\sqrt{\frac{D}{\rho_{eff}^t}} = \frac{1}{2\pi(0.610)^2}\sqrt{\frac{114{,}560}{1840*0.04143}} = 16.58Hz$

ii. **Chicken Mesh Fiber**, $T = \frac{1}{2\pi a^2}\sqrt{\frac{D}{\rho_{eff}^t}} = \frac{1}{2\pi(0.350)^2}\sqrt{\frac{90{,}683}{1260*0.04143}} = 54.23Hz$

iii. **Glass Fiber**, $T = \frac{1}{2\pi a^2}\sqrt{\frac{D}{\rho_{eff}^t}} = \frac{1}{2\pi(0.300)^2}\sqrt{\frac{85{,}345}{1170*0.04143}} = 74.318Hz$

Model Frequencies:

$f_{11} = (3.50)^2 * 16.58 = 203Hz$	$f_{11} = (3.50)^2 * 54.23Hz = 664.31Hz$	$f_{11} = (3.50)^2 * 74.318 = 910.93Hz$
$f_{12} = (6.98)^2 * 16.58 = 808Hz$	$f_{12} = (6.98)^2 * 54.23Hz = 2642.10Hz$	$f_{12} = (6.98)^2 * 74.318 = 3620.80Hz$

$f_{22} = (7.00)^2 * 16.58 = 812Hz$	$f_{22} = (7.00)^2 * 54.23Hz = 2654.27Hz$	$f_{22} = (7.00)^2 * 74.318 = 3641.58Hz$
$f_{13} = (8.00)^2 * 16.58 = 1061Hz$	$f_{13} = (8.00)^2 * 154.23Hz = 3470.7Hz$	$f_{13} = (8.00)^2 * 74.318 = 4756.35Hz$
$f_{23} = (9.00)^2 * 16.58 = 1343Hz$	$f_{23} = (9.00)^2 * 54.23Hz = 4392.63Hz$	$f_{23} = (9.00)^2 * 74.318 = 6019.75Hz$
$f_{33} = (10.0)^2 * 16.58 = 1658Hz$	$f_{33} = (10.0)^2 * 54.23Hz = 5423Hz$	$f_{33} = (10.0)^2 * 74.318 = 7431.8Hz$
$f_{14} = (11.0)^2 * 16.58 = 2006Hz$	$f_{14} = (11.0)^2 * 54.23Hz = 6561.83Hz$	$f_{14} = (11.0)^2 * 74.318 = 8992.47Hz$
$f_{24} = (12.0)^2 * 16.58 = 2388Hz$	$f_{24} = (12.0)^2 * 54.23Hz = 7809.12Hz$	$f_{24} = (12.0)^2 * 74.318 = 10701.8Hz$

4.3.5.1.3.2 Thickness-Shear Mode (4000Hz)

Shear Modulus

i. Steel Mesh Fiber

$$G_{eff} = \frac{E_{eff}}{2(1 + v_{eff})} = \frac{18.4}{2(1 + 0.22)} = 7.54GPa$$

Shear Wave Speed:

$$v_s = \sqrt{\frac{G_{eff}}{\rho_{eff}}} = \sqrt{\frac{7.54x10^9}{1840}} = 2024\, m/s$$

Fundamental Thickness-shear Frequency:

$$f_{ts} = \frac{v_s}{2t} = \frac{2024.5}{2 * 0.04143} = 24400Hz$$

ii. Chicken Mesh Fiber

$$G_{eff} = \frac{E_{eff}}{2(1 + v_{eff})} = \frac{12.6}{2(1 + 0.17)} = 5.38GPa$$

Shear Wave Speed:

$$v_s = \sqrt{\frac{G_{eff}}{\rho_{eff}}} = \sqrt{\frac{7.54x10^9}{1260}} = 2446.24\ m/s$$

Fundamental Thickness-shear Frequency:

$$f_{ts} = \frac{v_s}{2t} = \frac{2446.24}{2 * 0.04143} = 29522Hz$$

iii. Glass Fiber

$$G_{eff} = \frac{E_{eff}}{2(1 + v_{eff})} = \frac{11.7}{2(1 + 0.17)} = 5GPa$$

Shear Wave Speed:

$$v_s = \sqrt{\frac{G_{eff}}{\rho_{eff}}} = \sqrt{\frac{7.54x10^9}{1260}} = 25385.91\ m/s$$

Fundamental Thickness-shear Frequency:

$$f_{ts} = \frac{v_s}{2t} = \frac{25385.91}{2 * 0.04143} = 306371Hz$$

4.3.5.1.3.3 Fiber Reinforcement Impact:

Stiffness Enhancement:

$$\Delta E = V_{fiber}\left(E_{fiber} - E_{matrix}\right) = 0.08 * (20 - 5) = 1.2GPa$$

Frequency Shift:

$$\frac{\Delta f}{f} = \frac{1}{2}\sqrt{\frac{\Delta E}{E_{eff}}} = \frac{1}{2}\sqrt{\frac{1.2}{18.4}} = 9.1\%$$

Table 13: **Frequency Shift**		
1	Steel Mesh Fiber	9.1%
2	Chicken Mesh Fiber	7%
3	Glass Fiber	6%

Table 14: **Summary of Results of experimental and radical frequencies**		
Mode	Frequency(Hz)	Experimental Range(Hz)
(1,2)	808	1000
(1,3)	1061	1000-4000
(2,2)	812	
(2,3)	1343	
(3,3)	1658	
(1,4)	2006	

(2,4)	2388	
(3,4)	2802	
(4,4)	3250	
(4,5)	3730	4000
(5,5)	42044	

Best Steel Mesh Fiber

Thickness-shear Mode: 24400Hz (not observed in 1-4 kHz)

Keyway stiffness: Increased frequency by 400% vs surface mount

Fiber Effect: +9.1% frequency shift.

4.4 Diagonal Shear Test

The shear strength of masonry walls was assessed through the diagonal shear test, as per ASTM E519 standards. Total specimens, each with dimensions of 50.8 cm × 50.8 cm × 11.43 cm (20 in × 20 in × 4.5 in), constructed in an English bond pattern, were tested. Diagonal loading was applied, and precise measurements of the load and deformation along both diagonals were taken. The walls exhibited notable deformation under shear forces without collapsing, demonstrating their structural robustness. Although diagonal cracks appeared, there were no signs of localized failure, indicating effective stress distribution and the absence of concentrated failure points. The walls also maintained stability, showing no rocking motion even under substantial deformation. A cohesive failure pattern was evident in both the inter-brick bonding and within the bricks themselves, reflecting an excellent deformation response. These findings are vital for understanding the behaviour of masonry walls under stress and provide valuable insights for constructing resilient structures capable of withstanding various loads. Shear stress-strain curves

were plotted for each specimen, illustrating their load-bearing capacity and deformation behaviour under diagonal loading. Reinforced walls, especially those wrapped with dried thread, displayed enhanced shear strength, rigidity modulus, and strain performance. The incorporation of fiber reinforcement significantly improved the structural response compared to untreated walls.

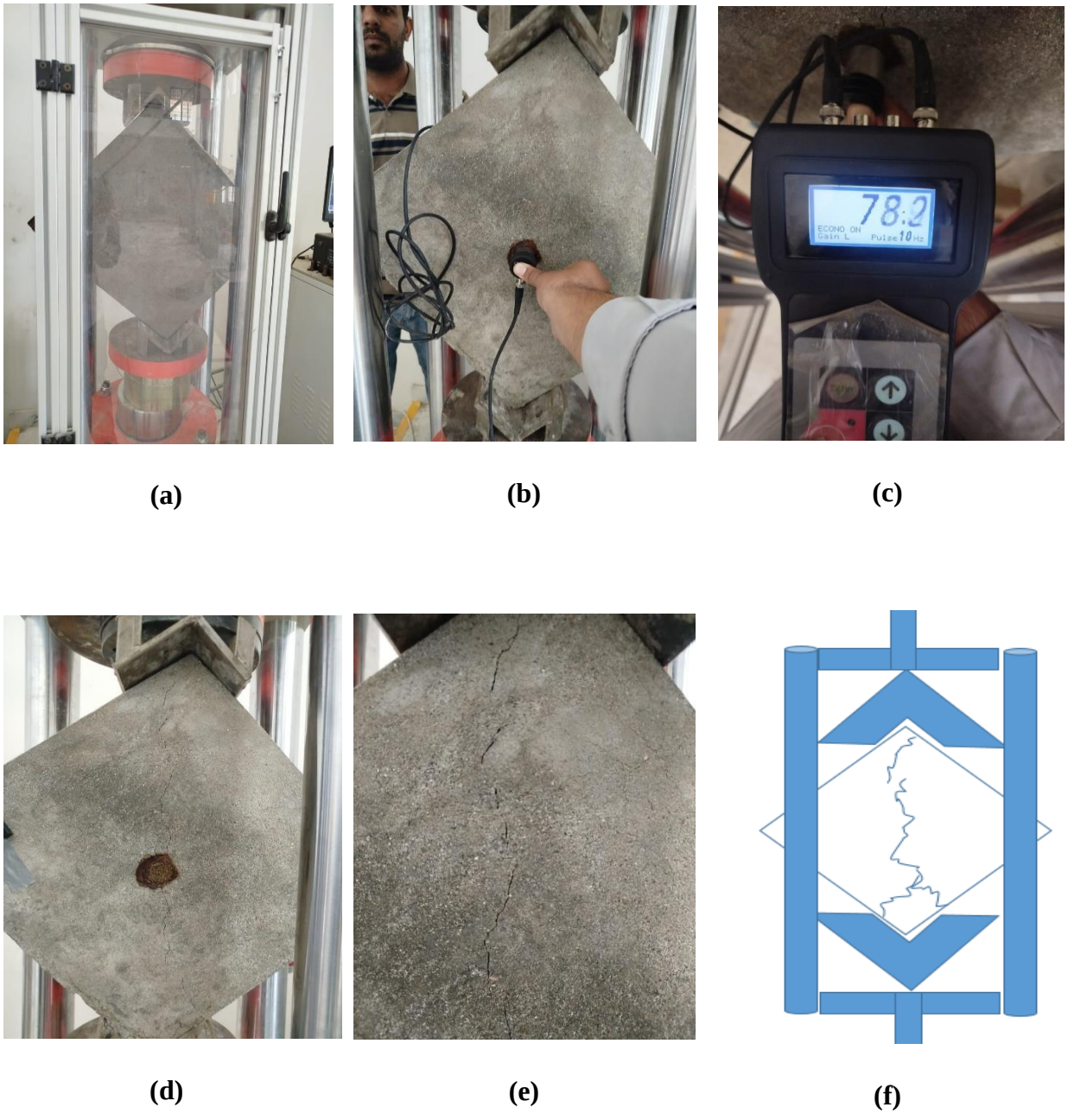

(a) **(b)** **(c)**

(d) **(e)** **(f)**

Figure 4.26: Diagonal Shear Test of Crack Pattern (a)Specimen in UTM (b)UPV Test (c)UPV Device (d)Grease Mark & Crack (e)Crack Appeared (f)Schematic View

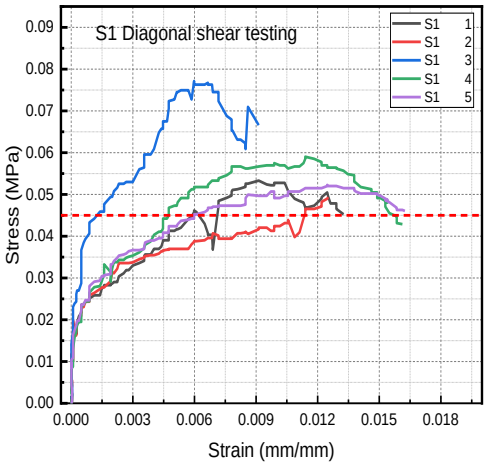

(a)

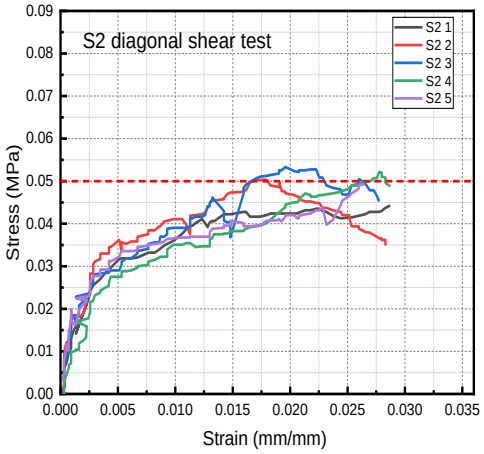

(b)

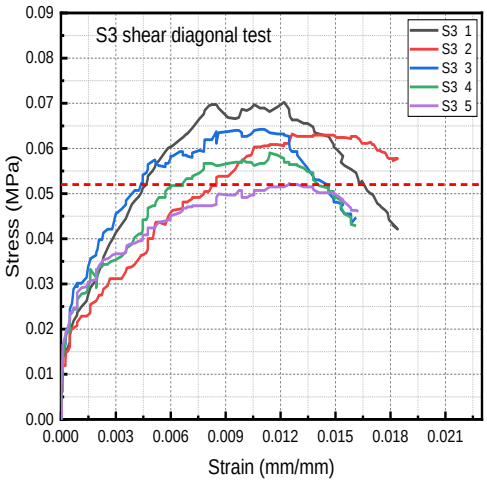

(c)

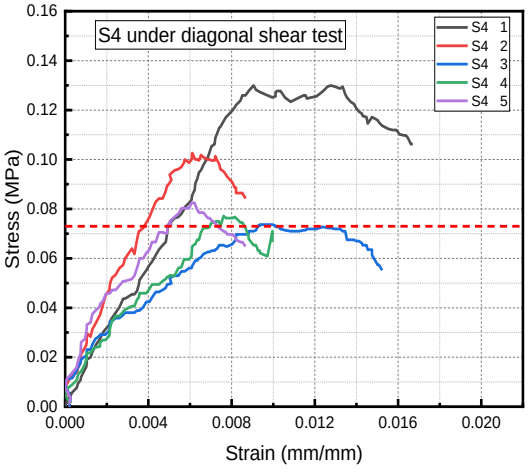

(d)

Figure 4.27: Diagonal Shear Test Data (a)S1 (b)S2 (c)S3 (d)S4

By employing the secant modulus approach, which spans from 1/20th to 1/3rd of the maximum shear strength, the shear modulus was calculated from the shear stress-strain curves. The findings revealed a notable enhancement in energy absorption capacity and ductility in the strengthened walls. This data underscores the effectiveness of fiber-reinforced masonry in dissipating energy and controlling deformation, making it an ideal solution for regions susceptible to seismic activity.

Stiffness analysis was conducted by assessing the rate of change in diagonal force (P) relative to displacement (D). The initial stiffness (K_0) was calculated by examining the fluctuation in diagonal force and displacement immediately before the formation of the initial crack, following Equation (6).

$$\mathbf{K_0 = P_0 / D_0}$$

Where P_0 denotes the initial cracking load, and D_0 represents the corresponding displacement.

Residual stiffness (K_r) was calculated using Equation (7):

$$\mathbf{K_r = (Pmax - P_0) / (Dmax - D_0)}$$

Where P-max is the maximum load and D-max is the corresponding displacement.

The stiffness ratio α is defined as the relationship between the initial and residual stiffness values. These parameters play a crucial role in evaluating the effectiveness of structural reinforcement and understanding the post-cracking behaviour of walls. This study closely parallels my research on Fibers-reinforced mortar masonry (RMM). The findings further substantiate Fiber's potential as a reinforcement material, not only for boosting shear strength and ductility but also for preserving structural integrity under impact or vibratory loading, such as in seismic zones.

Table 15. **Shear strength, Modulus of Rigidity, Strain, Ko, Kr, α**

Property	S1 / Simple Walls (1B) MPa (psi)	S2 / Glass Fiber Walls (2A) MPa (psi)	S3 / Chicken Mesh Fiber Walls (UMW) MPa (psi)	S4 / Steel Mesh Fiber Walls (2B) MPa (psi)
Shear Strength fv	0.088 (12.75)	0.138 (20.04)	0.059 (8.55)	0.131 (18.98)
Modulus of rigidity	29.1 (4225.9)	35.8 (5190.62)	19.4 (2806.51)	27.8 (4027.58)
Strain at max stress	0.016	0.027	0.009	0.018
Ko	111.49	187.32	89.57	161.59
Kr	11.74	5.16	23.76	4.81
$\boldsymbol{\alpha}$	9.5	36.3	3.77	4.81

The emphasis on stiffness enhancement through Fiber reinforcement offers valuable insights for optimizing masonry construction designs. The shear strength f_v presented in the table for various wall specimens (S1, S2, S3, and S4) is typically calculated using the diagonal compression test method, as outlined in ASTM E519. This method involves applying a compressive load along the diagonal of a square masonry panel, inducing pure shear stress in the central portion of the specimen. During the test, the applied load at failure is recorded and used to compute the shear strength of the wall using the following equation:

$$f_v = \frac{P}{2A} \quad (3)$$

Where:

f_v is the shear strength (MPa),

P is the peak compressive load applied along the diagonal (N),

A is the net cross-sectional area resisting the shear (typically calculated as the wall thickness multiplied by the gauge length between the strain gauges or the effective shear area).

In this test, strain gauges or LVDTs are used to measure the diagonal deformation, enabling the calculation of shear strain and ultimately, the modulus of rigidity (G). However, the shear strength f_v itself is calculated solely based on the applied load and the effective area, regardless of strain measurement. The values reported such as 0.088 MPa for the simple wall (S1) and 0.138 MPa for the Glass fiber reinforced wall (S2) indicate the maximum shear stress each configuration could withstand before failure. These values reflect the improved shear capacity resulting from the inclusion of fiber reinforcement. The modulus of rigidity (G), also known as shear modulus, is a measure of a material's resistance to shear deformation. In masonry testing, particularly under diagonal compression tests (ASTM E519), this property is determined by measuring the relationship between shear stress (τ) and shear strain (γ) within the elastic range. The modulus of rigidity is then calculated using the basic shear equation:

$$G = \frac{\tau}{\gamma} \quad (4)$$

Where:

G = Modulus of rigidity (MPa),

τ = Shear stress (MPa),

γ = Shear strain

The shear stress (τ) is calculated as:

$$\tau = \frac{P}{2A} \quad (5)$$

Where:

P = Applied diagonal load (N),

A = Effective shear area (m^2), typically taken as wall thickness × gauge length (the vertical/horizontal dimension between diagonally placed sensors).

The shear strain (γ) is obtained from the relative displacement measured along the diagonals of the wall using LVDTs or strain gauges, following:

$$\gamma = \frac{\Delta V + \Delta H}{g} \quad (6)$$

Where:

ΔV and ΔH = Vertical and horizontal diagonal displacements (mm),

g = Gauge length between sensors (mm)

Substituting into the equation:

$$G = \frac{P \cdot g}{2A\,(\Delta V + \Delta H)} \quad (7)$$

This formulation is widely used in experimental masonry research and allows for a reliable determination of the material's stiffness under shear loads. The value of G gives insight into the wall's ability to resist lateral deformations, especially in unreinforced vs. reinforced configurations like those in your study.

The reported values of the modulus of rigidity (G) for the four wall configurations S1 (29.1 MPa), S2 (35.8 MPa), S3 (19.4 MPa), and S4 (27.8 MPa) provide valuable insight into the shear stiffness and deformation behavior of each specimen under lateral loading conditions. The highest rigidity observed in the S4 (Steel Fiber Mesh Wall with Steel Reinforcement) indicates that the presence of fiber strips significantly enhances the wall's ability to resist shear deformation, thereby increasing its overall stiffness. In contrast, the lowest value recorded for the S1 highlights the detrimental effect of the masonry.

Furthermore, the S1 (simple wall and steel reinforcement) exhibits a moderate rigidity value (27.8 MPa), which, although lower than the fully solid fiber-reinforced wall (S4), is considerably higher than the unreinforced wall (S1). This demonstrates that fiber reinforcement partially compensates for the structural weakness introduced by the simple walls, thereby improving the overall shear performance. The baseline specimen (S1), with a G value of 29.1 MPa, serves as a control for comparison and represents typical shear stiffness in unreinforced solid masonry. Overall, the variation in rigidity among the different wall types confirms the effectiveness of fiber

reinforcement in enhancing the lateral stiffness of brick masonry walls, especially under conditions where discontinuities such as openings are present.

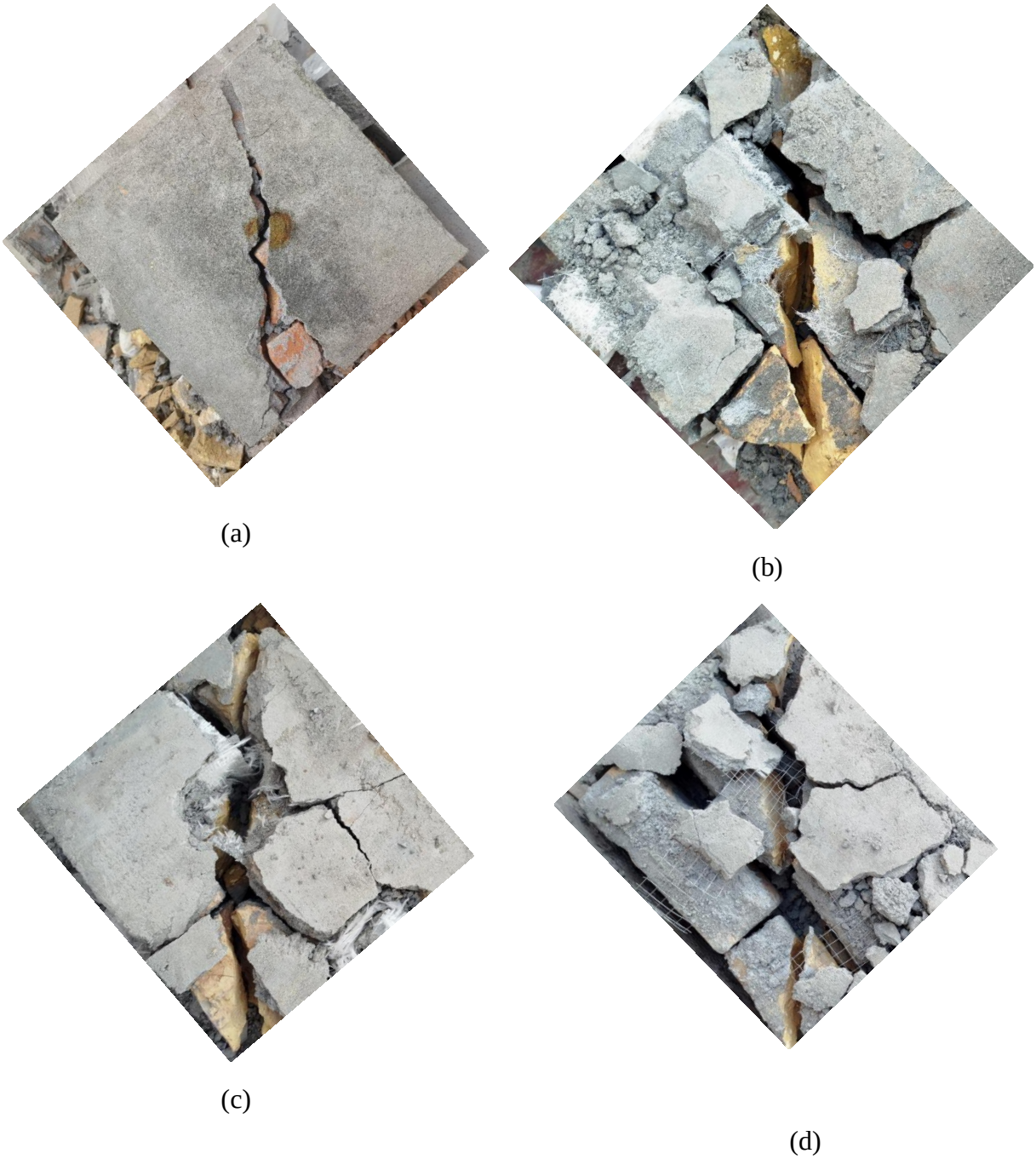

(a)

(b)

(c)

(d)

Figure 4.28: Diagonal Shear Testing (Fully Damaged Specimens) (a)Simple Walls (b)Glass Fiber Walls (c)Chicken Mesh Fiber Walls (d)Steel Mesh Fiber Walls

4.4.1 Ultrasonic Pulse Velocity (UPV) Test Results and Analysis

The Ultrasonic Pulse Velocity (UPV) test was performed on all wall specimens both before and after the application of loading to evaluate the internal condition and material integrity. As shown in Table 13, a significant decrease in UPV values was observed following the tests. This reduction indicates the formation of internal cracks and a decline in structural integrity, attributed to the effects of impact loading. These findings highlight the test's effectiveness in detecting subsurface damage and evaluating the overall health of the masonry walls.

Among the various specimens tested, the Steel Mesh Fiber Walls demonstrated the highest initial Ultrasonic Pulse Velocity (UPV) at 139.2 m/sec, indicating enhanced density and structural integrity attributed to Fiber reinforcement. Post-testing, the UPV decreased to 97.8 m/sec, suggesting internal damage; however, it still retained superior structural integrity compared to other specimens. In contrast, the Glass Fiber Walls and Simple Walls, both lacking reinforcement, exhibited significant UPV reductionsfrom 126.5 m/sec to 94.4 m/sec and from 114.7 m/sec to 85.5 m/sec, respectivelyimplying substantial internal cracking and diminished material continuity. Notably, the Chicken Mesh Fiber Walls experienced the most pronounced UPV decline, from 124.2 m/sec to 75.7 m/sec, indicating that the combination of unreinforced and reinforced elements led to increased stress concentrations and internal cracking under impact loading.

The observed reduction in Ultrasonic Pulse Velocity (UPV) across all specimens confirms the development of internal damage resulting from impact loading. However, specimens incorporating fiber reinforcement exhibited superior post-impact structural integrity compared to their unreinforced counterparts. This outcome underscores the efficacy of fiber reinforcement in mitigating structural damage and preserving internal cohesion under impact conditions. The presence of fibers enhances the material's ability to absorb energy and resist crack propagation, thereby contributing to improved durability and performance under dynamic loading scenarios.

Table 16. UPV data before and after the test for Diagonal shear wall specimens

Type of category	Specimens	UPV (m/sec) Before test	UPV (m/sec) Mid Test	UPV (m/sec) After test
Category 2	Simple Walls	114.7	93.3	75.7
	Glass Fiber Walls	124.2	99.1	85.5
	Chicken Mesh Fiber walls	126.5	105.7	94.4
	Steel Mesh Fiber Walls	139.2	120.9	97.8

4.5 Compression Testing

A total of twelve masonry prism specimens were tested to determine their average compressive strength and modulus of elasticity, with three specimens allocated to each category, as summarized in Table 14. An analysis of the failure modes revealed a consistent pattern across all specimens, characterized by vertical cracking, noticeable crushing along the vertical axis, and splitting, as depicted in Figure 4.29. The uniformity in failure behaviour underscores the reliability and repeatability of the test results, offering valuable insights into the structural performance of the masonry prisms.

The compressive stress-strain behaviour of the masonry prisms, illustrated in Figure 4.30, reflects their response under applied loading. A detailed summary of the results comprising the average prism compressive strength, masonry compressive strength, modulus of elasticity, and strain at peak stress is presented in Table 14. For specimens with an hp/tp ratio of 2.33, a correction factor

of 1.0266, as recommended by ASTM C1314, was incorporated to accurately compute the masonry compressive strength.

The modulus of elasticity (E) for masonry prisms under compressive loading was determined in accordance with the procedures outlined in ASTM C469 and ASTM C1314. This parameter quantifies the material's elastic deformation capacity when subjected to stress and is critical for evaluating the structural performance of masonry walls under loading conditions.

The process begins by applying a controlled compressive load (P) to the specimen using a reaction frame, ensuring that the force is evenly distributed. The cross-sectional area (A) of the specimen is determined by multiplying its width by its thickness. The compressive stress (σ) is then calculated using the formula:

$$\sigma = \frac{p}{A}$$

Here, P represents the applied force in Netons, while A denotes the cross-sectional area of the specimen in square millimeters (mm^2). Simultaneously, deformation and strain are measured using a Linear Variable Differential Transformer (LVDT) along with a laser displacement sensor. These instruments precisely track the change in length (ΔL) of the specimen during the compression process. The corresponding strain (ε) is then calculated using the following relation:

$$\varepsilon = \frac{\Delta L}{L}$$

Where L is the initial gauge length of the specimen and ΔL is the recorded displacement.

Based on the acquired stress-strain data, the modulus of elasticity (E) is calculated by identifying the slope of the linear segment of the stress-strain curve. According to ASTM C1314 guidelines, this linear portion is typically defined between 5% and 33.33% of the ultimate compressive strength. The modulus of elasticity is computed using the following equation:

$$E = \frac{\Delta\sigma}{\Delta\varepsilon}$$

where Δσ represents the change in stress (MPa), and Δε is the corresponding change in strain.

The findings offer valuable insights into the stiffness and deformation characteristics of masonry under compressive loading. Where necessary, the correction factor specified by ASTM C1314 is

applied to adjust the modulus of elasticity, taking into account the specimen's height-to-thickness ratio. These calculations are essential for evaluating the structural integrity of fiber-reinforced masonry walls and for optimizing their performance under diverse loading conditions.

Table 17. Summary of masonry wall specimens under Compression test

Specimen types	**Compressive strength of prism (MPa)**	**Elastic modulus (GPa)**	**Maximum displacement (mm)**
S1	3.4	2.5	5.32
S2	3.99	3. 68	4.99
S3	4.91	3. 77	3.96
S4	5.89	4.26	2.72

Ilustrates the load-displacement curves for all tested wall specimens, showcasing their structural response under applied loading. These curves provide essential insights into the stiffness, deformation behaviour, and overall load-bearing capacity of each wall configuration.

The Simple Wall, serving as the baseline reference, exhibits a gradual linear-elastic behavior followed by a consistent decline post-cracking. Although it maintains moderate strength, the absence of reinforcement results in greater displacement at peak load, indicating reduced structural integrity compared to its reinforced counterparts. In contrast, the wall reinforced solely with unreinforced walls shows a noticeable reduction in both strength and stiffness, likely due to premature cracking and increased deformation under loading. Conversely, the Simple Wall reinforced with fiber strips demonstrates a significantly steeper load-displacement curve, reflecting enhanced stiffness and improved load-bearing capacity.

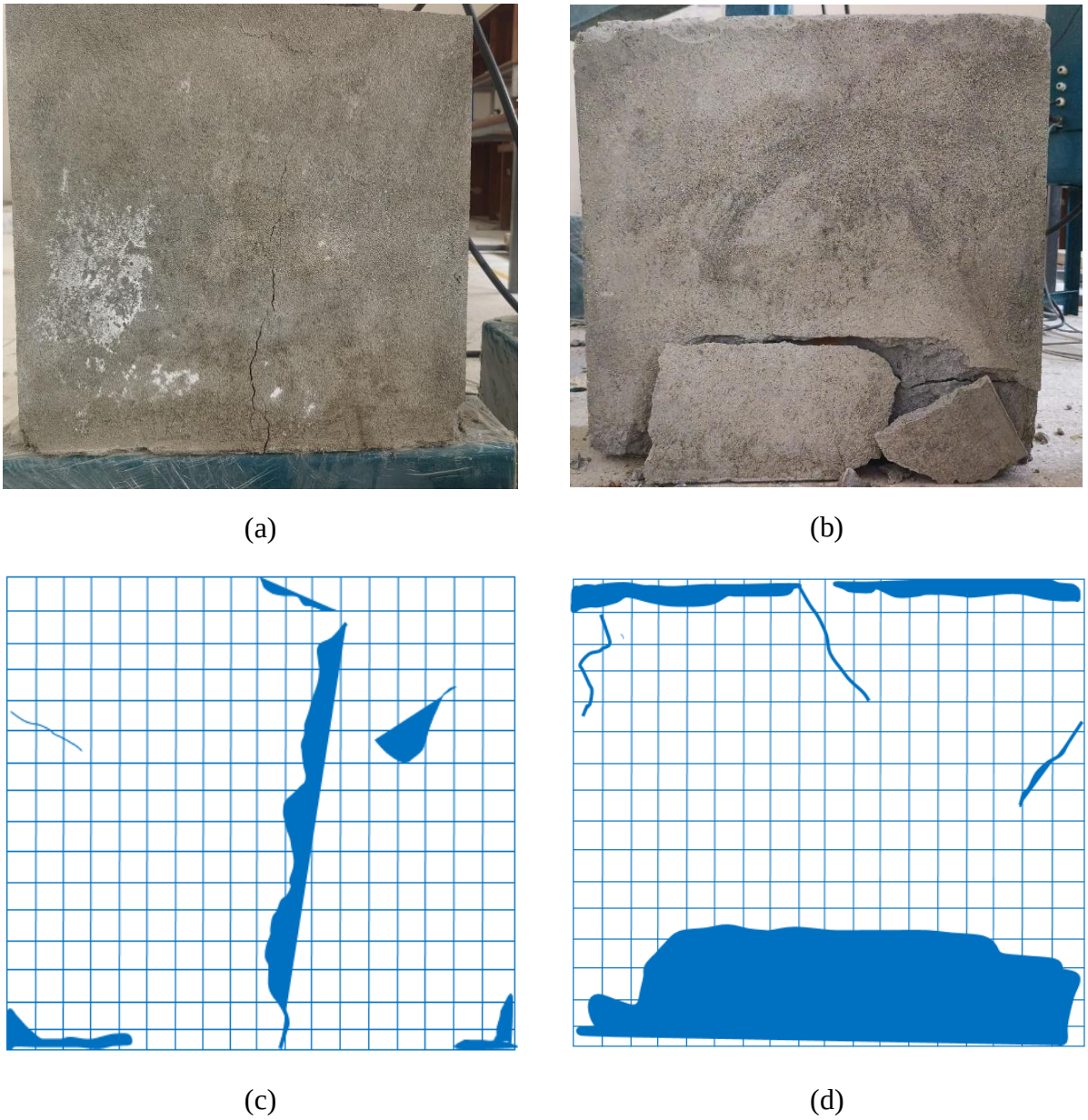

Figure 4.29: Compression Testing Specimens (load performance) (a)Damage mode of S1 (b)Damage mode of S2 (c)Schematic View of S1 (d)Schematic View of S2

The reduced displacement at peak load is indicative of improved structural integrity, positioning this configuration as the most robust among all tested specimens. While fiber reinforcement improves the wall's stability and strength, it may slightly limit the ultimate load capacity; however, the failure progression is more gradual and controlled compared to unreinforced walls.

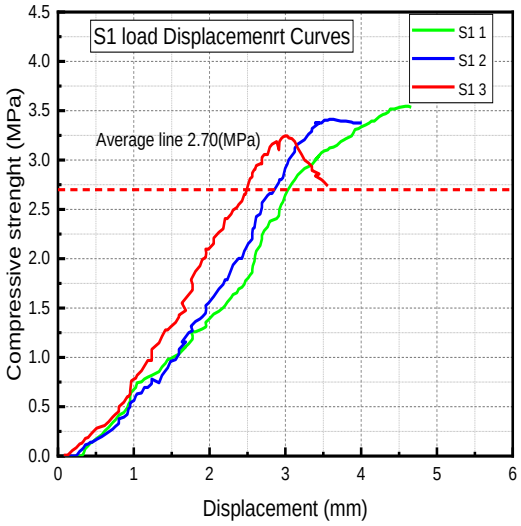

(a)

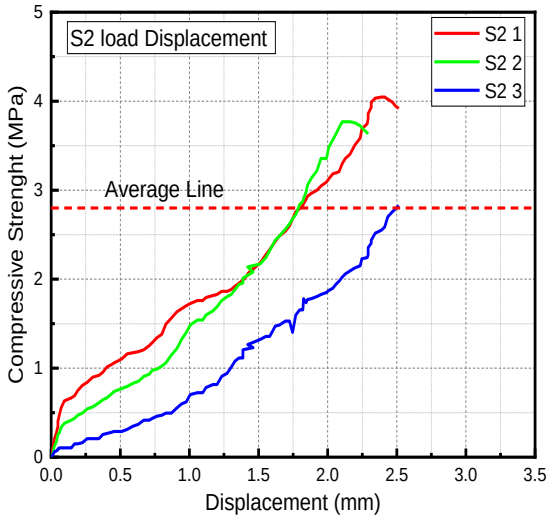

(b)

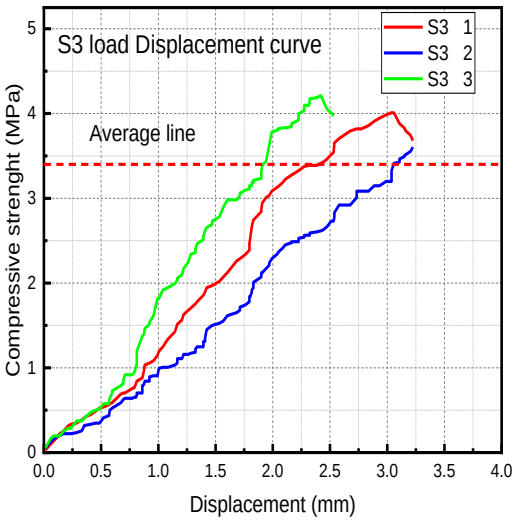

(c)

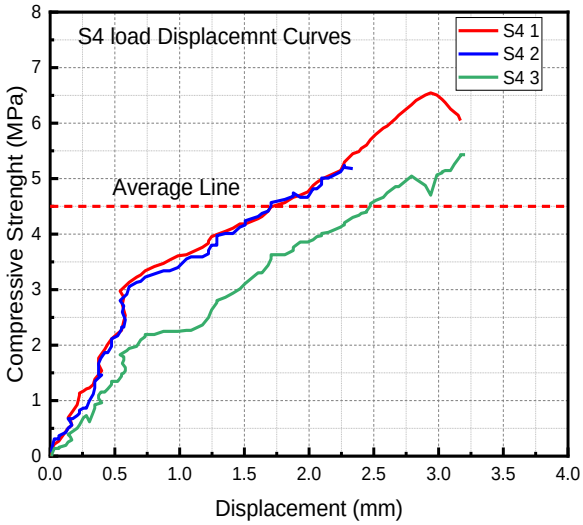

(d)

Figure 4.30: Load Displacement Curves (a)S1 (b)S2 (c)S3 (d) S4

(a)

(b)

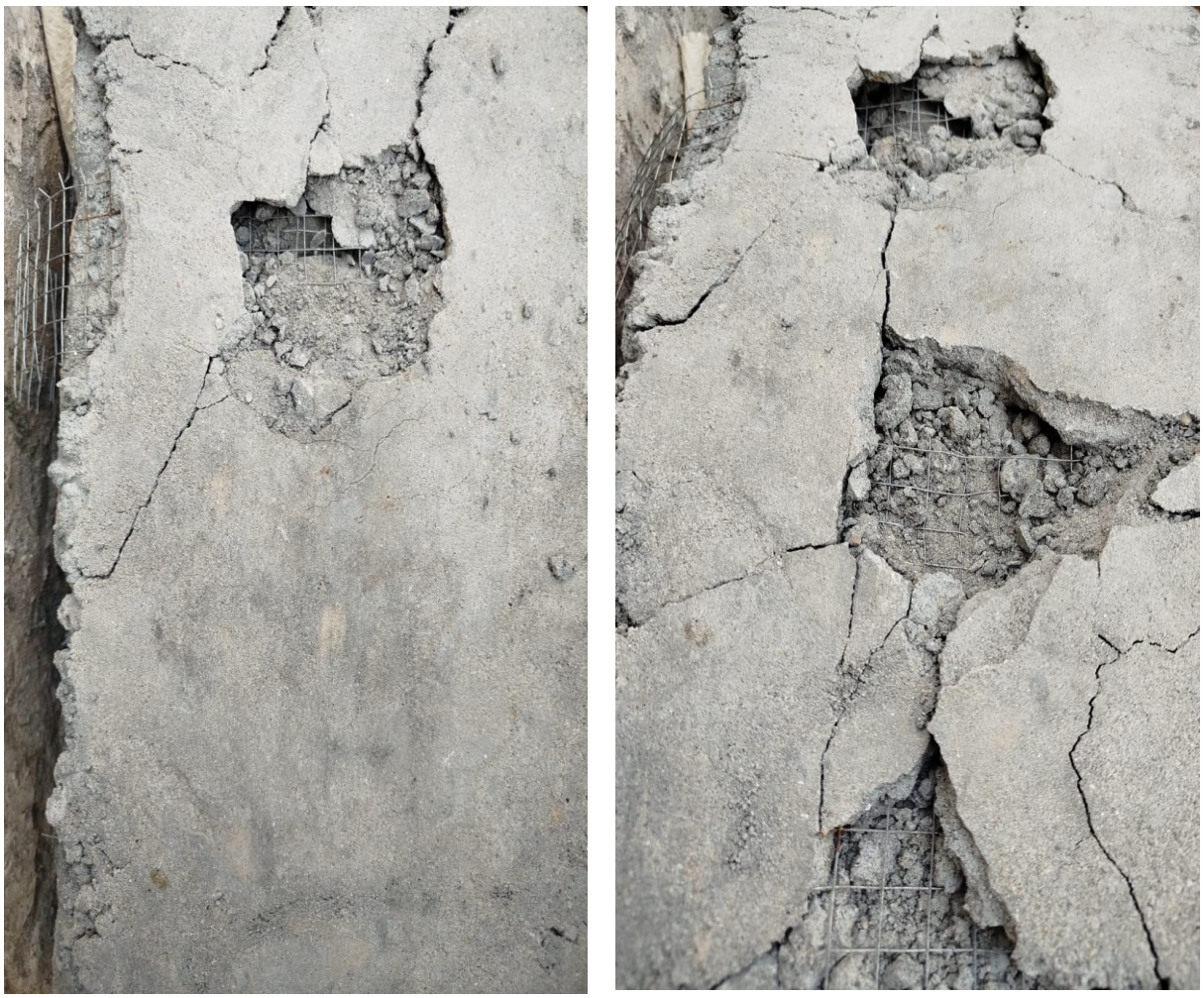

(c)

Figure 4.31: Compression Testing (Fully Damaged Specimens) (a)Glass Fiber Wall (b)Chicken Mesh Fiber Wall (c) Steel Mesh Fiber Walls

4.6 Summary

The dynamic performance evaluation of fabric-reinforced brick masonry walls aimed to enhance structural behaviour by incorporating Glass Fiber, Steel Mesh Fiber, and chicken mesh. Using solid red clay bricks, 24 specimens were tested through static load tests, Diagonal Shear Test (Prism Test), and Pendulum Impact Tests to assess mechanical and dynamic properties. The Pendulum Impact Test and Diagonal Shear Test (ASTM E519) revealed that reinforced walls exhibited superior crack resistance, load-carrying capacity, and energy dissipation. Under low and high-velocity impact conditions, steel mesh fiber walls demonstrated the highest impact force and damping ratio, while glass and chicken mesh fibers also significantly improved energy absorption. Diagonal shear tests showed that reinforced walls had enhanced shear strength, modulus of rigidity, and strain performance. Using the secant modulus approach, the shear modulus was calculated, revealing improved ductility and energy absorption. Stiffness analysis highlighted that fiber reinforcement effectively prevented localized failure and maintained stability even under substantial deformation. The findings validate the potential of fiber-reinforced masonry for seismic resilience and structural optimization in masonry construction.

Chapter 5

Conclusion and Recommendations

- Post-impact analysis revealed a significant decrease in resonance frequency across all wall configurations, indicating a substantial loss in effective stiffness due to crack propagation. Unreinforced walls dropped from 2596 Hz to 1730.5 Hz, while reinforced walls decreased from 3528.5 Hz to 1564.25 Hz.

- The damping ratio increased with damage progression; unreinforced walls rose from 2.2% to 4.2%, and reinforced walls from 1.4% to 3%, highlighting enhanced energy dissipation through internal friction and micro-crack activity.

- Fiber-reinforced walls (S3 and S4) exhibited superior damping properties and higher energy absorption compared to unreinforced counterparts, albeit with a moderate trade-off in stiffness reduction.

- Dynamic elastic modulus decreased post-impact, reflecting stiffness degradation; however, fiber reinforcement effectively mitigated this effect more than in unreinforced walls.
- A pronounced effect of fiber mesh spacing was noted: diagonal tension strength improved by 96% with 4-inch spacing, modulus of rigidity by 82%, and energy absorption by 195%, indicating that wider fiber mesh spacing offers optimal performance.

- In compression tests, the S4 configuration exhibited the highest strength (5.89 MPa) and stiffness (4.26 GPa), while S1 and S2 showed the lowest performance (3.4 MPa and 3.99 MPa; 2.5 GPa stiffness).

- Maximum displacement was better controlled in S4 (2.72 mm), indicating enhanced resistance to deformation.

- Wall specimens with reinforced fiber strips (S1, S2) consistently showed reduced compressive strength and stiffness, highlighting structural vulnerabilities in these configurations.

- Failure modes across all configurations included vertical cracking, crushing, and splitting; however, the presence of fiber reinforcement helped contain crack propagation.

- These findings suggest that fabric-reinforced brick masonry walls not only enhance structural resilience and energy dissipation but also maintain adequate stiffness and load-bearing capacity, validating their use in earthquake-prone and vibration-sensitive environments.

References

1. Matthys, H. and L. Noland, *Evaluation, strengthening and retrofitting of masonry buildings.* TMS, Colorado, 1989.
2. Tumialan, J.G., et al. *Strengthening of masonry with FRP bars*. in *3rd. Int. Conf. on Composites in Infrastructure (ICCI 2002)*. 2002.
3. Korany, Y. and R. Drysdale, *Enhancing seismic flexural resistance of historic masonry walls using carbon fiber rope.* TMS Journal, 2004: p. 27-38.
4. Chuang, S.-W., et al., *Seismic Retrofitting of Unreinforced Masonry Walls by Frp Strip*. 2003, New Zealand Society for Earthquake Engineering.
5. Tomazevic, M., P. Weiss, and M. Lutman, *Influence of floors and connection of walls on seismic resistance of old brick masonry buildings.* Institute for testing and research in materials and structures, ZAG, Ljubijana, 1994.
6. ElGawady, M., P. Lestuzzi, and M. Badoux. *A review of conventional seismic retrofitting techniques for URM*. in *13th international brick and block masonry conference*. 2004. Citeseer.
7. Borri, A., M. Corradi, and A. Vignoli, *Experimental evaluation of in-plane shear behaviour of masonry walls retrofitted using conventional and innovative methods.* Masonry International, 2008. **21**: p. 29-42.
8. Tumialan, J., et al. *Strengthening of masonry walls by FRP structural repointing. Non-metallic reinforcement for concrete structures*. in *5th International research symposium on fiber reinforced polymer for reinforced concrete structures. Cambridge, UK*. 2001.
9. Mahmood, H., A. Russell, and J. Ingham. *Monotonic testing of unreinforced and FRP-retrofitted masonry walls prone to shear failure in an earthquake*. in *Proceedings of the 14th world conference on earthquake engineering*. 2008.
10. Faella, C., et al. *Tuff masonry walls strengthened with a new kind of C-FRP sheet: experimental tests and analysis*. in *Proceedings of the 13th World Conference on Earthquake Engineering, Vancouver, BC, Canada*. 2004.
11. Gattesco, N., I. Boem, and A. Dudine, *Diagonal compression tests on masonry walls strengthened with a GFRP mesh reinforced mortar coating.* Bulletin of Earthquake Engineering, 2015. **13**: p. 1703-1726.
12. Code, P., *Eurocode 8: Design of structures for earthquake resistancePart 3: Assessment and retrofitting of buildings.* Incorporating corrigendum March, 2010.
13. Gattesco, N. and I. Boem, *Out-of-plane behaviour of masonry walls strengthened with a GFRP reinforced mortar coating.* 2014.
14. Engineering, A.S.o.C. *Seismic rehabilitation of existing buildings*. 2007. American Society

of Civil Engineers.

15. Ascione, L., et al., *Il documento CNR N. 203/2006: Istruzioni per la progettazione, l'esecuzione ed il controllo di strutture di calcestruzzo armato con barre di materiale composito Fibrorinforzato.* 2006.

16. Shabdin, M., N. Khajeh Ahmad Attari, and M. Zargaran, *Experimental study on seismic behaviour of unreinforced masonry (URM) brick walls strengthened in the boundaries with shotcrete.* Journal of Earthquake Engineering, 2021. **25**(7): p. 1381-1407.

17. Park, J.-R., et al., *Shaking table tests of veneer masonry wall retrofitted with long-rawlplug screw anchors.* Journal of Building Engineering, 2023. **76**: p. 107163.

18. Bruggi, M. and G. Milani, *Optimal FRP reinforcement of masonry walls out-of-plane loaded: A combined homogenization–topology optimization approach complying with masonry strength domain.* Computers & Structures, 2015. **153**: p. 49-74.

19. Halici, O.F., et al., *Out-of-plane seismic performance of bed-joint reinforced Autoclaved Aerated Concrete (AAC) infill walls damaged under cyclic in-plane displacement reversals.* Engineering Structures, 2023. **286**: p. 116077.

20. Attari, N.K., et al. *Seismic evaluation of cladded exterior walls considering the effects of facade installation details and out-of-plane behaviour of walls*. in *STRUCTURES*. 2020. ELSEVIER SCIENCE INC STE 800, 230 PARK AVE, NEW YORK, NY 10169 USA.

21. Koutas, L.N. and C.G. Papakonstantinou, *Flexural strengthening of RC beams with textile-reinforced mortar composites focusing on the influence of the mortar type.* Engineering Structures, 2021. **246**: p. 113060.

22. Azadvar, N., et al., *Experimental comparison of cyclic behaviour of RC columns strengthened with TRC and FRP.* Bulletin of Earthquake Engineering, 2021. **19**: p. 2941-2970.

23. Williams Portal, N., L. Nyholm Thrane, and K. Lundgren, *Flexural behaviour of textile reinforced concrete composites: Experimental and numerical evaluation.* Materials and Structures, 2017. **50**: p. 1-14.

24. Chen, Z., et al., *Macro-modelling method for the in-plane behaviour of the damped masonry infill wall in a frame structure.* Journal of Building Engineering, 2023. **80**: p. 108114.

25. Majumder, A., et al., *Seismic and thermal retrofitting of masonry buildings with fiber reinforced composite systems: a state of the art review.* International Journal of Structural Glass and Advanced Materials Research, 2021. **5**: p. 41-67.

26. Arisoy, B., E. Ercan, and A. Demir, *Strengthening of brick masonry with PVA fiber reinforced cement stucco.* Construction and Building Materials, 2015. **79**: p. 255-262.

27. Costa, A.A., et al., *Experimental testing, numerical modelling and seismic strengthening of traditional stone masonry: comprehensive study of a real Azorian pier.* Bulletin of Earthquake Engineering, 2012. **10**: p. 135-159.

28. D'Ambrisi, A., et al., *Analysis of masonry structures strengthened with polymeric net reinforced cementitious matrix materials.* Composite Structures, 2014. **113**: p. 264-271.

29. Juhásová, E., Z. Zembaty, and M. Kowalski, *Experimental investigations of dynamic effects on brick masonry buildings and their strengthening.* Archives of Civil Engineering, 2000. **46**(1): p. 83-106.

30. Papanicolaou, C.G., et al., *Textile-reinforced mortar (TRM) versus FRP as strengthening material of URM walls: in-plane cyclic loading.* Materials and structures, 2007. **40**: p. 1081-1097.

31. D'Ambrisi, A., L. Feo, and F. Focacci, *Experimental and analytical investigation on bond between Carbon-FRCM materials and masonry.* Composites Part B: Engineering, 2013. **46**: p. 15-20.

32. Gams, M., M. Tomaževič, and A. Kwiecień, *Strengthening brick masonry by repointing–an experimental study.* Key Engineering Materials, 2014. **624**: p. 444-452.

33. De Felice, G., et al., *Mortar-based systems for externally bonded strengthening of masonry.* Materials and structures, 2014. **47**: p. 2021-2037.

34. Balsamo, A., et al., *Masonry walls strengthened with innovative composites.* Special Publication, 2011. **275**: p. 1-18.

35. Carozzi, F.G. and C. Poggi, *Mechanical properties and debonding strength of Fabric Reinforced Cementitious Matrix (FRCM) systems for masonry strengthening.* Composites Part B: Engineering, 2015. **70**: p. 215-230.

36. Codispoti, R., et al., *Mechanical performance of natural fiber-reinforced composites for the strengthening of masonry.* Composites Part B: Engineering, 2015. **77**: p. 74-83.

37. De Santis, S. and G. de Felice, *Tensile behaviour of mortar-based composites for externally bonded reinforcement systems.* Composites Part B: Engineering, 2015. **68**: p. 401-413.

38. Huang, X., et al., *Properties and potential for application of steel reinforced polymer and steel reinforced grout composites.* Composites Part B: Engineering, 2005. **36**(1): p. 73-82.

39. Papanicolaou, C., T. Triantafillou, and M. Lekka, *Externally bonded grids as strengthening and seismic retrofitting materials of masonry panels.* Construction and Building Materials, 2011. **25**(2): p. 504-514.

40. Kayali, O., M. Haque, and B. Zhu, *Some characteristics of high strength fiber reinforced lightweight aggregate concrete.* Cement and concrete composites, 2003. **25**(2): p. 207-213.

41. El-Diasity, M., et al., *Structural performance of confined masonry walls retrofitted using ferrocement and GFRP under in-plane cyclic loading.* Engineering Structures, 2015. **94**: p. 54-69.

42. Dizhur, D. and J. Ingham, *Diagonal tension strength of vintage unreinforced clay brick masonry wall panels.* Construction and Building Materials, 2013. **43**: p. 418-427.

43. Triantafillou, T.C. and C.G. Papanicolaou, *Shear strengthening of reinforced concrete members with textile reinforced mortar (TRM) jackets.* Materials and structures, 2006. **39**: p. 93-103.

44. Prota, A., et al., *Experimental in-plane behaviour of tuff masonry strengthened with cementitious matrix–grid composites.* Journal of Composites for Construction, 2006. **10**(3): p. 223-233.

45. Erdogmus, E., *Use of fiber-reinforced cements in masonry construction and structural rehabilitation.* Fibers, 2015. **3**(1): p. 41-63.

46. Natalli, J.F., et al., *A review on the evolution of Portland cement and chemical admixtures in Brazil.* Revista IBRACON de Estruturas e Materiais, 2021. **14**: p. e14603.

47. Balaguru, P. and A. Foden, *Properties of fiber reinforced structural lightweight concrete.* Structural Journal, 1996. **93**(1): p. 62-78.

48. Pierre, P., R. Pleau, and M. Pigeon, *Mechanical properties of steel microfiber reinforced cement pastes and mortars.* Journal of materials in civil engineering, 1999. **11**(4): p. 317-324.

49. Banfill, P. and A. Forster. *A relationship between hydraulicity and permeability of hydraulic lime*. in *International RILEM Workshop on Historic Mortars: Characteristics and Tests, Cachan, France: RILEM Publications sarl*. 2000.

50. Concrete, A.C.C.o., et al., *Standard test method for flexural toughness of fiber reinforced concrete (using centrally loaded round panel)*. 2012: ASTM International.

51. Shah, S.P., *Do fibers increase the tensile strength of cement-based matrix?* Materials Journal, 1992. **88**(6): p. 595-602.

52. Erdogmus, E. and C. Armwood. *Feasibility of Fiber-Reinforced Mortar for the Reconstruction of an Ancient Roman Temple*. in *Proceedings of Historical Mortars Conference HMC08, Lisbon, Portugal*. 2008.

53. Küçükdoğan, B., *An investigation of strengthening of historical masonry constructions by steel skeleton*. 2007, Middle East Technical University.

54. Ehsani, M., H. Saadatmanesh, and J. Velazquez-Dimas, *Behaviour of retrofitted URM walls under simulated earthquake loading.* Journal of Composites for Construction, 1999. **3**(3): p. 134-142.

55. Di Ludovico, M., et al. *Experimental behaviour of masonry columns confined using advanced materials*. in *The 14th world conference on earthquake engineering*. 2008.

56. Ehsani, M., H. Saadatmanesh, and A. Al-Saidy, *Shear behaviour of URM retrofitted with FRP overlays.* Journal of composites for construction, 1997. **1**(1): p. 17-25.

57. Albert, M.L., A.E. Elwi, and J.R. Cheng, *Strengthening of unreinforced masonry walls using FRPs.* Journal of Composites for Construction, 2001. **5**(2): p. 76-84.

58. Hamid, A.A., et al., *Behaviour of composite unreinforced masonry–fiber-reinforced polymer wall assemblages under in-plane loading.* Journal of Composites for Construction, 2005. **9**(1): p. 73-83.

59. Krevaikas, T.D. and T.C. Triantafillou, *Masonry confinement with fiber-reinforced polymers.* Journal of composites for construction, 2005. **9**(2): p. 128-135. Baek, J.-W., Kwon, J.-H., Kang, S.-M., & Park, H.-G. (2024). Cyclic loading test for brick masonry veneer anchored to reinforced concrete walls. *Journal of Building Engineering*, *96*, 110369.

60. Branco, J. M., & Araújo, J. P. (2012). Structural behaviour of log timber walls under lateral in-plane loads. *Engineering Structures*, *40*, 371-382.

61. Ganbaatar, A., Mori, T., Matsumoto, S., & Inoue, R. (2022). Reinforced effect on brick wall using timber wall as a retrofitting method. *Buildings*, *12*(7), 978.

62. H. Okail, A. Abdelrahman, A. Abdelkhalik, and M. Metwaly, "Experimental and analytical investigation of the lateral load response of confined masonry walls," *HBRC journal*, vol. 12, no. 1, pp. 33-46, 2016.

63. W. Wang and N. Chouw, "Flexural behaviour of FFRP wrapped CFRC beams under static and impact loadings," *International Journal of Impact Engineering*, vol. 111, pp. 46-54, 2018.

64. W. Zhang, S. Chen, N. Zhang, and Y. Zhou, "Low-velocity flexural impact response of steel fiber reinforced concrete subjected to freeze–thaw cycles in NaCl solution," *Construction and Building Materials*, vol. 101, pp. 522-526, 2015.

65. M. P. Salaimanimagudam, C. R. Suribabu, G. Murali, and S. R. Abid, "Impact response of hammerhead pier fibrous concrete beams designed with topology optimization," *Periodica Polytechnica Civil Engineering*, vol. 64, no. 4, pp. 1244-1258, 2020.

66. W. Zhang, S. Chen, and Y. Liu, "Effect of weight and drop height of hammer on the flexural impact performance of fiber-reinforced concrete," *Construction and Building Materials*, vol. 140, pp. 31-35, 2017.

67. Y. Pan, C. Wu, X. Cheng, V. C. Li, and L. He, "Impact fatigue behaviour of GFRP mesh reinforced engineered cementitious composites for runway pavement," *Construction and Building Materials*, vol. 230, p. 116898, 2020.

68. A. R-89, "Measurement of properties of fiber reinforced concrete," *Reported by ACI Committee*, vol. 544, 1999.

69. T. Z. Batran, M. K. Ismail, and A. A. Hassan, "Behavior of novel hybrid lightweight concrete composites under drop-weight impact loading," in *Structures*, 2021, vol. 34, pp. 2789-2800: Elsevier.

70. M. Ziada, S. Erdem, Y. Tammam, S. Kara, and R. A. G. Lezcano, "The effect of basalt fiber on mechanical, microstructural, and high-temperature properties of fly ash-based and basalt powder waste-filled sustainable geopolymer mortar," *Sustainability*, vol. 13, no. 22, p. 12610, 2021.